Understanding wrinkle formation in roll-to-roll top encapsulant production process for thin-film solar cells

Modelling aproach

T. Alkanbar

TU Delft

Understanding wrinkle formation in roll-to-roll top encapsulant production process for thin-film solar cells

Modelling aproach

by

T. Alkanbar

to obtain the degree of Master of Science

at the Delft University of Technology,

to be defended publicly on Thursday February 25, 2021 at 01:00 PM.

Student number:	4842685	
Project duration:	July 1, 2020 – February 25, 2021	
Thesis committee:	Prof. dr. ir. A. Smets,	PVMD, TU Delft
	Dr. P. Manganiello,	PVMD, TU Delft
	Dr. A. Lekic,	IPEG, TU Delft
	Dr. G. Limodio,	PVMD, TU Delft

This thesis is confidential and cannot be made public until February 25, 2023.

An electronic version of this thesis is available at `http://repository.tudelft.nl/`.

TU Delft

Abstract

Thin-film flexible solar panels can be utilized on many surfaces where conventional solar panels are hard to be used such as side walls of buildings, ship roofs or curved surfaces. In conventional solar cells, glass is used to protect the panels from external damage. However due to its heavy weight and rigidity, glass is not an option for thin-film flexible solar cells. HyET Solar, a company based in the Netherlands that produces flexible thin-film solar cells uses a transparent foil produced using a roll-to-roll process to encapsulate and protect their solar panels. In order to reduce the amount of materials used and cut the costs, a thinner foil is being developed. Producing the thinner foil in a roll-to-roll process causes different defects in the foil, among which half sinusoidal waves forming mostly in the bottom side of the foil, these waves are called wrinkles.

The process of manufacturing the top encapsulant layer involves changing temperatures and mechanical stresses applied on the foil. Therefore, two models were developed to understand the effect of three process parameters (web force, web speed and temperatures of each production zone) on wrinkle formation. First, a thermal model of the process using ANSYS program was developed to understand the temperature profile of the produced foil along the process. Then, a mechanical model that uses the output of the thermal model and the applied mechanical forces to study the effect of the investigated production parameters on wrinkle formation was worked out.

The results show that operating at higher temperatures and reducing the thickness of the foil are directly responsible for decreasing the threshold of the critical stress that causes wrinkle formation and thus reducing the range and the magnitude of the force to 1.4 N is needed to perform the process without forming wrinkles in the foil. Varying web speed between 0.3 m/min and 3m/min is found to have a minor effect when varied under high temperatures. Finally, decreasing the temperature of the first and second zones by 10 °C is found to extend the range of the web force that can be applied.

Performing the process under lower temperatures or reducing the mechanical forces that act on the foil will reduce wrinkle formation in the developed foil; web speed should not be considered in mitigating wrinkle formation.

Preface

Finishing my bachelor's degree in Mechanical engineering, I wanted to work in an area where I can make the biggest impact possible in the world. The idea of contributing to a better world by improving the way of utilizing energy has intrigued me because of the multidisciplinary challenges involved varying from economical and political to technological aspects. After long years of studying at schools and universities, I wanted to have the opportunity to do my thesis project in an industrial environment to gain an insight on the situation of the renewable energy industry. Due to the collaboration between TU Delft and HyET solar, I was able to do what I wanted.

First, I would like to thank my supervisor Prof. Arno Smets for his role in establishing this master's program and initiating such collaborations that give students the opportunity to work on multidisciplinary challenging subjects in an industry environment. I would also like to thank Dr. Gianluca Limodio because of his support along the process of my thesis project, and to my fellow master students Seba Makhlouf, Zakariya Asalieh and Mohammed Hannan for their help and collaboration.

The opportunity to do my thesis project at HyET Solar, was a way to meet people who taught me a lot beyond the technical knowledge. I have to express my gratitude to my supervisor at the company Dr. Ekaterina Khadikova with her continuous support and supervision. I was always looking forward for my meetings with her to hear her insights and her critical questions about my work, Dr. Edward Hamers for the intellectual discussions and the insights he provided me with, Willem Scheerder for giving me the time to discuss ideas and teaching me a lot about work ethics by his example, Herbert Lifka who gave me the opportunity to work on small projects and gain experience next to working on my thesis project. I also should not forget to mention Zafar Idu who was always there to guide me in the laboratories and all people working at HyET Solar and HyET Hydrogen.

Furthermore, I would like to thank my parents, my sister, my friend and mentor Joseph Vreeburg, my second family in Istanbul (Belli Family) and my friends everywhere in the world for being always beside me in all circumstances.

This page will not be enough to mention all people who made a difference in my life. Therefore, I'd like to thank all people I did not mention by name whom presence was enough to charge my life with positivity.

Lastly, it is important for me to thank all kind people in this world who make the life of people around them or far from them better.

T. Alkanbar
Nijmegen, February 2021

Contents

List of Figures

List of Tables

1

Introduction

As humanity develops and the economic situation of human beings improves to reach some level of prosperity, their basic needs get fulfilled, and they start paying more attention to other issues surrounding them as their environmental footprint. Svante Arrhenius (1859-1927) described the green-house effect in 1886, after which the understanding of the role of CO_2 and other greenhouse gases on climate change has increased enormously. Despite that fact, it was not before the energy crisis in 1973, when the interest in developing alternative energy sources started gaining acceleration. The following nuclear accidents and disasters as Chernobyl (1986) and Fukushima (2011) had convinced many governments to rely less or even eliminate nuclear energy sources. All of that opened the door wide for alternative energy sources, among which solar energy and other sustainable energy technologies. This interest has created a huge industry worth billions of dollars trying to develop the best and most cost effective technological solutions.

In this chapter, a general introduction about the problem this research is trying to understand and solve will be given. Starting with a general introduction about solar energy and thin film solar cells, the importance of encapsulating thin-film solar cells will be discussed. Following, a general introduction on roll-to-roll manufacturing process will be given. Later in the chapter, background information about the production of the encapsulation foil of thin film solar cells using a new and challenging technique by laminating different layers in a roll-to-roll process is presented and the efforts to produce the foil using a thinner layer of ETFE (ethylene tetrafluoroethylene) without defects are explained, in addition, the literature dealing with buckling and wrinkling in thin foils will be introduced and discussed. Finally, the aim of the research and the outline will be stated.

1.1. Solar Energy and Thin film solar cells

Solar photovoltaic energy has been growing exponentially in the 2010s [14] and it is likely to continue this trend in the in the sustainable development scenario. Such scenario is expected to become a reality with China's proposal to achieve net zero emission and surely, taking existing Paris agreement into account in addition to the willingness of many countries to achieve net zero emission levels.

Converting sunlight into electrical energy can be achieved by different solar cell technologies. One promising technology in terms of flexibility and light weight is thin-film solar cell technology, as these characteristics open the door for many new applications.Thin-film flexible solar panels can be utilized on many surfaces where conventional panels can not be mounted as side walls of buildings or ship roofs as examples.

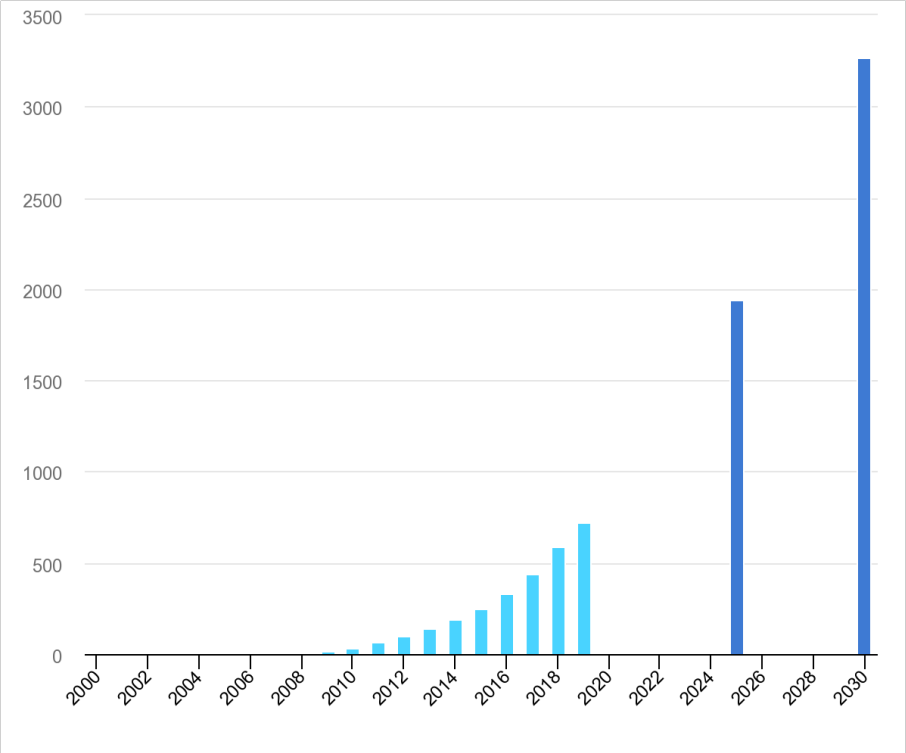

Figure 1.1: Growth in solar PV generation in the sustainable development scenario (IEA)

Thin-film solar cell technologies are rather new technologies compared to wafer based technologies with a market share of around 10%[31]. Thin film solar cells are favorable due to being cost effective in terms of the harnessed energy obtained from a certain amount of raw materials [21]. Three technologies are the most widely spread commercially, amorphous silicon solar cells (a-si), cadmium telluride solar cells (CdTe) and copper indium gallium diselenide (CIGS).

In HyET Solar, amorphous silicon solar cells are produced using Plasma Enhanced Chemical Vapour Deposition (PEVCD) on an aluminum foil. Figure 1.2 depicts the main layers in an amorphous silicon solar cell.

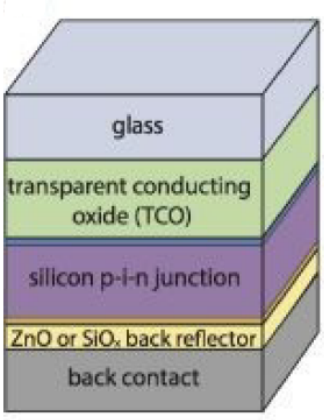

Figure 1.2: General structure and layers of a thin film solar cell[25]

1.2. Encapsulation of thin-film solar cells

A long lifetime with stable operation is vital to make a certain solar cells technology competent. In a world of competitive profit-maximizing firms, each extra year of stable operation means a drastic de-

crease in LCOE (Levelized Cost of Energy), thus a more competent product. In conventional crystalline silicon solar cells, glass is usually used as a protection layer, however, when it comes to flexible thin-film solar cells, glass is not an option as the technology promises light weight and flexibility. HyET Solar, a company that produces low cost flexible thin-film solar cells, uses abundant elements and utilizes roll-to-roll manufacturing processes that allow to curb the costs of production to achieve a product with nearly 30% lower LCOE [26]. Despite the previous fact, there is still room for improvement and cost reduction. One of the most costly parts is the top encapsulation foil that consists of a sandwich structure of two ETFE plastic foils and fiber glass fabric in between, these three layers are bonded with silicon glue. Reducing only the thickness of the ETFE foils to half is enough to make the whole product 10% less expensive. Producing a thinner encapsulation foil brings its own technical challenges with it as more defects appear in the manufacturing process.

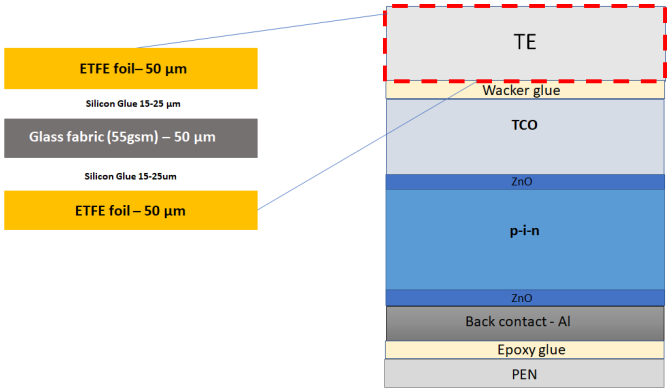

Figure 1.3: Position of TE (Top encapsulation foil) on top of the solar cell structure and TE layers of the solar cells of HyET solar

In order to achieve operational stability of the produced solar cells and protect the active layers and the whole solar cell from external damage, a protective layer should be added. This layer has to have some characteristics as high light transmittance, light weight, flexibility, low gas/water permeability, and should be strong enough to protect the layers beneath it from damage. Minimizing the thickness of the encapsulation layer, will result in less material used which affects the weight and the cost of the product in addition to reducing its environmental impact.

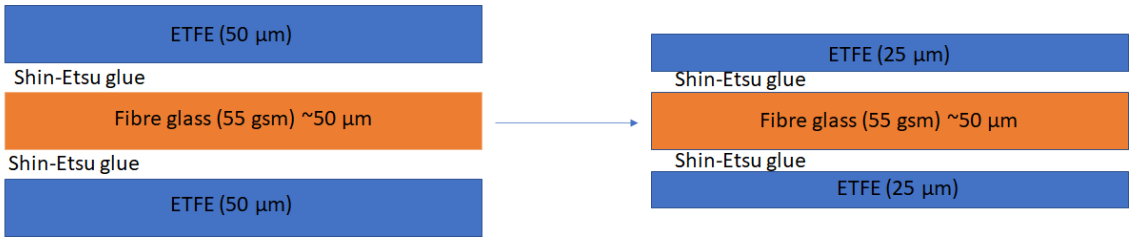

Figure 1.4: The aimed improvement in the top encapsulation foil

The aims to produce a thinner top encapsulation foil using 25μm ETFE layers instead of 50μm ETFE layers were faced with different types of defects happening in the encapsulation foil. Some of these defects are air entrainment,*Battleships* and wrinkling. Air entrainment happens when small air bubbles form in the glue layer, Battleships, as shown in Figure 1.5b is a defect thought to be a cluster of air bubbles formed in the glass fibre layer which is impregnated by silicon glue, the defect was called ”Battleship” because it interestingly looks like a big battleship. The other kind of defects is wrinkling (Figure1.5a. When wrinkling happens, the foil forms half sinusoidal waves filled with glue, usually forms on the bottom ETFE layer. This kind of defects is also referred to as ”Sand wrinkles”. The focus of this research will be to understand the process parameters that cause the wrinkling defect and find the optimal parameters to avoid them.

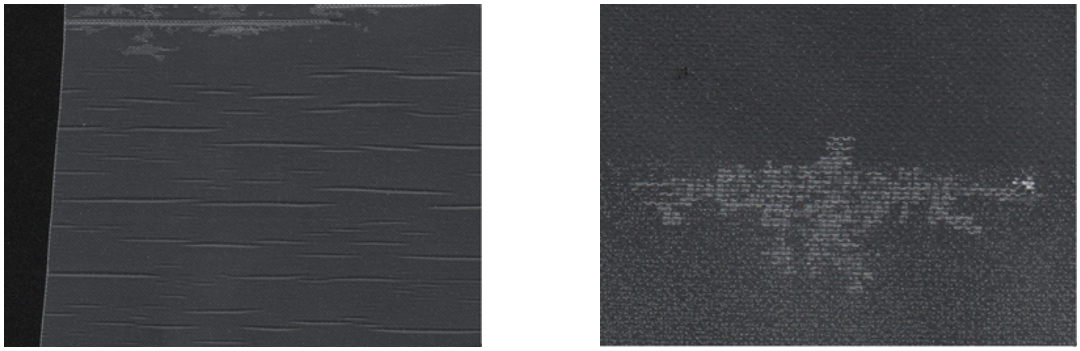

(a) wrinkling defect (b) Battleship defect

Figure 1.5: different defects that appear in the encapsulation foil

The reason that wrinkling is considered a defect is beyond the visual appearance of the foil. As it can be seen in Figure 1.6, The foil is visually degraded after 1134 of aging the foil in a Weather Ometer (WOM), a machine in which weathering effects (light exposure, humidity, temperatures) can be applied to a certain material and thus the effect of exposure to external weather conditions can be simulated. This degradation is a big concern in terms of reliability as it indicates to failure of the foil to protect the product within its lifetime. In addition the foil loses its transparent appearance, this translates into worse light transmittance to the cell the foil should protect as shown in Figure 1.7.

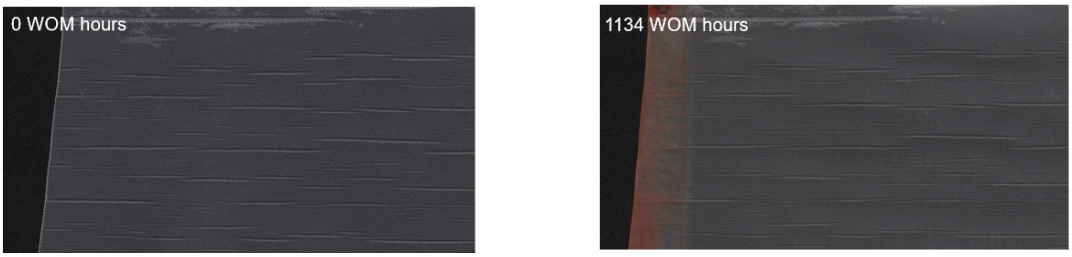

(a) The foil before WOM aging process (b) The foil after 1134 WOM aging process

Figure 1.6: Top encapsulatio foil with wrinkling defects are a big concern for the reliability. The effect of aging the foil in Weather Ometer (WOM) for 1134 hours

In the figure below, it is clear that the top encapsulation foil is losing its ability to transmit light the longer it is aged in the WOM machine. Relative efficiency here is the efficiency of the cell at a certain moment divided by its initial efficiency (predefined to be 1.15).

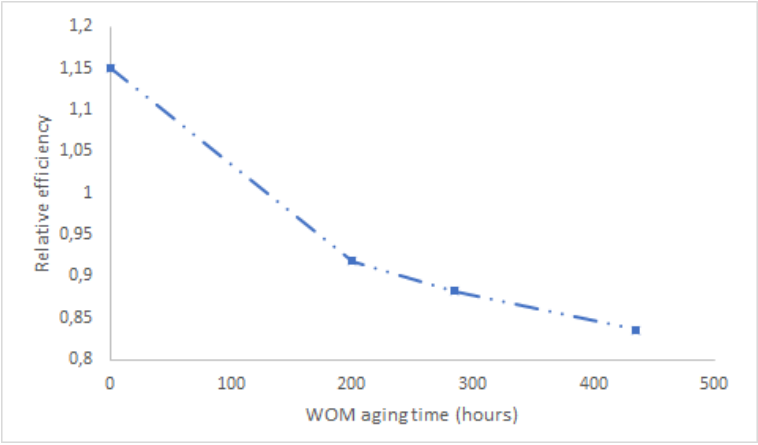

Figure 1.7: Relative efficiency of the foil plotted against time spent in WOM. Adapted from data of [17]

1.3. Roll-to-Roll (R2R) manufacturing process

Roll-to-Roll manufacturing process (also called web processing) is a fabrication process at which a roll of material is inserted into a machine where it undergoes one or different processes and leaves the machine in form of output roll, this output roll can be a final product or an input for the next process. A variety of additive or substractive manufacturing techniques as depositing, embedding, printing, etching or laminating might be used to process the roll. Therefore, roll-to-roll has found application in multiple industries such as flexible electronics, flexible Photovoltaics, fuel cells, paper industry and many other industries. According to NREL (National Renewable Energy Laboratory), the advantages of roll-to-roll processing include reducing manufacturing costs, high production rates and yields, and increased production efficiency. These characteristics allow the manufacturers to produce large quantities as the processes can be continuous and consequential which makes the products more competitive taking advantage of the economy of scales to compete with established technologies.

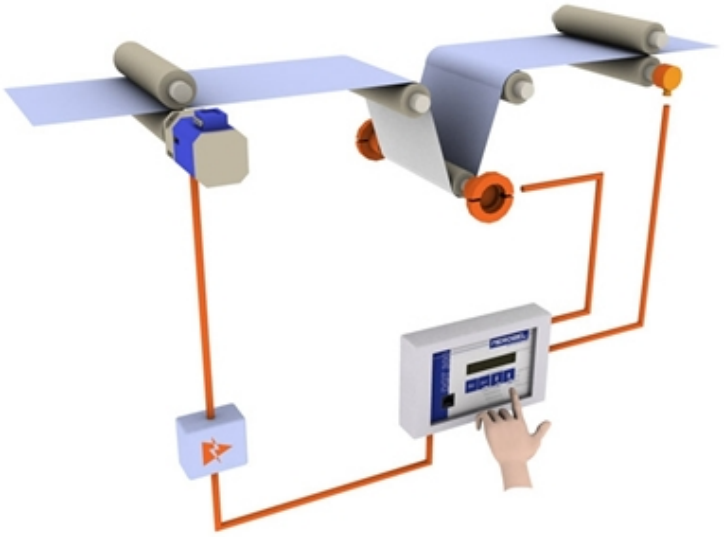

Figure 1.8: An example of R2R manufacturing process [1]

Despite the promising side of R2R technology in terms of large scale production and increased production efficiency, a lot of challenges are still present. These challenges can be divided into technical and economical. Technical challenges include the huge differences between lab-scale manufacturing and the real process, the variations in incoming materials such as incoming material tolerances and lot-to-lot variations to give some examples. Furthermore, the process itself adds some technical challenges, some of these challenges were addressed in[11] and include guiding the path of the web, controlling the tension in each part of the process, and controlling temperature or moisture and their effects. Not being able to get a grip on these parameters leads to defects such as baggy webs, wrinkling, buckling. On the other hand, the most important economical and financial challenge is the cost of R2R manufacturing equipment and machines can be very expensive which makes it a less attractive option for low scale production. A manufacturer should be guaranteed to be able to produce and sell large amounts of a certain product to make such a high start-up investment. This will make it harder for smaller companies to enter the market.

1.4. Production of encapsulation foil at HyET Solar

Top encapsulation foil at HyET Solar is produced by laminating two ETFE layers on a non-woven glass fibre fabric with the help of silicon glue (as discussed in 1.2 . The process consists of multiple consequent stages. First, glass fiber gets impregnated by the silicone glue and the ETFE foils are preheated in the first sections of the machine (Z9 and Z8). Afterwards, the three layers are joined

in the mangle section as shown in Figure 1.10 and all layers enter the oven zones (Z1 to Z6) where they are heated up to achieve the curing (hardening) of the glue. The glue mix used is a silicon glue produced by the company named Shin-Etsu. The glue starts curing at 65 °C and and the curing reaction gets the highest value at 122.23 °C [8]. Due to the changing temperature, the viscosity of the glue is changing during the process as well as the dimensions of the ETFE layers, and to a much smaller extent the glass fibre layer. When the winder and the drum (right in Figure 1.9) start turning, they pull all three foils, thus turning the unwinders. The stress in a certain foil is determined by the braking force applied on the unwinders. Winders and unwiders are no more than rollers with a motor or braking system mounted on its side to control its motion.

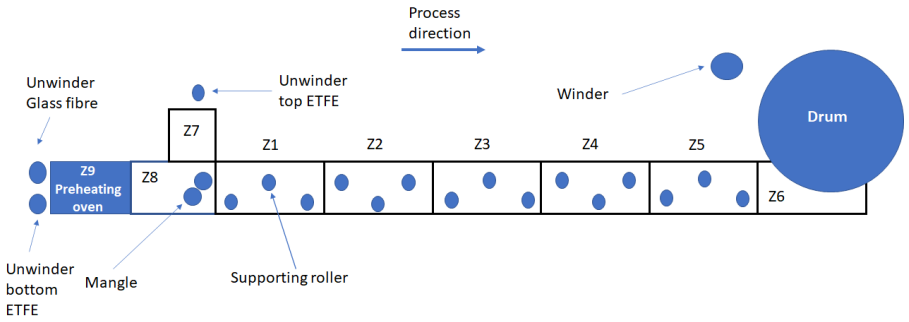

Figure 1.9: Scheme of the machine used to produce the top encapsulation foil

The chambers shown in 1.9 and named Z1 to Z9, are ovens with specific temperatures and lengths. The foil passes through all of these chambers in order to construct the encapsulation foil. The foils and glue are preheated in Z9, Z7 and Z8 before they are joined in the Mangle section. The foils then pass between Z1 to Z6 and around the drum where the glue hardens (cures) gradually ending as a top encapsulation roll around the winder.

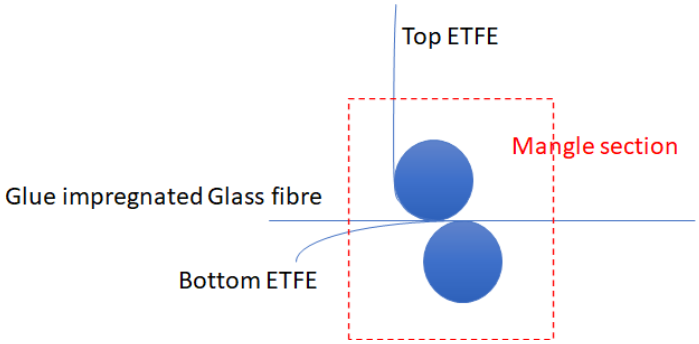

Figure 1.10: Joining the three foil before Z1

Set temperatures and lengths of each zone are given in the following table.

Zone number	Z9	Z8	Z1	Z2	Z3	Z4	Z5	Z6	Drum
Set temperature (°C)	48	75	100	120	120	128	135	145	135
Length (cm)	103	76	86.5	85.5	88	84.5	82	108	N/A

Table 1.1: Temperatures and lengths of each zone in the machine

1.5. Literature review

Wrinkling is a well-known phenomenon, it can almost be seen everywhere, in aging skin, the outer bark of an old tree, they can even appear in the cornea of the in uncommon situations [15] or the geological

process of mountain formation. A lot of research has been done on wrinkling of thin-films not only to mitigate them as defects, but also to make creative use of them in many applications as in stretchable electronics [19], anti reflective coating applications[13] Wrinkling in two dimensional materials has been studied by [4]

1.5.1. Reasons for wrinkling in webs

Wrinkles in webs appear due to compressive stresses in the transverse direction (perpendicular to the process direction). Despite the fact that these stresses do not form directly due to an external force, many reasons might cause these stress as studied by[10, 16]. Some of these reasons are:

A.Roller misalignment: If a roller has a misaligned rotation axis, the web will seek aligning itself perpendicular to the mentioned axis of the misaligned roller, this will cause lateral compressive stress in the web.

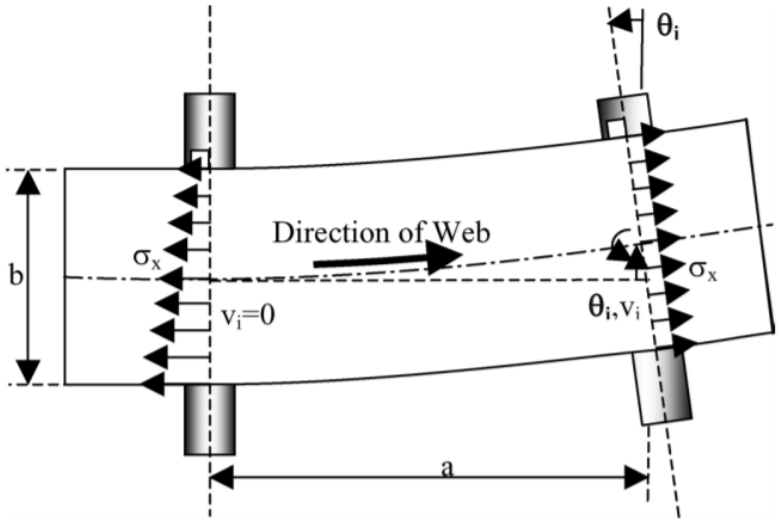

Figure 1.11: The effect of a misaligned roller [16]

B.Roller imperfections: Due to manufacturing-related imperfections, the roundness of the roller might be far from good when it comes to transporting a web without wrinkling. In a tapered roller as in 1.12, The roller will have the same angular velocity along x, however due to the bigger radius at x=L, the speed of the surface and thus the speed of the web will be higher at this side. This mismatch in speeds of both sides of the web will induce wrinkling in it.

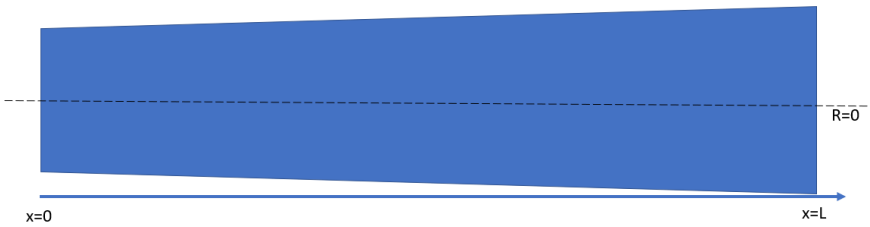

Figure 1.12: An exaggerated tapered roller

C.Tension variation: When handling a web a tensile load is usually applied on the web in order to make it move. This tension changes during the process due to many effects. The strain caused by the load in process direction (PD) is given as ϵ_{PD}, this strain causes a strain in the transverse direction (TD)

equal to $\epsilon_{TD} = -\nu\epsilon_{PD}$ where ν is Poisson's ratio of the material. When the tension decreases in PD, the strain in TD becomes positive and the web expands. This case is especially relevant in the case where the web is in continuous contact with a fluid, as shear stresses caused by the resistance of the fluid to the transverse motion of the web can induce wrinkles. This is different from wrinkling caused directly by external forces which will be discussed later.

D.Temperature variations: The increase in temperature causes expansion of the web, this in its role leads to the same effect of decreasing tension as the foil will expand in all directions. Especially in polymer materials that have a high coefficient of thermal expansion (CTE) in the range of $100 * 10^{-6} K^{-1}$. The symbol α is usually used to point to the coefficient of thermal expansion.

1.5.2. Review of earlier trials to mitigate wrinkling

At HyET Solar, multiple attempts were done to mitigate wrinkling in the foils with 25 μm ETFE in[12]. The main focus of the trials was to reduce whitening in the encapsulation foil, but some work has been done on avoiding wrinkle defects. Ultimately, the problem was solved by using 50 μm ETFE foil instead of 25 μm ETFE foil.

First trial

In the first tial, February 2020, a new structure of the foil had been tried. Namely, using 50μm thick ETFE foil in the bottom and 25μm ETFE foil in the top layer as wrinkles tend to appear in the bottom foil. The result was buckled foil as seen in 1.13b. The stated reason is the difference in stress release between the top and the bottom foil. This is a logical conclusion, if the top foil shrinks more than the bottom one, this will cause compressive stresses in the top part of the encapsulation foil, creating a bending effect as seen in the trial.

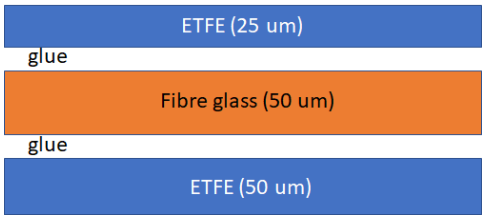

(a) The structure of produced top encapsulation foil

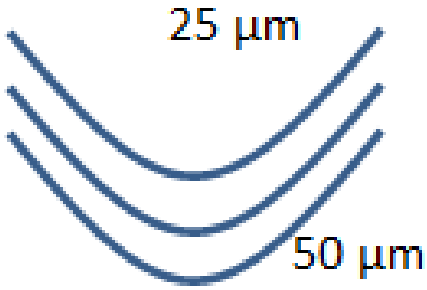

(b) Buckled foil

Figure 1.13: Trial of using 50μm foil in the bottom layer and 25μm in the upper foil

Second trial

In the second trial in February 2020, multiple hardware changes were applied for the production process of the top encapsulation foil, the observations were made during the production process. Three changes were effective in increasing or reducing wrinkling. The first one is preheating the bottom ETFE foil with IR heaters, causing buckling at the location of heating, thus increasing wrinkle forming, no reason was stated for this phenomena. The second one is covering all rollers in the oven zones one to five with plastic to avoid excessive heating due to the direct contact between the ETFE foil and the metal rollers, this increased wrinkling, the stated cause of the increase in wrinkling is friction difference. The third one is increasing the temperature of zone eight (Z8) from 75 °C to 110 °C, which caused reduction in wrinkling, the cause of that is the higher glue viscosity in locations of wrinkle formation, as higher viscosity will hold the foil better to the much stiffer fibre glass foil.

Series 900 trials

In series 900, the relationship between the gap between the two rollers of the mangle section and the thickness of the glue has been quantified, also the relationship between the thickness and sand wrinkles (in the figure given as SW) was observed. From Figure 1.14, mangle position is a number that tells about the situation of the mangle gap. When mangle position is zero the mangle is closed, and a value

of three means that the mangle is closed which means that the two rollers are at the closest distance to each other. In the figure below, it is seen that the thickness of the encapsulation foil is proportionally related to the status of the gap. OS and DS are the two long sides of the foil. A conclusion has been drawn that the number of observed sand wrinkle defects decreases with decreased thickness of the glue.

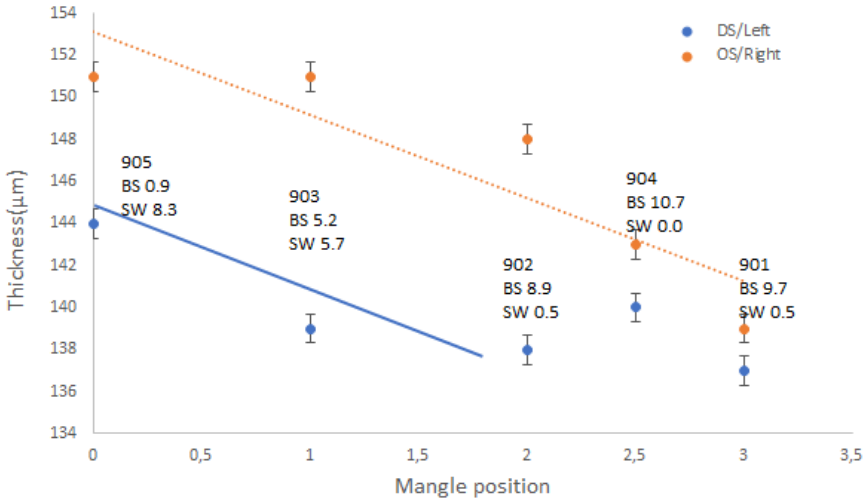

Figure 1.14: The relationship between the mangle gap and the thickness of the glue with indications about the number of sand wrinkle defects per meter

Viscosity of the glue during the process In [18], The viscosity of the glue has been measured using viscometer with a plate that can be heated at the same temperatures and times as happening during the process. The viscosity was found to be very low in the first four meters after the beginning of Z1 as shown in

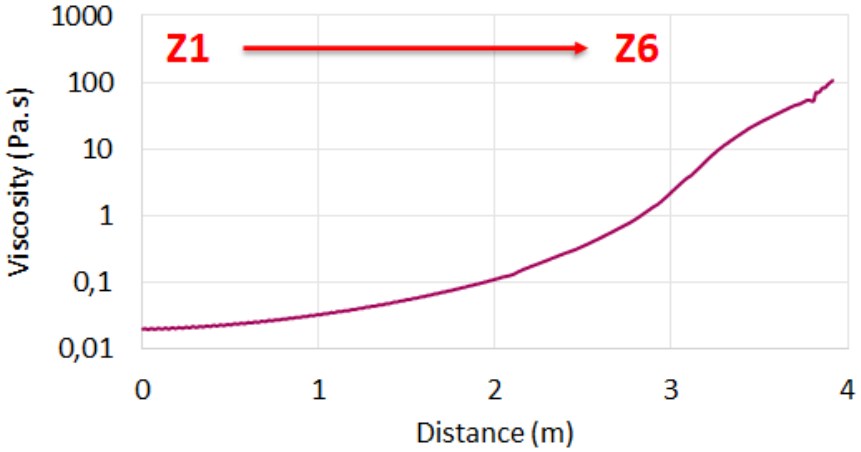

Figure 1.15: The viscosity of the glue measured using a viscometer for the first four meters of the process

1.5.3. Wrinkling of thin plates and foil under tensile loads

Before delving into the literature of buckling in thin foils or thin plates. It is important to note that the process of laminating the different layers of the top encapsulation foil at HyET Solar is unique and has many aspects that make it more complex than applying loads on one foil. However, the best way to start exploring the problem is by understanding the mechanisms that cause a thin foil to wrinkle. Wrinkling in foils can be treated as a buckling problem. Buckling usually happens under compressive stress. In [23]

buckling in center cracked plates has been studied, wrinkles in this case develop due to compressive stresses around the cracks and they argue that buckling in a thin plate under tensile loads will happen only in a situation of discontinuity. The effects of crack length, boundary conditions and bi-axial force in addition to the effect of initial imperfection on the critical loads were studied. Boundary conditions in this context is the situation of the edges of the plate, whether one or more of the edges is clamped, simply supported or free.

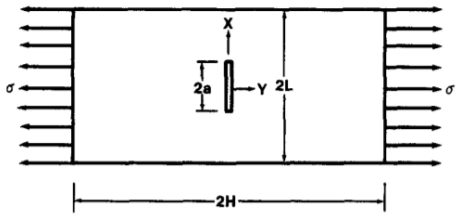

(a) A plate with crack under tensile load[23]

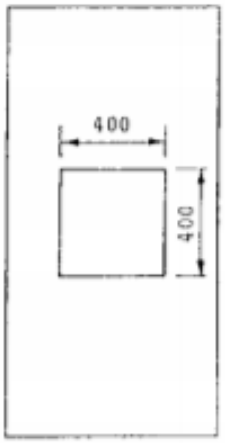

(b) Plate with a square-shaped hole [24]

Figure 1.16: Plates with different situations of discontinuity

In another paper [24] buckling of thin plates under another kind of discontinuity has been discussed, buckling in plates with holes under tension. Local lateral compressive stress around the holes was causing local buckling, the magnitude of buckling caused by tensile loads was found to be smaller than buckling under compressive loads.

Wrinkling in thin foils can also happen without any geometric discontinuity as a result of special boundary conditions, [9] studied . In [5], wrinkling phenomenon in thin sheets constrained from the short edges as shown in 1.17 and under tensile loads has been studied and a model that predicts the wavelength and the amplitude of wrinkles in a stretched sheet as given in1.11.2.

$$\lambda = \frac{(2\pi Lt)^{1/2}}{[3(1-\nu^2)\gamma]^1/4} \tag{1.1}$$

$$A = (\nu Lt)^{1/2}\left[\frac{16\gamma}{3\pi^2(1-\nu^2)}\right]^1/4 \tag{1.2}$$

where, λ is the wavelength of one wrinkle, L is the length of the sheet, t is the thickness of the sheet, γ the stretching strain and ν is Poisson's ratio.

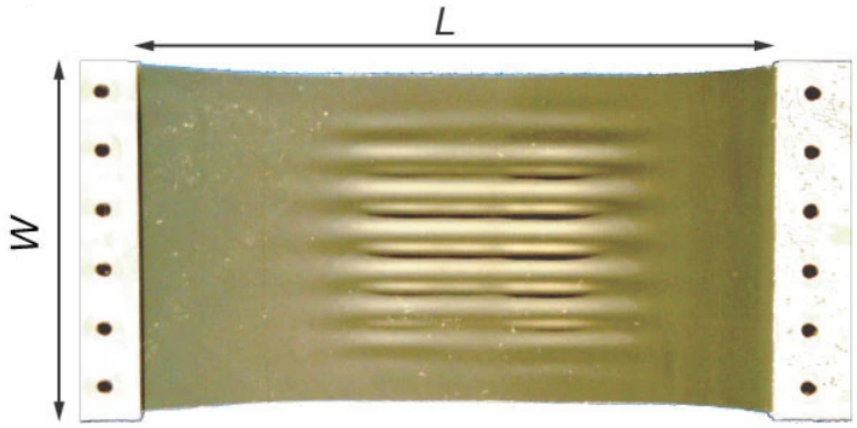

Figure 1.17: A sheet under tensile loads and constrained short edges [6]

The link between compressive stresses caused in the transverse direction and tensile loads has been studied in [9], the reason of wrinkling was stated to be the compressive stresses in the transverse direction caused by constraining the movement of the edges. The foil will tend to shrink in transverse direction as a result of stretching it, however, the clamped edges will prevent this movement, these compressive stresses are much smaller in magnitude than the tensile loads, however, the magnitudes of the compressive loads were not quantified. Finally, a diagram of the buckling coefficient k_c for different different ratios was introduced (Figure 1.18), which makes it easier to calculate the critical tensile load for wrinkling in a practical way. More about this topic will be covered later in Chapter 2.

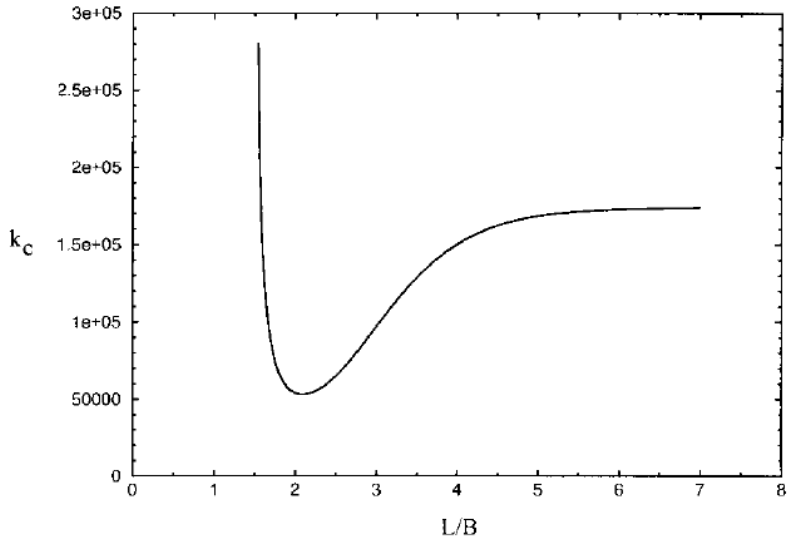

Figure 1.18: The buckling coefficient plotted against different aspect ratios[9]

1.6. Aim and outline of the thesis

As discussed earlier, there are many factors that cause wrinkling in webs used in R2R manufacturing processes. Some of these factors are related to imperfections and tolerances of machine parts, other factors are related to process parameters and the behaviour of the web used in production. In this thesis project, the focus will be only on the process parameters that will affect the stresses in the web.

The aim of this research is to evaluate the influence of production parameters of the encapsulation foil

by studying and modelling the effect of the three directly controllable process parameters which are web force, web speed and zone temperatures.

The questions this thesis is aiming to answer are:

1. How do process parameters (i.e. temperature, web speed, web force) affect wrinkle forming?
2. Which force ranges cause wrinkling in a thin foil under different process settings?
3. What are the optimal process parameters to avoid wrinkling?

Earlier in this chapter, after a short introduction about solar energy thin-film solar cells and the encapsulation of these cells, the process and problem this research is dealing with were described. Further, the literature of research dealing with related to this problem has been studied. In chapter 2, the theory of heat transfer, some principles of mechanics followed by the theory of buckling and wrinkling in thin plates and thermal expansion in multilayered materials will be discussed, paving the way to understand the performed work. In chapter 3, The modelling process will be explained, starting with the thermal model which provides the temperature of the studied foil during the process. Later in the chapter, a proposed model that uses the results of the previous model and the process parameters then calculates the stresses in the foil during the process will be explained. In Chapter4, the results gathered using the model quantifying the effect of the three process parameter discussed before on the formation of wrinkles in the bottom ETFE foil will be shared and explained. Lastly, in Chapter 5, these results will be discussed and based on them recommendations for further research or process development will be presented.

2

Theoretical background

2.1. Heat transfer mechanisms:

Heat can move in several ways depending on the medium and the conditions. There are 3 main mechanisms of heat transfer. Conduction, convection, and radiation. These mechanisms can happen simultaneously or separately. Conduction is the result of energy transfer in a material from high energetic particles to the adjacent particles with less energy, convection happens due to the interaction between fluid and solid surfaces and combines the effects of conduction and the dynamics of the surrounding fluid. Radiation does not involve any interaction of matter, the energy moves in the form of electromagnetic waves caused by changes in the electronic configuration of the atoms or molecules. These mechanisms are explained in [3].

2.1.1. Conduction

Conduction is the way energy, in form of heat, moves in a quiescent fluid or a solid body due to interactions between its particles. Conduction happens in solids as a result of the vibrations of molecules since they can not move, while in fluids, it happens as the molecules move randomly and collide with each other. This process implies energy moving from particles with a relatively high level of energy to the ones with lower energy levels. A potato put in the oven, for example, will start warming at the outer layer and the heat will move gradually inwards to the parts with lower temperature due to conduction.

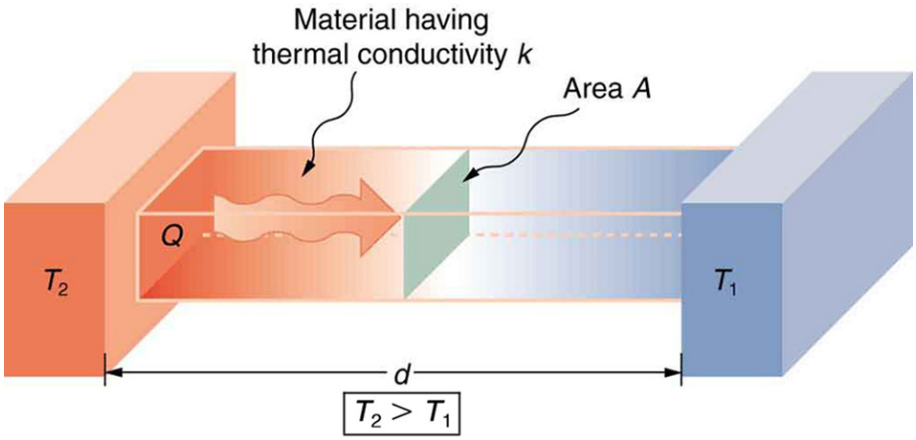

Figure 2.1: Conduction mechanism in a solid material

The rate of heat conduction in a certain medium will depend on several factors as thermal difference, geometry, thickness, and material properties. The larger the heat difference, the larger the energy variation between adjacent particles and thus the larger the heat transfer. A body with larger surface

area will increase the possibility of heat transfer as more heat exchange can take place. It is well known that the thicker an insulation material is, the less heat can pass through and that a plate of copper and a plate of polystyrene will not conduct heat at the same rate.

Considering a steady heat transfer in a body with a surface area (A), thickness (ΔL), and a temperature difference (ΔT), the rate of heat transfer will be proportional to A, ΔT and inversely proportional to t as seen in

$$\text{Rate of conductive heat transfer} \propto \frac{A * \Delta T}{\Delta L} \tag{2.1}$$

$$\dot{Q}_{cond.} = kA\frac{\Delta T}{\Delta L} \tag{2.2}$$

k is a constant of proportionality and is different for each material, thus it is a measure of the ability of a material to conduct heat. Materials with low conduction coefficient (k) are insulators and used in insulation applications and materials with high coefficient (k) are good heat conductors and are used in applications where heat should be transferred efficiently as cooling applications. When ΔL→0 the above-mentioned equation becomes:

$$\dot{Q}_{cond.} = kA\frac{dT}{dL} \tag{2.3}$$

This equation is called Fourier's equation of conduction and it relates the temperature gradient dT/dL to the rate of conductive heat transfer.

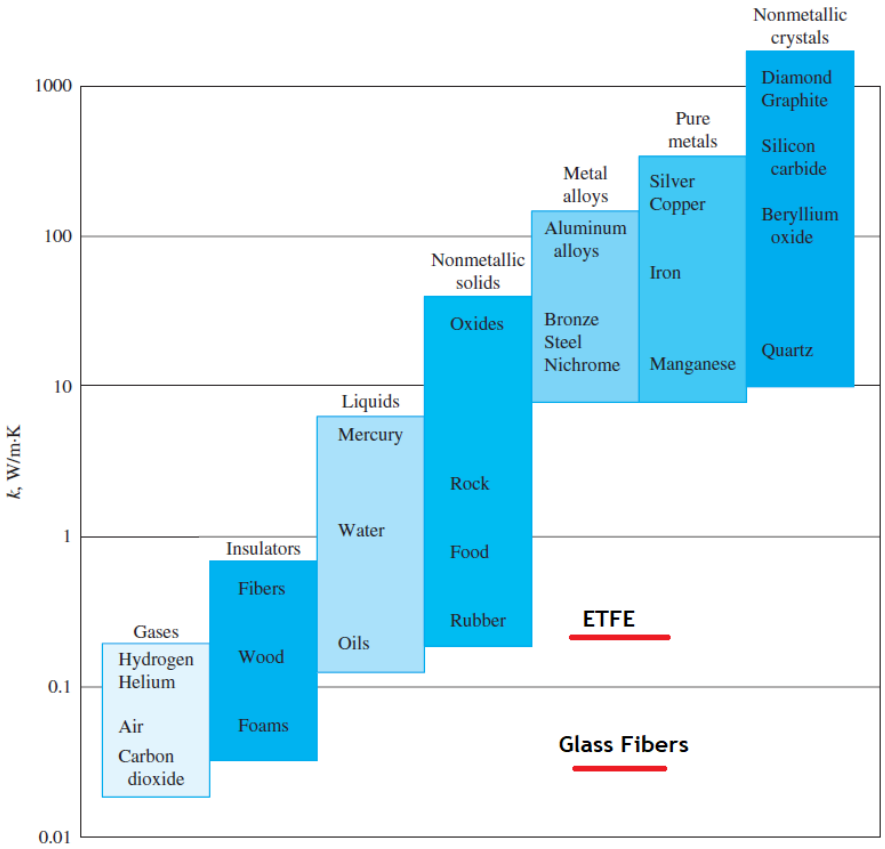

Figure 2.2: conduction coefficient (k) for different types of materials [3]. Added material properties are taken from [28] [2]

2.1.2. Convection

Convection is the heat transfer mechanism where heat moves due to the movement of a fluid. This movement causes parts of the fluid with different temperatures to come into contact, increasing the chance of conductive heat transfer within the fluid. Therefore, higher heat transfer rates are achieved by higher fluid velocities. In case the fluid is constant the mechanism becomes pure conduction.

In the graph below, cooling of plate by blowing a fluid (air for example) with a lower temperature is demonstrated. First, the interaction happens between the uppermost layer of the solid plate and the lowest layer of the fluid by conduction due to the no-slip condition which is a consequence of a small constant layer at the bottom. Then, an amount of heat is carried away by the fluid and transferred gradually upwards, away from the plate.

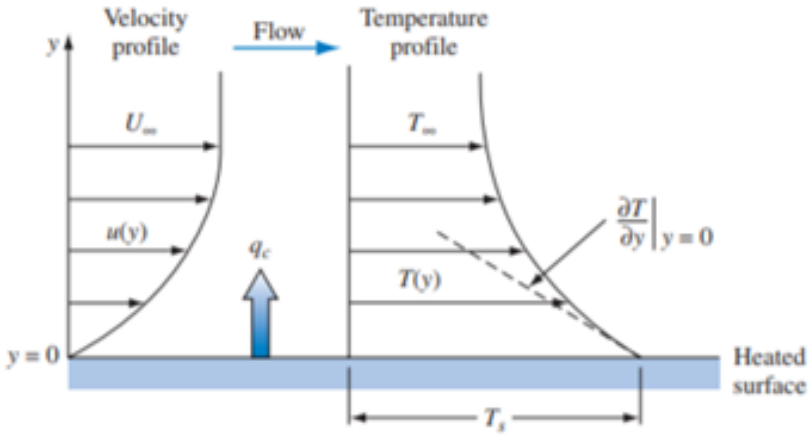

Figure 2.3: temperature profile when cooling a hot plate by blowing air [20]

Two types of convection are present:

Forced convection: The fluid is forced to flow by an external effect such as a fan or a pump.
Natural convection: The fluid moves due to the effect of changing densities of different layers of the fluid, as naturally the warmer parts of fluid tend to move upwards, leaving its space to molecules with a lower temperature. If the temperature difference is not enough to cause even this movement of the fluid, heat will still flow due to conduction.

The rate of heat transfer due to conduction depends on the geometry of the solid (surface area A_s), temperature difference (ΔT) and both the characteristics of the fluid and the geometry of the solid material as shown in the equation below

$$\dot{Q}_{conv.} = \overline{h} A \Delta T \tag{2.4}$$

$$\Delta T = (T_s - T_a) \tag{2.5}$$

Ts is the temperature of the surface and Ta is the ambient temperature.

The factor $\overline{h}$ is the convection coefficient, which does not only depend on the properties of the fluid and the geometry of the solid material, but it also depends on surface roughness, the flow properties of the fluid whether it is internal or external, and whether it is turbulent or laminar. The convection coefficient is rather a complex value to determine, therefore, many empirical ways were developed to define its value.

2.1.3. Calculating convection coefficients in the machine

What makes determining convection coefficients complex is the big number of parameters that can influence the rate at which convection will be happening. One of the most common ways to calculate convection coefficients is a method that uses dimensionless parameters, this method can give values with acceptable accuracy, but it is limited with predetermined geometries and conditions. In this section only relations for flow over a horizontal plate will be discussed.

As discussed earlier, there are two types of convection, natural and forced convection. When calculating the convection coefficients, each of the types has its own relations to be used in the calculations.

To find the convection coefficient at a certain setup, Nusselt number which is a dimensionless number should be found, knowing the characteristic length that depend on the geometry (L_c) and the conduction coefficient of the fluid (k) in addition to Nusselt number (Nu), the convection coefficient ($\overline{h}$) can be calculated as shown in 2.6.

$$\Delta Nu = \frac{\overline{h} L_c}{k} \tag{2.6}$$

The way Nusselt number is calculated depends on the flow of the fluid, whether it is forced or natural and the total Nusselt number is the sum of both calculated values in case of two flow regimes are present.

$$Nu_{total} = Nu_{natural} + Nu_{forced} \tag{2.7}$$

1) Natural convection

The relations used to determine the average $Nu_{natural}$ depend on the type of fluid flow, whether it is laminar or turbulent. The flow regime in natural convection is determined by the Rayleigh number.

$$Nu = \frac{\overline{h} L_c}{k} = C(Gr_L Pr)^n = CRa_L^n \tag{2.8}$$

Where,

Gr (Grashof number): a dimensionless number that determines the ratio of buoyancy to viscous forces in a fluid. Grashof number is calculated using 2.9

$$Gr_L = \frac{g\alpha(T_s - T_a)L_c}{\nu^2} \tag{2.9}$$

Where,

g: the acceleration of the earth gravity.
α: the coefficient of thermal expansion of the plate.
T_s: temperature of the surface of the plate.
T_a: ambient temperature.
L_c: the characteristic length of the plate A_s/p.
A_s: the surface area at which heat transfer occurs
p:the perimeter of the area at which heat transfer occurs.
ν: kenimatic viscosity of the fluid.

Pr (Prandtl number): A number that gives the ratio of the kinematic viscosity to thermal diffusivity of a fluid. The value of Prandtl number is obtained from the air properties table given in A and is evaluated at the film temperature $T_f = \frac{T_s + T_a}{2}$

Ra (Rayleigh number): Dimensionless number that determines the flow regime in natural flow.

C and n are constants related to the flow and geometry as given in the table below. Usually n is 1/4 if the flow is laminar and 1/3 if turbulent in case of natural convection.

Geometry	Lc	Range of Ra	Constants C	n
Lower surface of a heated horizontal plate	A_s/p	10^4 - 10^7	0.59	1/4
		10^7-10^{11}	0.1	1/3
Upper surface of a heated horizontal plate		10^5-10^{11}	0.27	1/4

Table 2.1: Constants C and n for a heated horizontal plate. Adapted from [3]

2) Forced convection
In case of enough relative motion between the heated plate and the fluid surrounding it, the flow is considered to be forced. The physics of forced convection is not different from natural convection and so is the procedure to calculate the convection coefficient for convective heat transfer.

$$Nu = \frac{\overline{h}L_c}{k} = CRe_L^m Pr^n \tag{2.10}$$

The flow regime in forced flow is determined by Reynolds's number (Re), given by the following relation.

$$Re = \frac{\rho u L_c}{\mu} \tag{2.11}$$

Where,
ρ: density of the fluid.
u: relative velocity between the fluid and the plate.
L_c: Characteristic length.
μ: dynamic viscosity of the fluid.

Flow regime	Range of Re	Range of Pr	Constants C	m	n
Laminar flow	Re < 5.10^5	Pr > 0.6	0.664	0.5	1/3
Turbulent flow	5.10^5 ≤Re ≤10^7	0.6≤Pr ≤60	0.037	0.8	1/3

Table 2.2: Constants C,m and n for each flow regime. Adapted from [3]

For forced flow over a vertical flat plate, the equations become:

$$\text{Laminar flow: } Nu = \frac{\overline{h}L_c}{k} = 0.664 Re_L^{0.5} Pr^{1/3} \tag{2.12}$$

$$\text{Turbulent flow: } Nu = \frac{\overline{h}L_c}{k} = 0.037 Re_L^{0.8} Pr^{1/3} \tag{2.13}$$

2.1.4. Radiation

Radiation is the form of energy emitted by matter in form of electromagnetic waves due to changes in electronic configurations. Radiation, unlike the previous two mechanisms, can happen without the presence of an intervening medium i.e. solid matter of a fluid. The energy of the sun is transferred to earth as a result of this mechanism. Thermal radiation is the form of energy emitted by bodies due to their thermal energy. Unlike other forms of radiative energy forms as gamma rays, radio waves or x-rays that has no relationship to the temperature of the emitting body. In the context of this thesis no special attention will be given to this form of heat transfer as it is neglected in the modelling process.

2.2. Basic concepts in mechanics of materials

To make it easier for readers from different backgrounds to understand the following sections, this short introduction to the basics of mechanics of materials is added to be used as a reference where some notions are explained.

Applying a certain force or pressure on a material, will cause an internal reaction counteracting the effects of the situation change. A basic example of that will be a beam with a surface area (A) fixed from one side and pulled with a force F from the other side as shown in Figure 2.5.

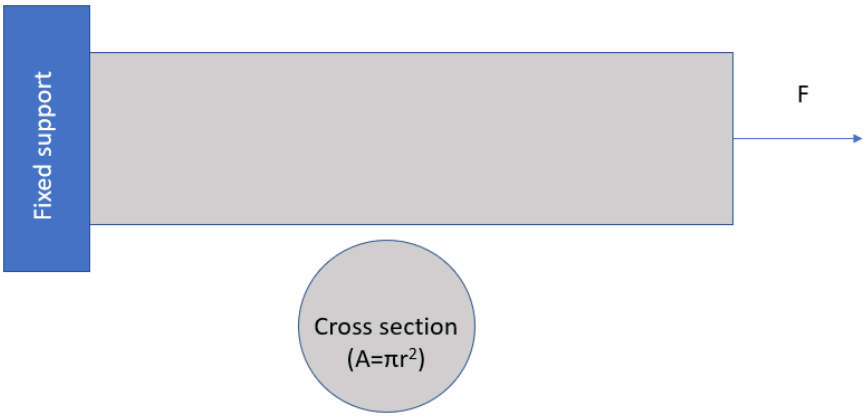

Figure 2.4: A beam fixed on one side and pulled from the other side with a force F

In this case stress is defined as the force per unit area (assuming that the force is applied uniformly on the cross section). The stress is called tensile if the force is pulling the beam away and compressive if it presses it towards the fixed support.

$$\sigma = \frac{F}{A} \tag{2.14}$$

Applying the force on the beam will cause elongation δL, The rate of elongation to the original length is called strain and given by the symbol (ϵ)

$$\epsilon = \frac{\delta L}{L} \tag{2.15}$$

The relation between the stress and strain is given by Hooke's law as shown in 2.16. E is called young's modulus and defined as a measure of the ability of a material to withstand changes in dimensions under a certain force.

$$\sigma = E\epsilon \tag{2.16}$$

Using equations 2.14,2.15 and 2.16, the elongation of the beam can be given as

$$\delta L = \frac{FL}{EA} \tag{2.17}$$

Such elongation can happen without the presence of any force when a beam is heated from a temperature T_1 to T_2, where $T_2 > T_1$. This elongation is calculated using the following equation.

$$\delta L = \alpha L \Delta T \tag{2.18}$$

α is the constant of thermal expansion and is a measurement of the amount of expansion per unit length under one unit of temperature change.

An interesting phenomenon that happens when putting a material under stress is the decrease in the width of the beam under tension as it becomes longer in the length direction, the opposite happens with compression. This is called Poisson's effect and it's expressed as

$$\nu = -\frac{\epsilon_w}{\epsilon_L} \tag{2.19}$$

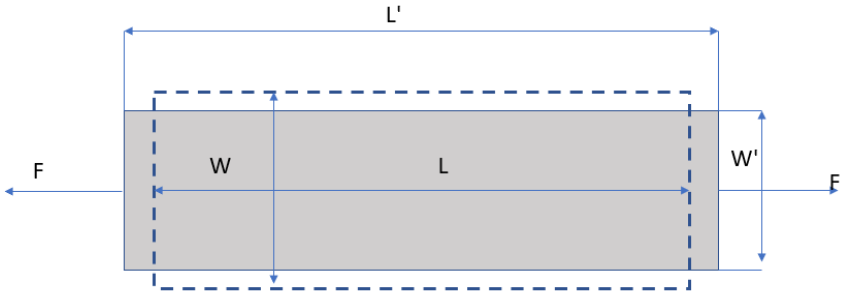

Figure 2.5: Poisson's effect. The beam elongates in the direction of the applied force while the width reduces in the transverse direction

2.3. Mechanical and thermal stresses in multi-layered membranes

Assuming three beams with a cross section (A) fixed together from both ends, one end is fixed in place and the other end can move freely as shown in Figure2.6. When these beams are heated equally, each beam will tend to expand an amount $\delta L = \alpha L \Delta T$, however, this will not be the case as the beams are made from different materials and are fixed to each other.

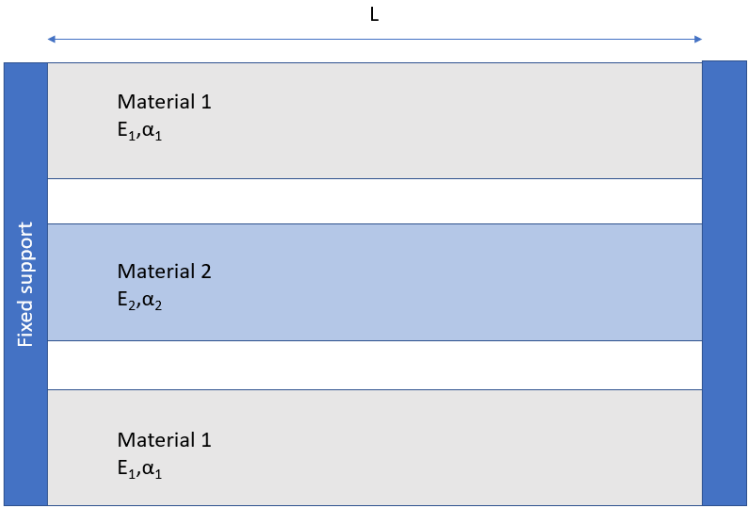

Figure 2.6: Three beams with length L fixed together from both edges

Assuming $\alpha_1 \gg \alpha_2$ and $E_2 \gg E_1$, The outer beams would expand more than the beam in the middle if the edges were not fixed. Accordingly, all beams will expand by a distance δL The outer beams will expand less than normal and the middle beam will expand more than normal, this will cause tension in the middle beam and compression in the outer beams.

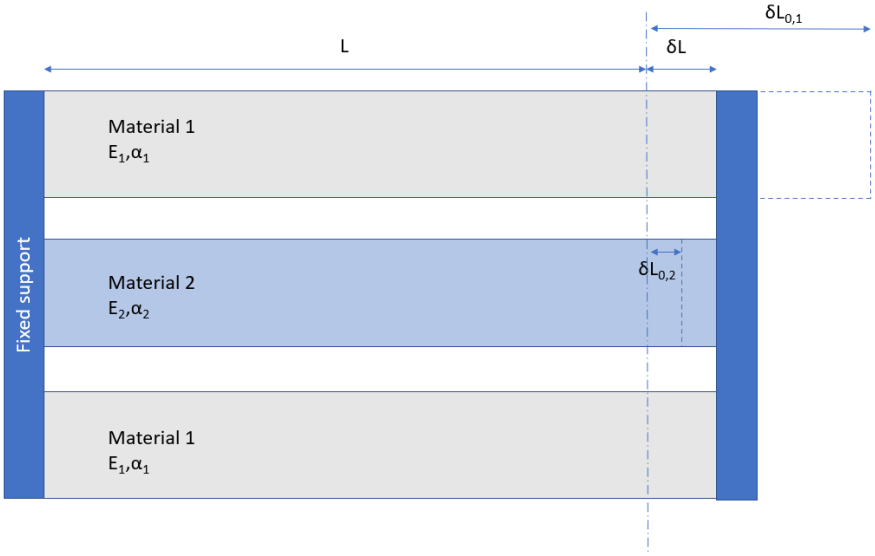

Figure 2.7: Heating three beams with length L fixed together from both edges

The previous analogy assumes a situation without a mechanical preload on the beams. If the beams were to be loaded with a force F as in Figure 2.9, the stresses generated are tensile stresses and can be defined as $\sigma_1 = E_1\epsilon_{force}$ in the outer beams and $\sigma_2 = E_2\epsilon_{force}$ in the middle beam. Assuming $E2 \gg E1$ and the moving support is rigid, the elongation and strain will be strongly determined by the middle beam, thus $\epsilon_{force} \approx \epsilon_2$. The stresses in the outer beams and middle beam will be given as

$$\sigma_2 = E_2\epsilon_2 \tag{2.20}$$

$$\sigma_1 = E_1\epsilon_2 \tag{2.21}$$

Fixing the elongation and heating the beams,

$$\sigma_2' = E_2(\epsilon_2 - \alpha_2\Delta T) \tag{2.22}$$

$$\sigma_1' = E_1(\epsilon_2 - \alpha_1\Delta T) = E_1(\frac{\sigma_2}{E_2} - \alpha_1\Delta T) \tag{2.23}$$

As $E_2 \gg E_1$ the stress is largely carried by the middle beam, so we can say that $\sigma_2 \approx \frac{F}{A_2}$

$$\sigma_1' = E_1(\frac{F}{A_2E_2} - \alpha_1\Delta T) \tag{2.24}$$

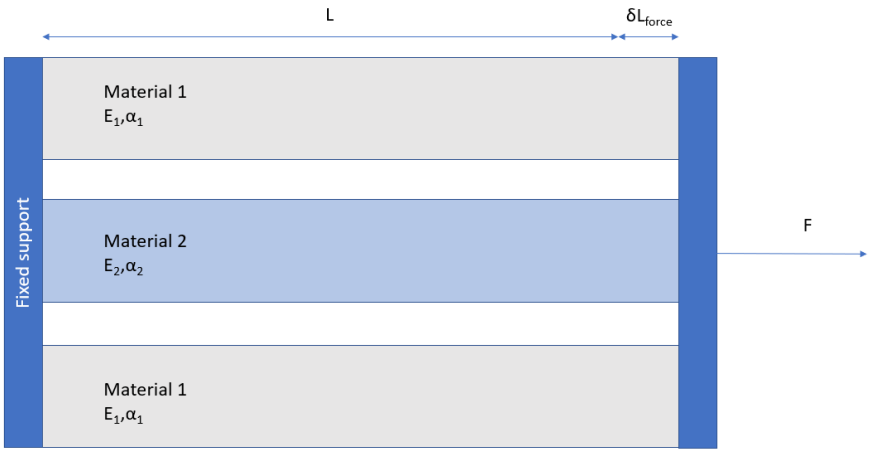

Figure 2.8: Applying force to Three beams with length L fixed together from both edges

The final condition is when the 3 beams are only fixed on one side, in this situation, the beams will behave as separate entities without influencing each other. In this case the effective stress after thermal relaxation can be given by 2.27. It is important to note here that the difference between this and the previous situation is that the length of any beam can become longer as the force will pull the beam as it elongates due to the temperature. However if the thermal relaxation fast and continuous, the thermal relaxation will persist.

$$\sigma_{Eff} = \sigma_{force} - \sigma_{thermal} \tag{2.25}$$

$$\sigma_{Eff} = E(\epsilon_{force} - \epsilon_{thermal}) \tag{2.26}$$

$$\sigma_{Eff}(t) = E\left(\frac{F}{AE} - \alpha\Delta T\right) \tag{2.27}$$

In this case $\Delta T = T_n - T_{n-1}$

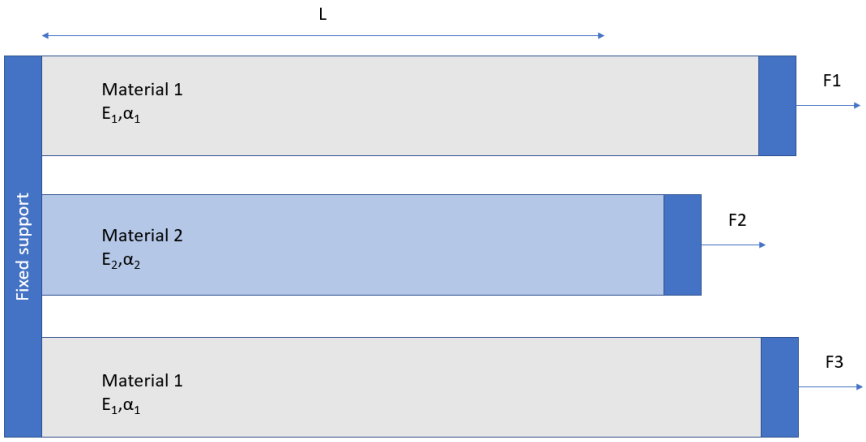

Figure 2.9: Three beams fixed on one side and pulled with three different forces on the other side

2.4. Buckling in plates

2.4.1. Buckling in plates under compressive stresses

Due to the similarity between the cross sections of wrinkled thin film and a buckled plate, it is possible to treat wrinkling in thin films as buckling in plates. Timoshenko and Gere [27] have studied the buckling in rectangular plates and the topic has been discussed in [29]. The governing equation of plate buckling for the case shown in Figure 2.10

$$D\left[\frac{\partial^4\omega}{\partial x^4}+\frac{\partial^4\omega}{\partial x^2\partial y^2}+\frac{\partial^4\omega}{\partial y^4}\right]+N\frac{\partial^2\omega}{\partial x^2}=0 \tag{2.28}$$

Where $D=\frac{Et^3}{12(1-\nu^2)}$ is bending rigidity of a plate, ω is the amount of deflection, N is the load applied on the plate, E is Young's modulus of the material, t is the thickness of the plate and ν is Poisson's ratio.

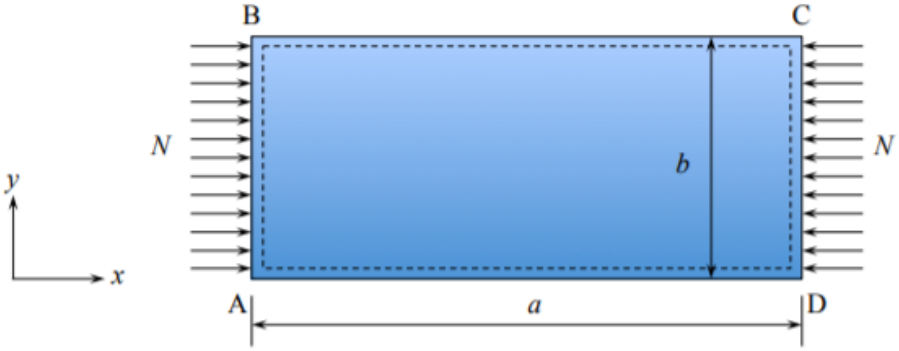

Figure 2.10: Geometry and loading conditions in a plate under buckling [29]

A product of two harmonic functions is considered to be the solution to 2.28, which is given as

$$\omega(x,y)=\sin\frac{m\pi x}{a}\sin\frac{n\pi y}{b} \tag{2.29}$$

solving equation 2.28 using the solution given in 2.29,

$$N=D\left(\frac{\pi a}{m}\right)^2\left[\left(\frac{m}{a}\right)^2+\left(\frac{n}{b}\right)^2\right]^2 \tag{2.30}$$

Where, m and n are integers that determine the number of half waves that will fit in the length and the width respectively. For all values of a, b, and m, n=1 gives the lowest value of N, This means that only one wave will form in the transverse direction to the load. Rearranging equation 2.31 we can determine the critical stress that will cause buckling in the plate using the following equations.

$$N_c=k_c\frac{\pi^2D}{b^2} \tag{2.31}$$

$$k_c=\left[\frac{mb}{a}+\frac{a}{mb}\right]^2 \tag{2.32}$$

Here, N_c is the critical load that causes buckling in the plate, k_c is the buckling coefficient for the situation shown above, D is bending rigidity, a and b are the length and width of the plate and the ratio $\frac{a}{b}$ is called the aspect ratio

This buckling coefficient (k_c) is special for the the load situation and boundary conditions shown in the figure above (simply supported plate with compressive loads acting on the short edges). Thus, for a simply supported plate with a compressive load applied on the short edges AB and CD as shown in 2.10. However, different k_c values are applicable under different boundary conditions and different load types.

2.4.2. Effect of boundary conditions

In plate buckling, boundary conditions have a big influence on the the buckling coefficient. There are three types of supports that are generally dealt with, free, clamped (c) or simply supported (ss), The loaded edges can be simply supported or clamped. In Figure 2.11 it can be seen that the buckling coefficient k_c depends heavily on the boundary conditions applied. The higher the buckling coefficient k_c, the higher the critical load that will cause buckling in the plate.

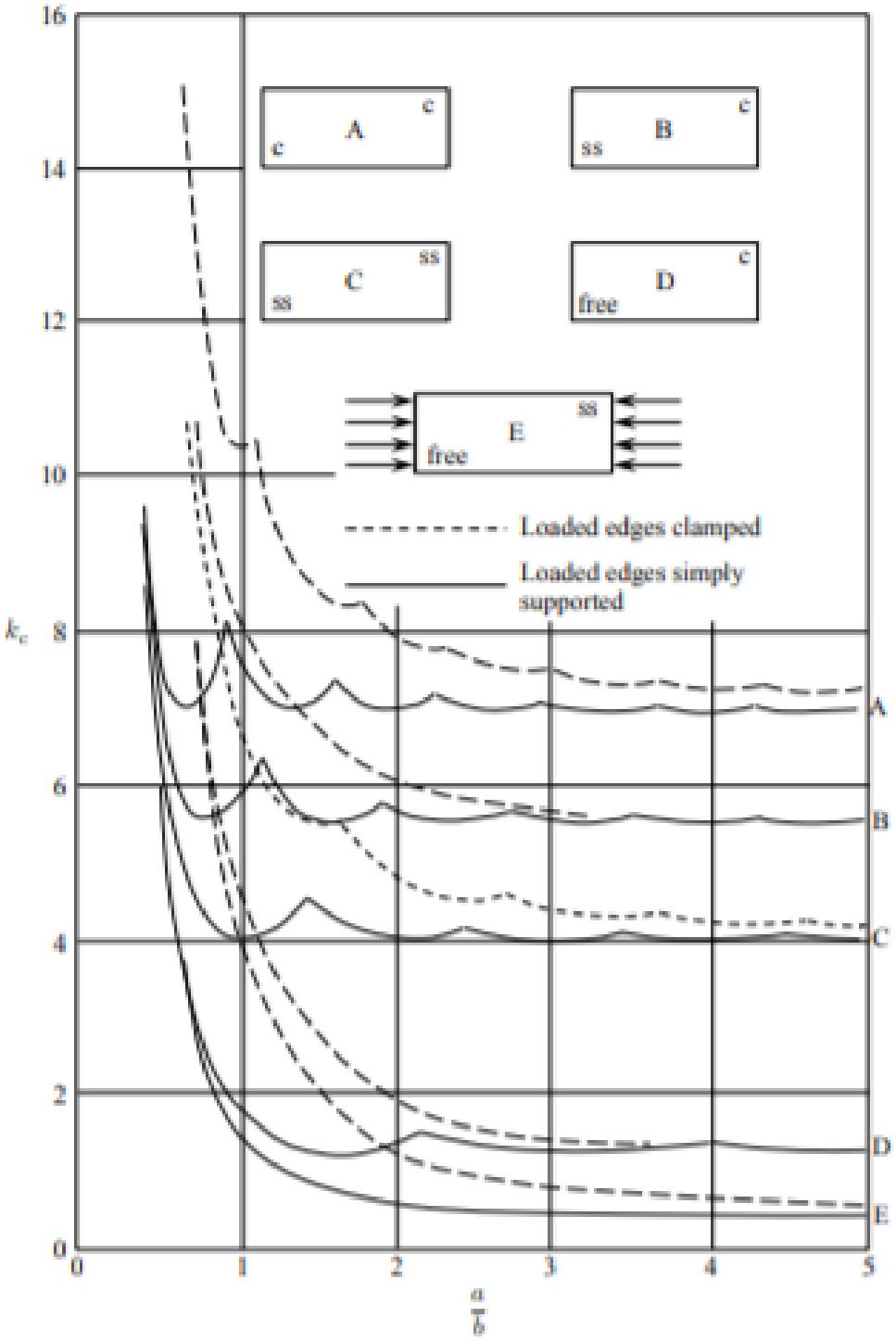

Figure 2.11: Buckling coefficient versus the aspect ratio (Length/Width) under different boundary conditions.[29]

2.4.3. Buckling in plates under tensile loads

Buckling phenomenon is typically studied under compressive loads, as compression is usually responsible for the loss of stability in structures. It is, however, important to know that especially in ultra-thin light weight structures as plates, buckling is observed to happen under tensile loads. It is important to note that buckling will happen even under uniform, external in-plane tensile loads applied to the edges of the plate. This has been studied and discussed in [22]and[9].

Buckling under tensile loads in thin plate with no presence of geometric discontinuity can happen under certain boundary conditions. When the movement in the transverse direction is constrained at the short edges, lateral compressive stresses will appear at a further distance from the edge due to constraining Poisson's effect and thus the contraction in the transverse direction. This effect can cause wrinkles in thin plates as it causes high wave number buckling modes that become permanent [9]. In the figure below, stress fields for two foils with different aspect ratios (ζ=Length/Width) is shown.

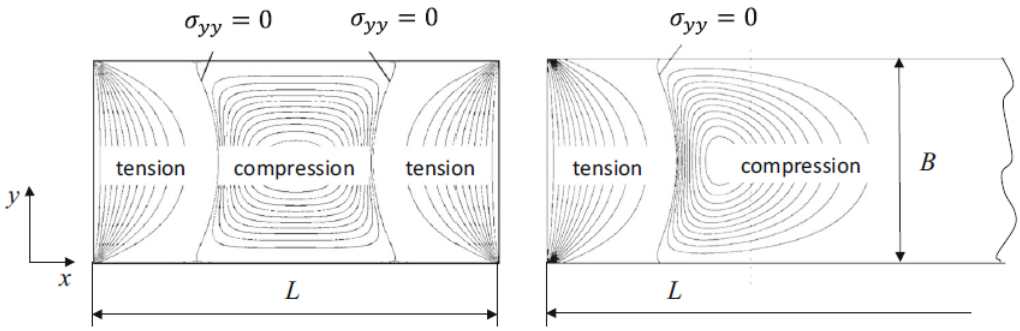

Figure 2.12: Stress field under tensile load with and a constrained short edges for two plates with L/B=2 (left) and L/B=7 (right)[22]

Buckling coefficients for a thin foil with a Poisson's ratio of $\nu = 0.3$ with different aspect ratios constrained from the edges and put under tensile loads is given in the figure below.

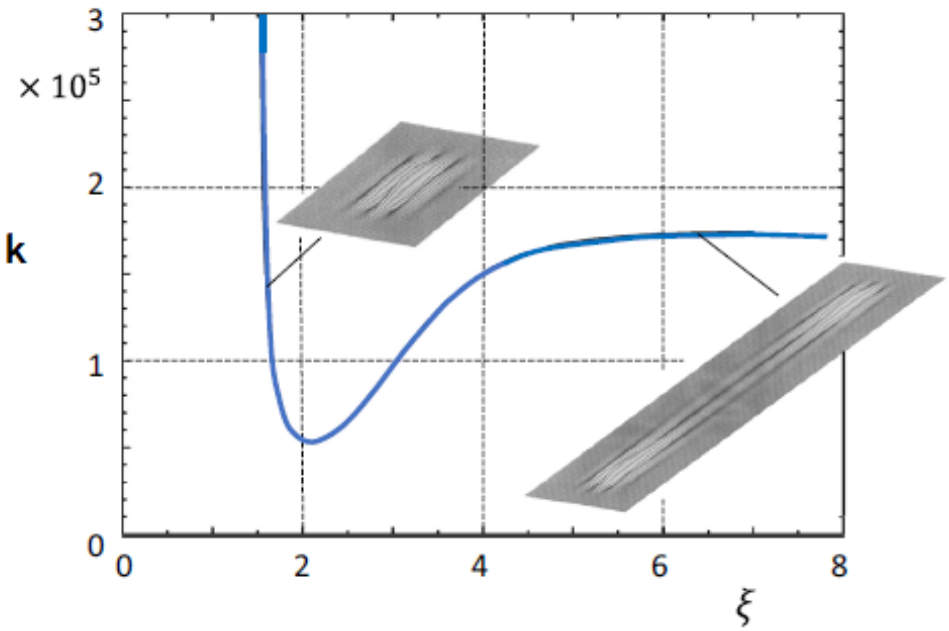

Figure 2.13: Buckling coefficient for a plate under tensile loads and with clamped edges as a function of aspect ratio ζ=L/B. [22]

The critical stress responsible for buckling in plates subjected to tensile loads can be calculated using the following equation.

$$\sigma_{cr} = k_c E\left(\frac{t}{B}\right)^2 \tag{2.33}$$

Where,
σ_{cr}: Critical wrinkling stress
E: Young's modulus
t: thickness of the plate
L: plate length
B: plate width
ζ: aspect ratio (L/B)
$k_c(\zeta)$: Buckling coefficient.

3

Methods

The process of laminating the three foils together includes the effects of different parameters. The controllable parameters that are to be studied in this project are web force, temperatures of zones along the process, and the web speed. Web force is the force acting directly on any layer and is important to keep the layer stable during the process, temperatures of the zones are important to harden the glue that joins the layer, but they have a negative effect on the dimensional stability of the ETFE layers which have high coefficient of thermal expansion, web speed has an effect on the heating rate of the foil during the process since the time spent in each zone under any given temperature will depend on this parameter.

To study the effects of these parameters, the strategy will be to develop two models. The first model will simulate how the foil is heating during the process including the effects of web speed and zone temperatures using ANSYS program. The second model will aim at understanding how the temperature is influencing the stresses in the foil along the process.

3.1. Thermal model of the process

3.1.1. Aim of modeling the process of production

Performing experiments in industry is usually very expensive and should be planned beforehand. The encapsulation foil is made in a R2R machine which produces some effects that are hard to be simulated in the lab. If a computer model is to be made to simulate the effects of this process, making calculated guesses about the effect of changing some variables should become easier, which makes the development of the product less expensive and limits the factors that need to be changed in real life experiments. The process will be modelled using ANSYS program's transient thermal package and the wanted output is the temperature of each point of the foil at a certain moment along the process.

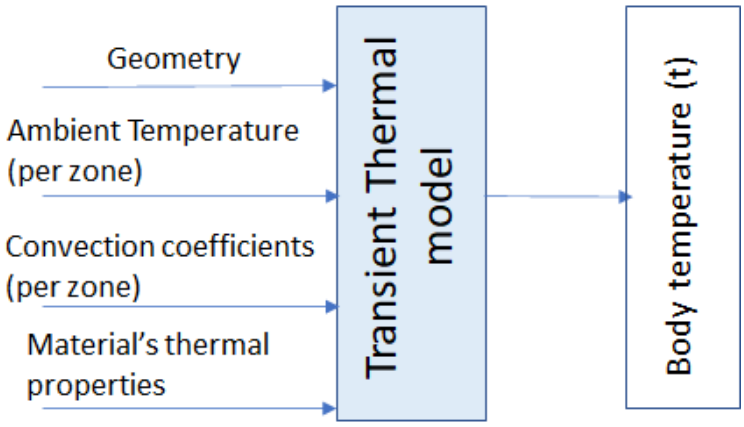

Figure 3.1: Scheme of the inputs and outputs of the thermal model

Varying temperatures will change the dimensions and the properties of ETFE drastically.[32].

The foil passes through different temperature zones in the machine, these different temperature zones lead to constant heat transfer from the air to the foil heating the foil up. As the temperature of the foil raises, the dimensions of ETFE foils and Glass fiber will also change as well as the viscosity of the glue. The interaction between all of these changes is complex and is suggested to be the reason of the defects that are happening in the end product.

3.1.2. Geometry

The geometry used in the simulation has a surface area of 10cm x 10cm and consists of five layers as shown in Figure 3.2a . Heat transfer in the foil will happen mainly in one dimension along the y-axis, no heat transfer happens along the x-axis as the temperature is homogeneous, and the temperature differences in z-axis are relatively small due to heating the foil gradually.

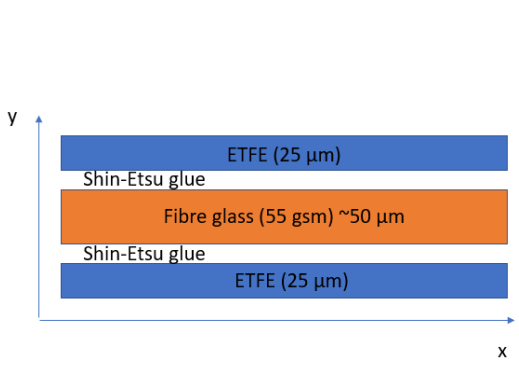

(a) Cross section of the geometry along TD

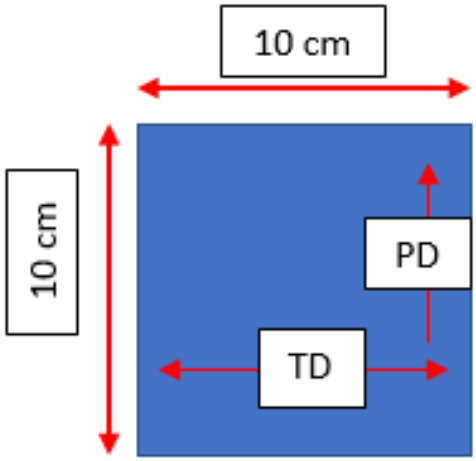

(b) Top view of the geometry

Figure 3.2: The geometry used to simulate the heating of the top encapsulation foil during the process

3.1.3. Model inputs

Material properties

Three materials will be involved in the modeling process, ETFE plastic foil, Shin-Etsu silicon glue, and non-woven Fibre glass fabric. For the purpose of this model, physical and thermal properties of the materials will be used. Table 3.1 summarizes material properties. The properties are taken from specification sheets provided by suppliers.

Property	Material		
	ETFE	Shin-Etsu silicon glue	Glass fibre
Density [g/cm^3]	1,7	1.05 (@25°C)	1.09
Thermal conductivity (k) [W/m.K]	0,238	0.2	0.04
Specific heat(c_p) [$J/kg^\circ C$]	2000	1000	887

Table 3.1: Physical and thermal properties used in the model

Ambient temperatures calculation
Steady heat loss is present during the process, this implies that the ambient temperature that heats the foils up is always lower than the set temperatures of the heaters. However, the air temperature at any given point is stable. Using four sets of thermocouples, the ambient temperature is measured at different points along the process and a correlation between the set temperatures and ambient temperatures is given in Figure 3.3.

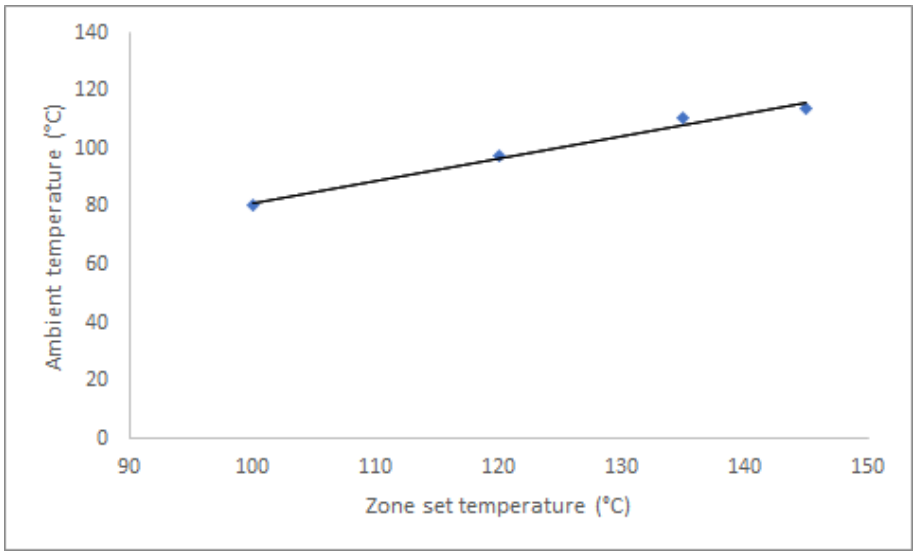

Figure 3.3: Correlation between set temperatures and ambient temperatures

This correlation is used to determine the ambient temperature corresponding to any set temperature. The equation obtained from the correlation is T_a=0,7657 T_{set} + 4,9935, the correlation has a value of $R^2 = 0,98$.

Calculating convection coefficients of the zones
Convection coefficients determine the speed of heating a body under certain circumstances. To find this rate in each zone along the process, Nusselt number (Nu) for each zone has been calculated as earlier explained in Section 2.1.3.

After Nu_{total} has been calculated for both sides, $\overline{h}$ can be calculated using the following equation.

$$\overline{h} = \frac{Nu.k}{L_c} \tag{3.1}$$

Air properties needed to perform the calculations as density (ρ), thermal conductivity (k), dynamic viscosity (μ), and Prandtl number (Pr) were taken from the table provided in Appendix A.

The characteristic length for a flat plate is defined as the area of the plate divided by its perimeter as shown in equation 3.2. The dimensions of the foil at each zone is the width of the foil multiplied by the

length of the specific zone. the film temperature (T_f) is taken as the film temperature of two consequent zones, this implies that the average temperature of the foil is equal to the temperature of the previous zone which might not be accurate. However, film temperature (T_f) is used to evaluate the average properties of the fluid in certain circumstances and this will not affect the results much, at least if the fluid is air.

$$L_c = \frac{A_s}{p} = \frac{L_z W}{2(L_z + W)} \tag{3.2}$$

Where,
A_s: surface area of a plate inside a certain zone.
p: the perimeter of a plate inside a certain zone.
L_z: the length of the zone.
W: width of the foil.

Tables with the calculations of the convection coefficients of the zones will be provided in Appendix B.

3.1.4. Methods of calculation

The thermal transient analysis package of ANSYS, the effect of changing boundary conditions through the process can be simulated. Ansys uses finite element method (FEM) to calculate the temperature at each point of the model using the following general equation.

$$k\left(\frac{\partial^2 T}{\partial x^2} + \frac{\partial^2 T}{\partial y^2} + \frac{\partial^2 T}{\partial z^2}\right) + q = \rho c_p \frac{\partial T}{\partial t} \tag{3.3}$$

Where,
k: conduction coefficient.
T: Temperature.
q: convective heat transfer.
ρ: density of the material.
c_p: Specific heat.
t: time.

The first term of the equation is to calculate the conduction in three dimensions, the equation for heat transfer in one dimension has been explained earlier in Section 2.1.1, the second term (q) represents the convective heat transfer which was explained in Section 2.1.2. The last term is related to the ability of the material to store energy.

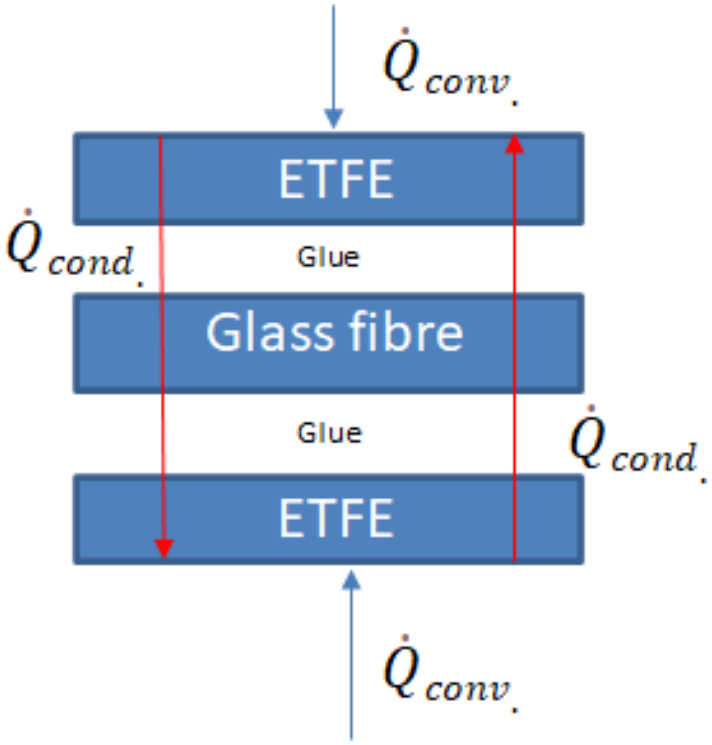

Figure 3.4: Demonstration of different heating mechanisms happening

3.1.5. Model output

Providing the input parameters i.e. geometry, material properties, zone ambient temperatures and the convection coefficients to Ansys mechanical (Transient thermal), the model will solve the heat transfer equations for each node and provide a temperature profile of all layers. As this study is interested only in the bottom ETFE layer, only the temperatures of this layer are obtained. The temperature profile is simply the average temperature of the foil along the process (between Z1 and Z6). An example of the temperature profile is given in Figure 3.5. The figure shows the temperature of the foil along the process compared with the ambient temperatures and the zone set temperatures in each zone.

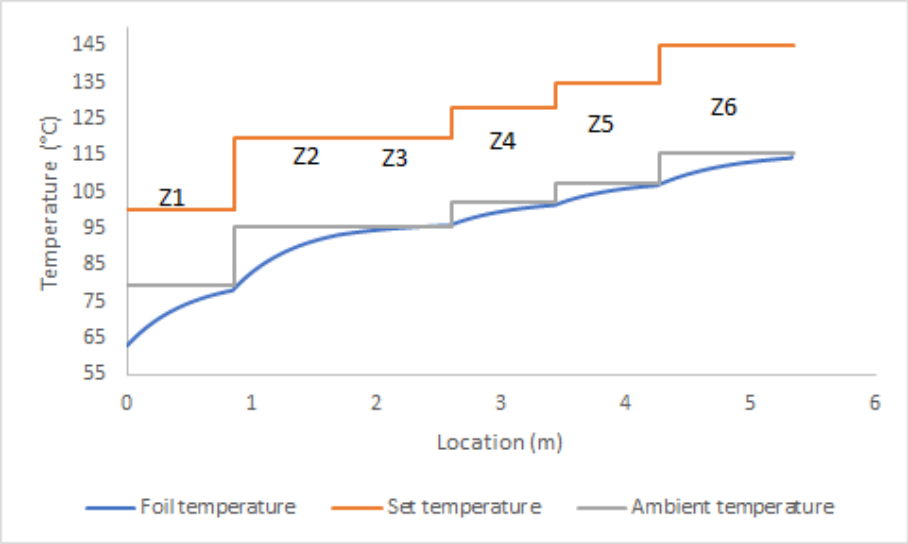

Figure 3.5: Example of the output of the thermal model

3.1.6. Model verification

A simple and effective approach has been used to verify the thermal model. Using old measurements of the foil performed with thermocouples touching the foil, the measurements were performed with different process parameters than the ones the model was designed for. A summary of the parameters of the simulated process is given in Table 3.2.

Zone number	Z1	Z2	Z3	Z4	Z5	Z6
Set temperature ($^{\circ}C$)	90	110	130	140	140	140
Ambient temperature ($^{\circ}C$)	73.9	89.2	104.5	112.2	112.2	112.2
Length (cm)	100	100	100	100	100	100
Velocity (cm/min)	100	100	100	100	100	100
Time (s)	60	60	60	60	60	60

Table 3.2: Process and machine parameters used for the experimental measurements and for model verification

Zone ambient temperatures and convection coefficients were inserted in ANSYS software as model inputs. These are summarized in the following figure. It is important to note that the foil enters the machine at room temperature.

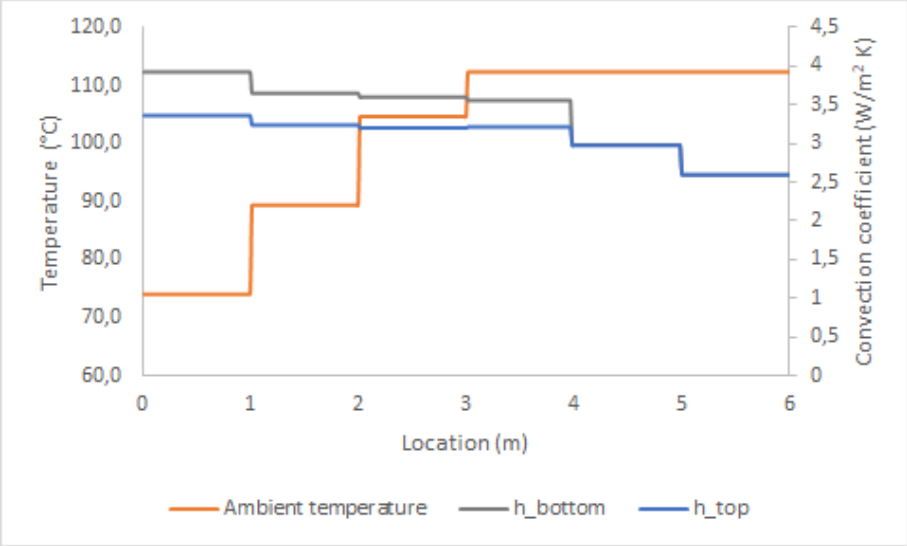

Figure 3.6: Model input parameters for the verification run

An overlap between the results of the simulation and the earlier performed experimental measurements can be seen as we plotted them against each other. Later in the process, the experimental measurements give slightly higher results, this is a result of the temperature generated by the exothermic reaction of glue curing which is not taken into account in the model.

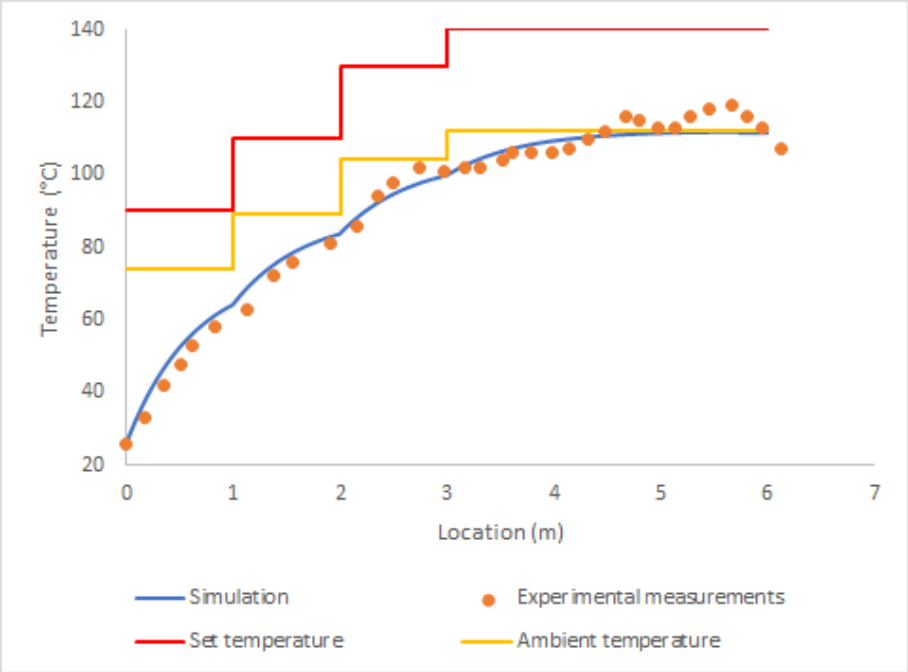

Figure 3.7: Model input parameters for the verification run

3.2. Mechanical model of the process

3.2.1. Aim of the model

As discussed earlier, the aim of this project is to determine the effect of process parameters (i.e. process temperatures, web speed, web force) on wrinkling formation and understand which process parameters can be causing the defect. Then, the optimal process parameters that will eliminate wrinkling are to be found.

As the temperature of the bottom ETFE foil (where wrinkling is happening mostly) can be known along the whole process from the results of the thermal model of the process, the mechanical effects combined with thermal effects can be simulated to determine the stresses along the process, these stresses should be compared to a wrinkling criteria in order to understand how every parameter can influence wrinkling in a positive or a negative way. The model will consider a situation where different forces are acting on each of the three solid layers of the encapsulation foil, focusing only the bottom layer where wrinkling is happening. The effect of other layers will be taken into account as boundary conditions.

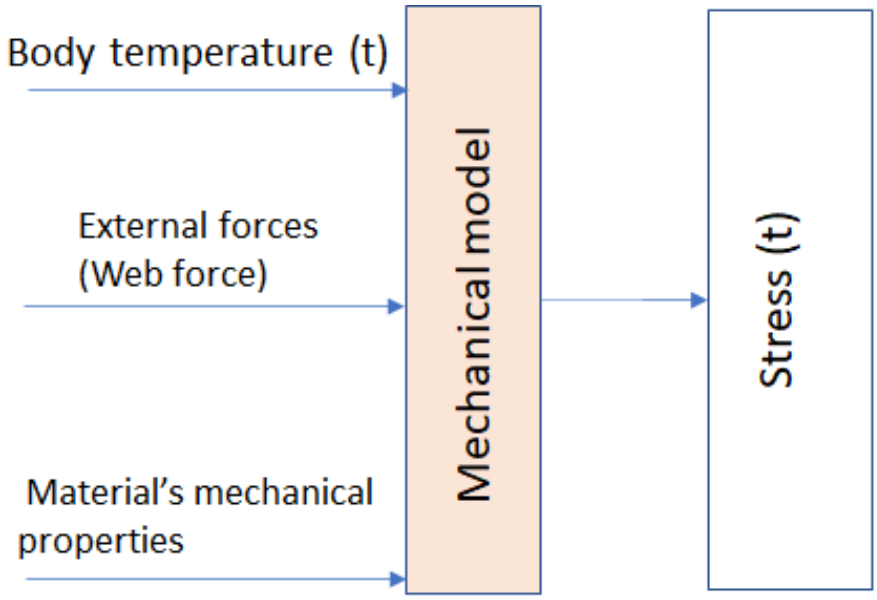

Figure 3.8: Scheme of the inputs and outputs of the thermal model.

3.2.2. Model Inputs

Three material properties are needed to perform the calculations for the mechanical model.
1. Young's modulus: Young's modulus in ETFE as in other polymers, depends to a large extent on temperature. In [7], the values of young's modulus under different temperatures have been measured. Figure 3.8 shows that young's modulus decreases with temperature until the temperature reaches 90 °C, which is the glass transition temperature of ETFE, before it stabilizes at around 0,05 GPa.

2. Coefficient of thermal expansion: The value of the coefficient of thermal expansion of ETFE has been taken from the material's property sheet [2] to be $9{\times}10^{-}5\ K^{-}1$.

3. Geometry: Thickness, width and length of each element are the important geometry parameters in this model. While thickness and width are constants, length of the element will be determined by the web speed (u) as it was defined as the distance covered by the foil in one second. The width of the foil is 0.4 m and the two thicknesses are present 25 μm and 50 μm.

4. Critical stress: Critical stress has been calculated using the following equation discussed in 2.4.3

$$\sigma_{cr} = k_c E\left(\frac{t}{B}\right)^2 \tag{3.4}$$

E is Young's modulus, t is thickness of the foil, B is the width of the foil. k_c is the buckling coefficient and is taken to be the value at large aspect ratios $\zeta > 8$ (k_c=1.8×$10^{-}5$).

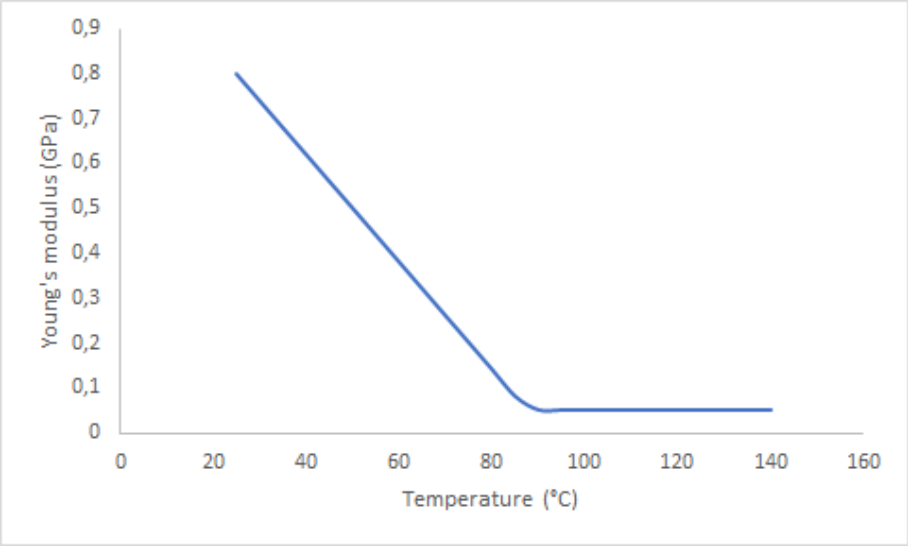

Figure 3.9: Young's modulus of ETFE under different temperatures.

3.2.3. Model description and boundary conditions

The model considers only one layer, the bottom ETFE foil, Glass fiber with its coefficient of thermal expansion in the range of 5.4×$10^{-}6cm/cm°C$ [30], 16 times smaller than ETFE, is considered to apply as two fixed supports at both sides of the foil as shown in 3.11 because the thermal expansion of glass fibres is very small compared to ETFE, therefore, ETFE will expand much more and glass fiber can be assumed as a rigid material. Fixed supports are also assumed to constrain the movement of the foil at the short edges in the transverse direction.

Every second the element will cover a distance (L) which is taken as the length of the element, so (L) will depend on the web speed (u). The stress is calculated for this element as shown in 3.5. taking the temperature difference with the previous position, Young's modulus under the new temperature into account, the effective stress can be calculated for each point of the process. The effective stress is the superposition of the mechanical stress applied by force and the stress release due to temperature differences along the process and thus, thermal expansion of the foil.

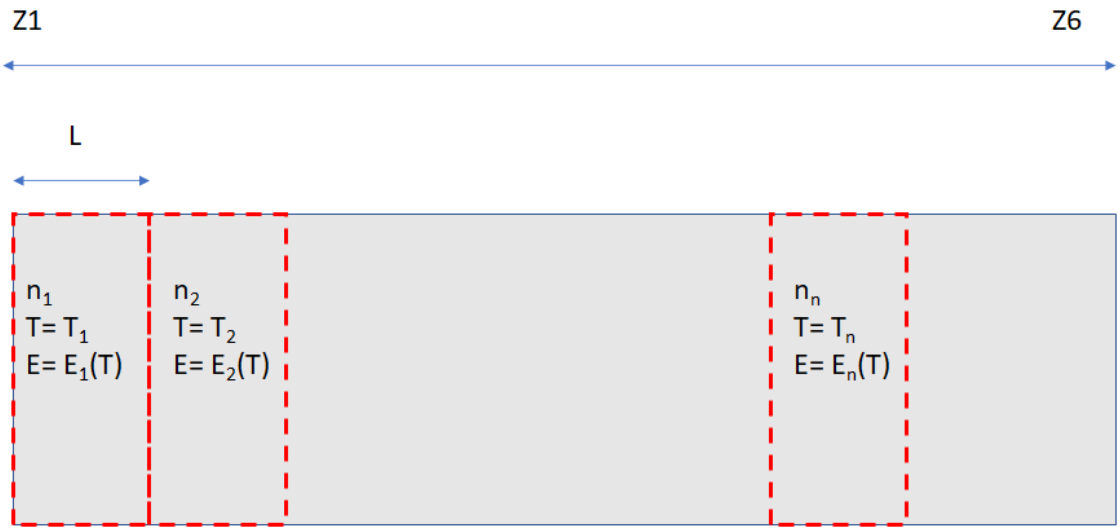

Figure 3.10: Demonstration of the boundary conditions applied on the foil along the process

The model assumes a pre-stretched foil between two fixed supports with a stress $\sigma = \frac{F}{A}$. As temperatures increase, the applied stress will start to decrease since higher temperatures lead to expansion in the foil. The behaviour of the foil will depend on the amount of stress release caused by the temperature change, if this is larger than the initially applied stress due to the web force, then compressive stresses will develop. What will happen afterwards will depend on the material and its geometry, whether it can carry this load or will buckle and delaminate as will be explained later.

$$\sigma_{Eff}(t) = E(t)\left(\frac{F}{AE(t)} - \alpha\Delta T\right) \tag{3.5}$$

Where,
$\sigma_{Eff}(t)$: Effective stress in the foil.
E: Young's modulus.
F: Applied force.
A: Cross section ($Width \times thickness$).
α: Coefficient of thermal expansion. $\Delta T = T_n - T_0$.

ΔT here is different from the case shown in Section 2.3, the main difference between the two cases is the applied force. Here, the force is not applied constantly, so the foil is stretched with a force one time and heated as shown in Figure 3.11.

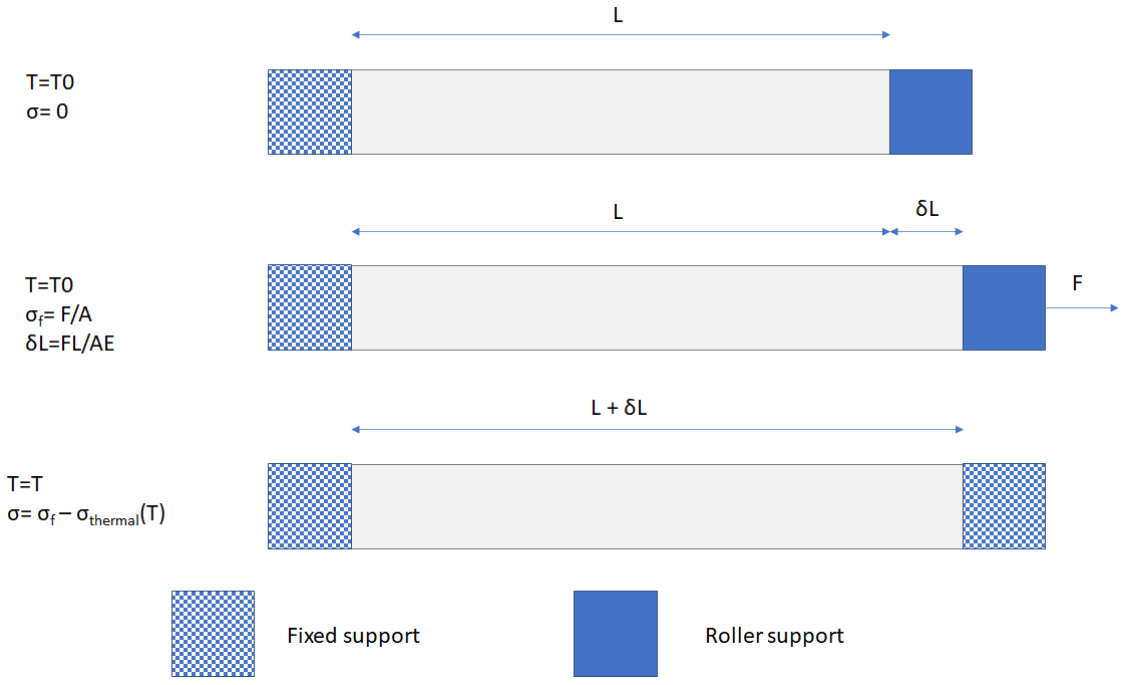

Figure 3.11: Demonstration of the boundary conditions applied on the foil along the process

These boundary conditions were assumed for the model as a result of analyzing the situation between Z1 and Z6 during the process. As shown in Figure 3.12, on one side the bottom foil will be constrained by the hardened glue in all directions near Z6, on the other side the high pressure caused by the two rollers of the mangle section will exert a similar boundary condition constraining its movement in all directions. As both ends of the foil are constrained and each element is expanding, thermal expansion of any element will be constrained by the thermal expansion of the neighbouring elements, therefore, the fixed ends boundary condition applies to all elements.

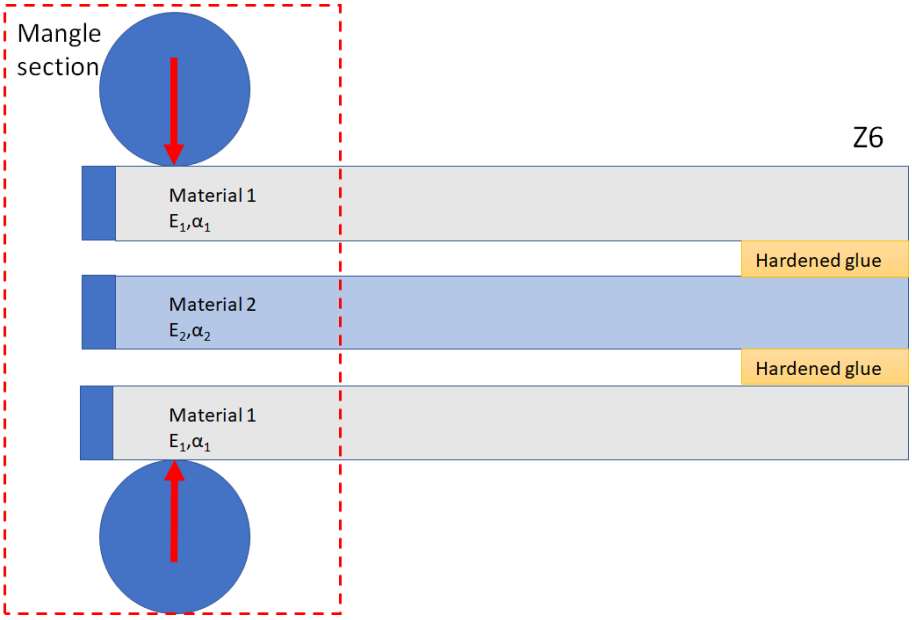

Figure 3.12: Demonstration of the two constrained sides of the foil in the machine

The results generated by this model are given in Appendix D

3.2.4. Wrinkling and delamination

In the figure below, an example of the generated results is given. Any stress above the critical stress will cause wrinkling in the foil. However, in web forces that do not exceed it, the effect of thermal expansion will be very high that it will generate compressive stresses as at web force of 1 N. These compressive stresses will cause the foil to hang down and delamination will occur. Presence of the glue might prevent this, however the effects of the glue are not taken into account in this model.

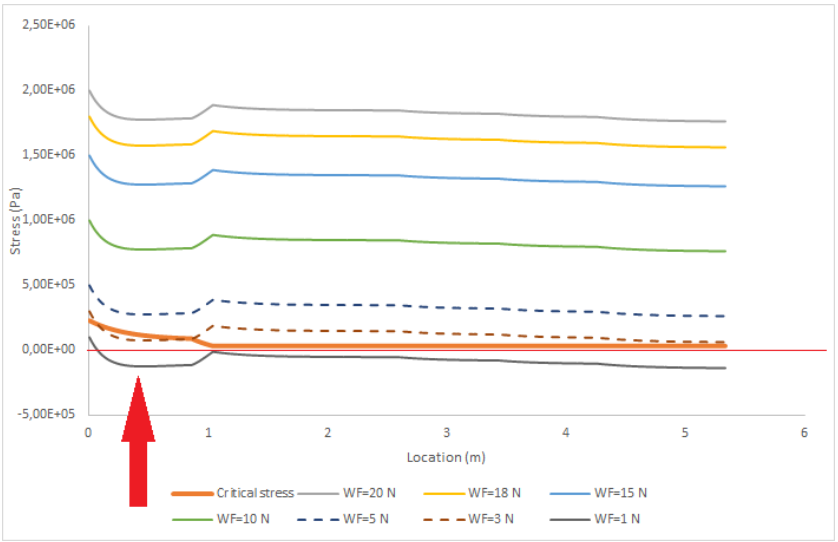

Figure 3.13: An example of the results showing negative stresses in 25 μm foil under web speed of 0.3 m/min

When temperatures rise the foil begins to expand. If tensile preload is present, the stress will be reduced. However, if the stress reduction due to higher temperature exceeds the preload compressive stresses start to form. A thin material as an ETFE foil will not be able to carry these stresses, thus, it delaminates as shown in Figure 3.14. The reason delamination will happen is the inability of a thin

plastic foil to carry compressive loads. If the foil of much thicker or made of another material as metal, delamination will need higher compressive stresses to happen.

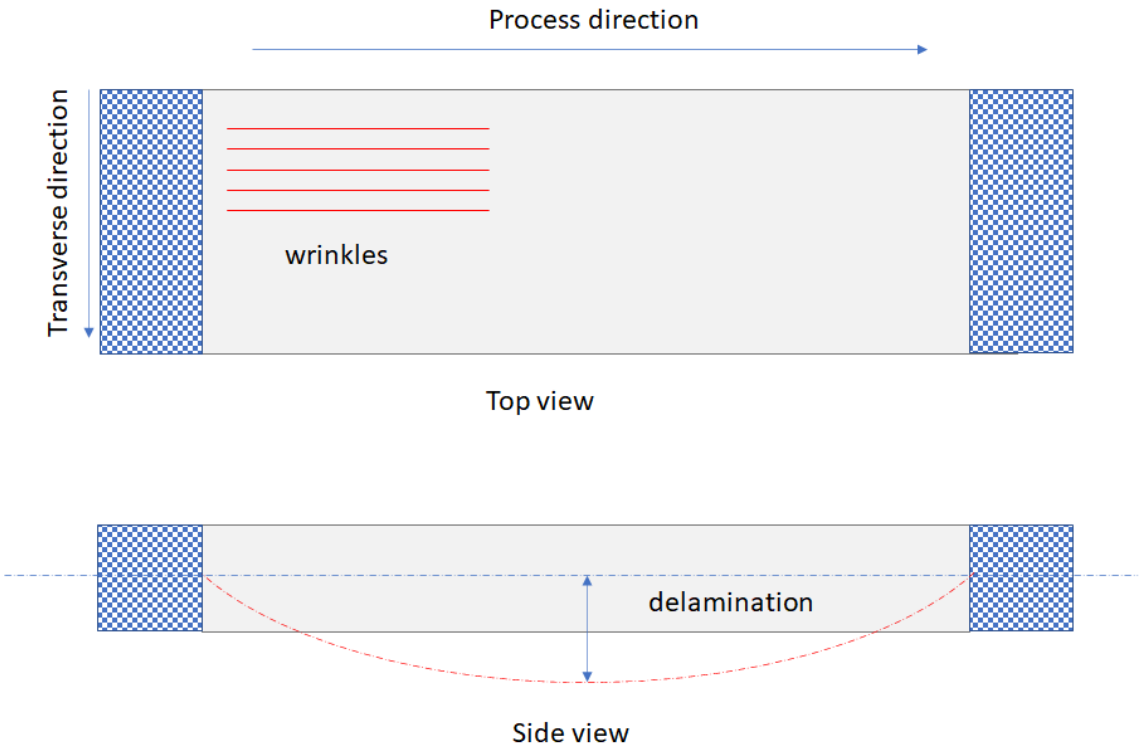

Figure 3.14

The difference between wrinkling and delamination is shown in the figure above. Wrinkling happens due to web stresses exceeding the critical limit for wrinkling along the process direction, while delamination will happen as a result of excessive thermal expansion along the transverse direction in this case. Te risk of delamination has been assessed based on the magnitude of compressive stress. A criteria of the assessment is given in the table below. The reason of the differences between 25 μm and 50 μm thicknesses is the stiffness of the two foils, the thicker a foil is the more stiffness it has and thus, the less it is likely to buckle and delaminate.

	Stress (Pa)		
Foil thickness	**<**-1×10^5	$-1 \times 10^{-}5$ **- 0**	**>0**
25 μm	High risk of delamination	Risk of delamination	No risk of delamination
50 μm	No need to use web forces that generate these stresses	Low risk of delamination	No risk of delamination

Table 3.3: Risk assessment of delamination in the foil

4

Results and discussion

4.1. The effect of web force

Applied web force has a direct influence on wrinkling as it increases the stress in the foil. A higher web force will directly cause an increase in the stress of the web. However, this effect will be decreased by the thermal expansion caused by temperature changes. As seen from the equation below, for the same force only the temperature will change the value of the effective stress. Therefore, all model calculations were made for seven different web forces and the effective stress has been compared to the critical stress for wrinkling.

$$\sigma_{Eff}(t) = E(t)\left(\frac{F}{AE(t)} - \alpha\Delta T\right) \tag{4.1}$$

4.2. The effect of web speed (WS)

Changing web speed during the process will cause a change in the heating rate of the foil. The higher the speed, the less steep the temperature profile will be. This will mean slower heating and smoother temperature changes.

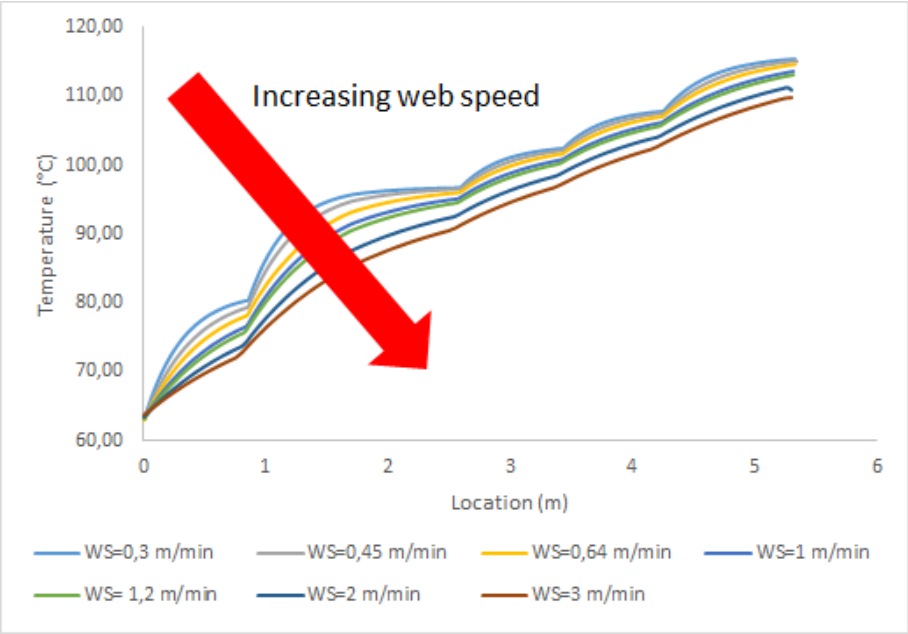

Figure 4.1: The effect of changing web speed on the temperature profile

The results of the mechanical model are given in Appendix D, a summary of these results with assessing the risk of delamination due to compressive stresses is presented in Figure 4.2 and Figure 4.3. The logic of risk assessment has been explained in Section 3.2.4

As Figure 4.2 and Figure 4.3 show, web speed has a minor to no effect on the web force operating range needed to avoid wrinkle formation. The reason web speed has such a small effect on avoiding wrinkling is operating under high temperatures, under all web speeds 90 °C where the critical stress reaches its lower value is reached in the first two meters. Therefore, the critical stress will be the same for all web speeds after the foil reaches 90 °C. It is also clear that the operating range of 50 μm foil is larger and the risk of delamination is lower than that of 25 μm

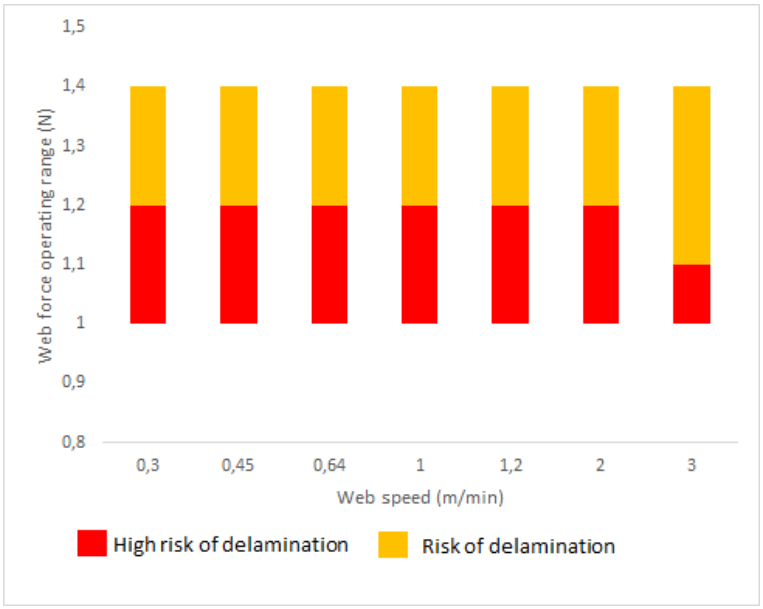

Figure 4.2: Operating range for 25 μ m wrinkle free ETFE foil and risks of delamination under different web speeds

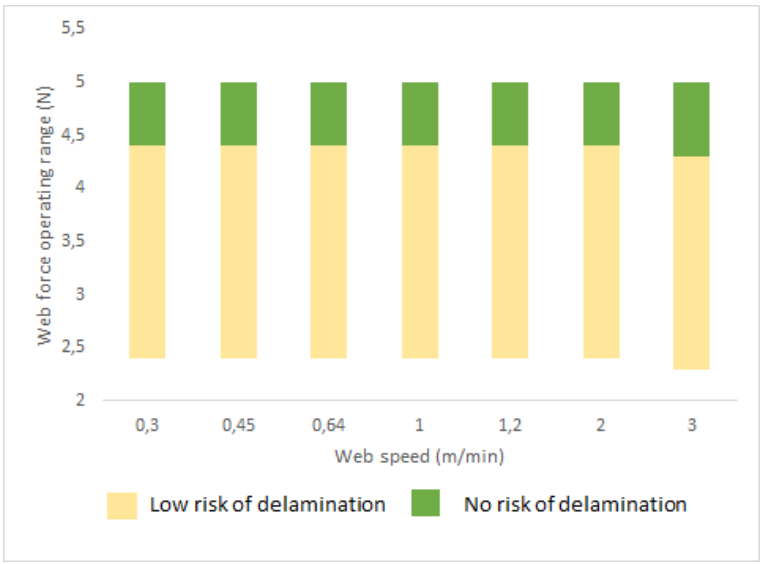

Figure 4.3: Operating range for 50 μ m wrinkle free ETFE foil and risks of delamination under different web speeds

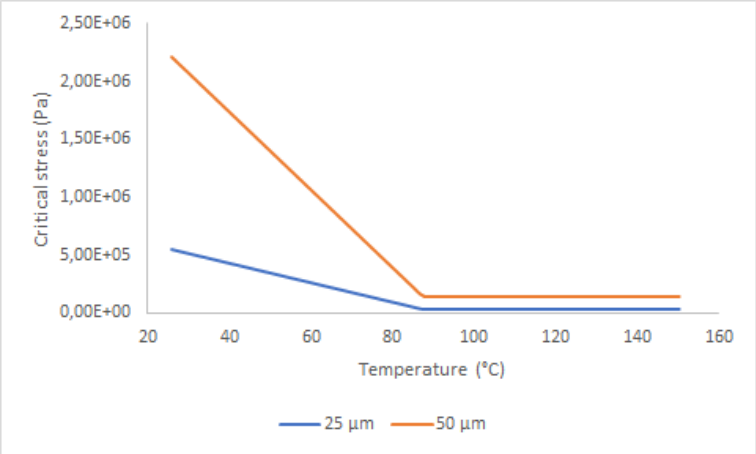

Figure 4.4: The effect of temperature on the critical wrinkling stresses in ETFE foils with different thicknesses

4.3. The effect of different zone temperatures

Five scenarios were simulated for 25 μm foil to understand the effect of different combinations of zone temperatures, web speed was varied between two values (0.64 m/min and 1.2 m/min). The results of the scenarios are to be compared to each other and with baseline settings.

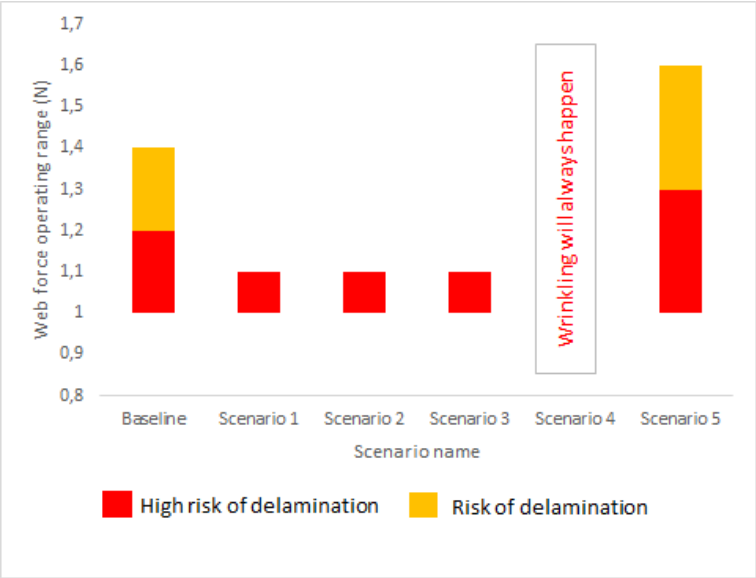

Figure 4.5: Comparison between operating web force ranges in different scenarios

From scenarios 1 and 3, it is again clear that web speed does not have a big influence on stresses. The effect of high temperatures at Z8 and Z1 is seen in scenario 4 as critical stress decreases to the lowest level quickly and wrinkling happens even at the smallest web forces. On the other side, lowering the temperatures of Z1 and Z2 by 10 °C leads to a stress profile that causes a stress profile similar to the one generated by baseline settings with higher critical stress covering longer distance along the process. From these insights it is possible see three trends. First, high temperatures are always not recommended as they reduce the critical stress for wrinkling in and increase the risk of delamination of the foil. Second, increasing the temperatures at Z8 and Z1 by 10 °C will lead to low critical stress and wrinkle formation early in the process. Third, lowering the temperatures of Z1 and Z2 leads to a higher operating range.

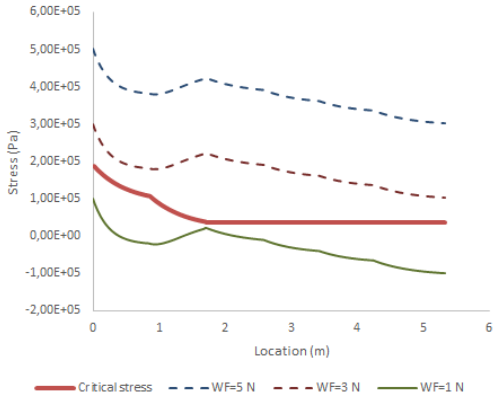

WS	Z8	Z1	Z2	Z3	Z4	Z5	Z6
m/min	deg C	deg C	deg C	deg C	deg C	deg C	deg C
0,64	85	100	110	120	128	135	145

(a) Scenario 1 settings

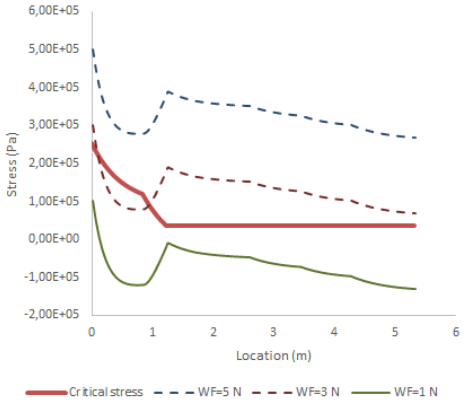

WS	Z8	Z1	Z2	Z3	Z4	Z5	Z6
m/min	degC	degC	degC	degC	degC	degC	degC
0,64	75	100	120	120	128	135	145

(b) Baseline settings

Figure 4.6: Comparison between stresses in the foil under scenario 1 settings and baseline settings. WS is web speed, WF is web force.

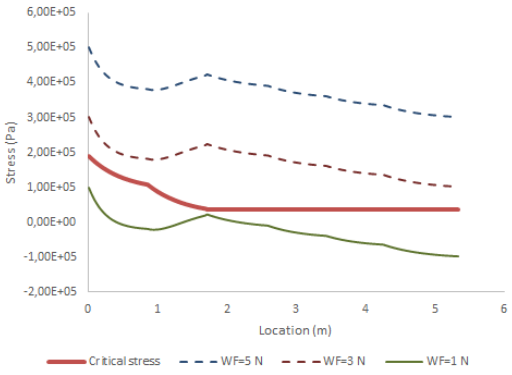

WS	Z8	Z1	Z2	Z3	Z4	Z5	Z6
m/min	degC	degC	degC	degC	degC	degC	degC
0,64	85	100	120	130	140	150	150

(a) Scenario 2 settings

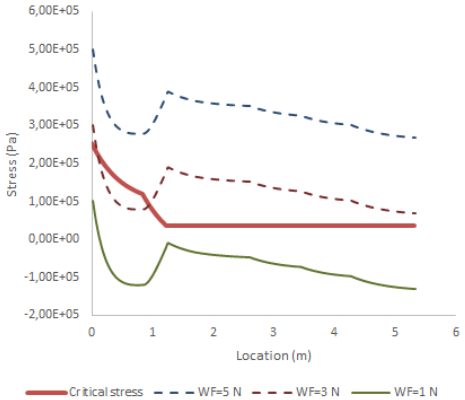

WS	Z8	Z1	Z2	Z3	Z4	Z5	Z6
m/min	degC	degC	degC	degC	degC	degC	degC
0,64	75	100	120	120	128	135	145

(b) Baseline settings

Figure 4.7: Comparison between stresses in the foil under scenario 2 settings and baseline settings. WS is web speed, WF is web force.

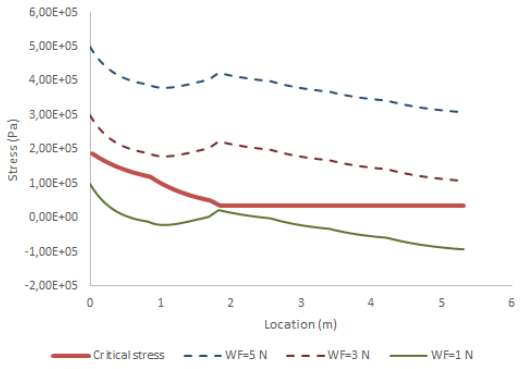

WS	Z8	Z1	Z2	Z3	Z4	Z5	Z6
m/min	degC	degC	degC	degC	degC	degC	degC
1,2	85	100	110	120	128	135	145

(a) Scenario 3 settings

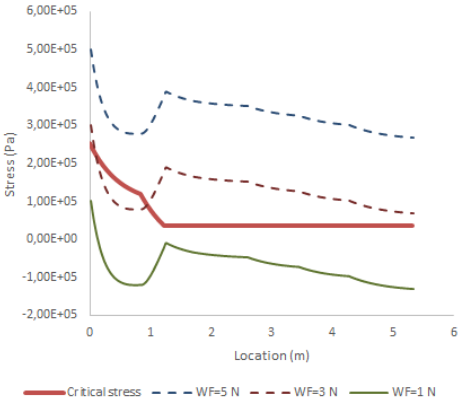

WS	Z8	Z1	Z2	Z3	Z4	Z5	Z6
m/min	degC	degC	degC	degC	degC	degC	degC
0,64	75	100	120	120	128	135	145

(b) Baseline settings

Figure 4.8: Comparison between stresses in the foil under scenario 3 settings and baseline settings. WS is web speed, WF is web force.

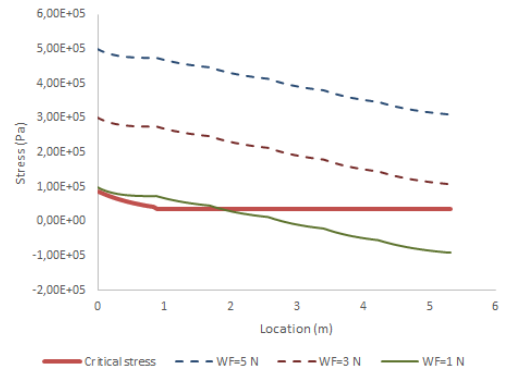

WS	Z8	Z1	Z2	Z3	Z4	Z5	Z6
m/min	degC	degC	degC	degC	degC	degC	degC
1,2	100	110	120	130	140	150	160

(a) Scenario 4 settings

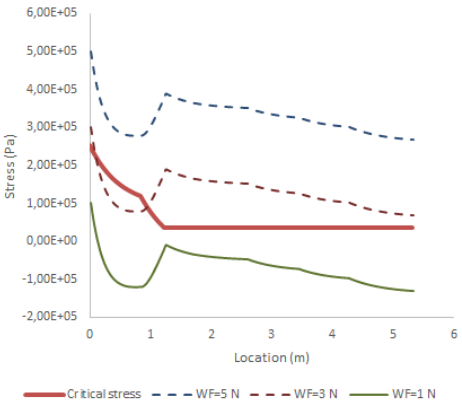

WS	Z8	Z1	Z2	Z3	Z4	Z5	Z6
m/min	degC	degC	degC	degC	degC	degC	degC
0,64	75	100	120	120	128	135	145

(b) Baseline settings

Figure 4.9: Comparison between stresses in the foil under scenario 4 settings and baseline settings. WS is web speed, WF is web force.

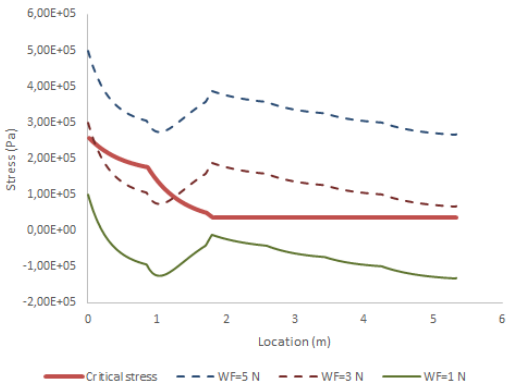

WS	Z8	Z1	Z2	Z3	Z4	Z5	Z6
m/min	degC	degC	degC	degC	degC	degC	degC
0,64	75	90	110	120	128	135	145

(a) Scenario 5 settings

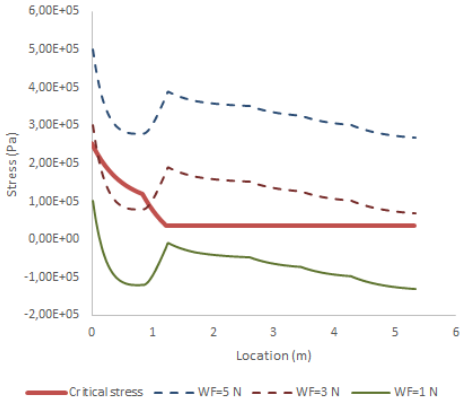

WS	Z8	Z1	Z2	Z3	Z4	Z5	Z6
m/min	degC	degC	degC	degC	degC	degC	degC
0,64	75	100	120	120	128	135	145

(b) Baseline settings

Figure 4.10: Comparison between stresses in the foil under scenario 5 settings and baseline settings. WS is web speed, WF is web force.

4.4. Critical reflecting on the model and the results

The ultimate goal of this study was to understand the effect of three process parameters (web force, web speed ,and zone temperatures) on wrinkling in the 25 μm ETFE foil and define the optimal parameters to a top encapsulation foil using 25 μm ETFE foil, using 25 μm ETFE foil is important to reduce the cost of top encapsulation foil. The first step was to define the temperatures of the foil along the process as temperature is playing a big role in changing the material's properties as Young's modulus (E), the stresses in the layers and determining the critical point at which the foil starts to wrinkle. The model has been successfully verified using older temperature measurements of the ETFE foil. Simulation values fitted the experimental measurements with a high accuracy, therefore, the model has been assumed valid to use for the next steps. Next, a model that calculates the stresses in the foil has been developed. To simplify the model, only the layer of interest has been simulated, the effects of the other layers were given as a boundary condition or were included in the process of discussing results. Glass fibre layer, for example, has been thought to apply two fixed supports at the beginning and end of the foil, this assumption has not been verified, but thought to be accurate enough to proceed with the modeling process. Another limitation of the model is the assumption that the environment is assumed to be perfect, for example all other causes of wrinkling discussed earlier in Section1.5.1 except temperature variations are not included in the model and temperatures are considered to be homogeneous around the foil. The effect of the glue that connects the ETFE foil to the core fiber glass layer and can play a role in stabilizing the foil has not been extensively included in the model as its effect is assumed to be small. Therefore, the model is considered to be a step into making the development of an encapsulation foil with thinner ETFE foils, but it can be developed further to include the other effects involved in the process and make the results more accurate. Finally, it is important to highlight the importance of having such a model in decreasing the costs of developing the top encapsulation foil further as it can give an indication to the parameters that are not worth testing. This for sure does not reduce the importance of testing the system in real life as many unpredicted parameters that are not included in the model may play a role.

5

Conclusions and Recommendations

In this section, the conclusions that have been reached will be presented with recommendations to improve the model on which this study is based and recommendations to go further with developing a thinner encapsulation foil for thin-film solar cells.

Conclusions:

- The process of making top encapsulation foils with 25 μm ETFE foils is a process that needs fine control and very strict tolerances of the process parameters as the process should be performed under narrow borders. Under temperatures higher than 90 °C a force slightly higher than 1.4 N will be enough to cause wrinkles in the foil, however, if the force is slightly lower the chance of having a delaminated foil is large.
- This study provides a thermal model of the machine that is fully developed and another mechanical model open for development. These two models provide a quick tool to predict the effect of different changes in the process or in the materials.
- At temperatures higher than 90 °C for ETFE, web speed plays a minor role in avoiding wrinkle formation as the critical stress for wrinkle formation reaches its lowest levels as shown in Figure 4.4.
- Hardware changes in the machine are needed to achieve web forces between (1-3 N).
- Decreasing the temperatures of Z1 and Z2 by 10 °C, is shown to increase the range of the web force that can be applied.

Recommendations for developing the model:

- The model does not explain the role of glue in holding the ETFE foil and preventing out-of-plane deformations as wrinkling.Knowing the behaviour of the used glue and knowing the optimal viscosity levels needed to stabilize the foil can expand the web force operating range to reach higher levels.
- The effect of glass fibre layer has not been included in the model. The model assumes the layer to be rigid and not expand with temperature, but glass fiber has a coefficient of thermal expansion of $5.4\times10^{-}6$, 16 times lower than that of ETFE. It is not expected that this will have a big effect on the results of the model. However, including it will help increasing the certainty of the results.

Recommendations for the strategy of developing a thinner encapsulation layer

- Bringing glue to a higher viscosity at the beginning of Z1 is a good solution to stabilize the foils and avoid wrinkling. If glue can hold the ETFE foil and prevent it from an out-of-plane movement wrinkling will not happen.
- Using an alternative to the current glue that cures under lower temperatures as high temperatures are the reason of lowering the critical stress for wrinkle formation.

A

Properties of air at 1 atm pressure

Properties of air at 1 atm pressure

Temp. T, °C	Density ρ, kg/m³	Specific Heat c_p, J/kg·K	Thermal Conductivity k, W/m·K	Thermal Diffusivity α, m²/s	Dynamic Viscosity μ, kg/m·s	Kinematic Viscosity ν, m²/s	Prandtl Number Pr
−150	2.866	983	0.01171	4.158×10^{-6}	8.636×10^{-6}	3.013×10^{-6}	0.7246
−100	2.038	966	0.01582	8.036×10^{-6}	1.189×10^{-5}	5.837×10^{-6}	0.7263
−50	1.582	999	0.01979	1.252×10^{-5}	1.474×10^{-5}	9.319×10^{-6}	0.7440
−40	1.514	1002	0.02057	1.356×10^{-5}	1.527×10^{-5}	1.008×10^{-5}	0.7436
−30	1.451	1004	0.02134	1.465×10^{-5}	1.579×10^{-5}	1.087×10^{-5}	0.7425
−20	1.394	1005	0.02211	1.578×10^{-5}	1.630×10^{-5}	1.169×10^{-5}	0.7408
−10	1.341	1006	0.02288	1.696×10^{-5}	1.680×10^{-5}	1.252×10^{-5}	0.7387
0	1.292	1006	0.02364	1.818×10^{-5}	1.729×10^{-5}	1.338×10^{-5}	0.7362
5	1.269	1006	0.02401	1.880×10^{-5}	1.754×10^{-5}	1.382×10^{-5}	0.7350
10	1.246	1006	0.02439	1.944×10^{-5}	1.778×10^{-5}	1.426×10^{-5}	0.7336
15	1.225	1007	0.02476	2.009×10^{-5}	1.802×10^{-5}	1.470×10^{-5}	0.7323
20	1.204	1007	0.02514	2.074×10^{-5}	1.825×10^{-5}	1.516×10^{-5}	0.7309
25	1.184	1007	0.02551	2.141×10^{-5}	1.849×10^{-5}	1.562×10^{-5}	0.7296
30	1.164	1007	0.02588	2.208×10^{-5}	1.872×10^{-5}	1.608×10^{-5}	0.7282
35	1.145	1007	0.02625	2.277×10^{-5}	1.895×10^{-5}	1.655×10^{-5}	0.7268
40	1.127	1007	0.02662	2.346×10^{-5}	1.918×10^{-5}	1.702×10^{-5}	0.7255
45	1.109	1007	0.02699	2.416×10^{-5}	1.941×10^{-5}	1.750×10^{-5}	0.7241
50	1.092	1007	0.02735	2.487×10^{-5}	1.963×10^{-5}	1.798×10^{-5}	0.7228
60	1.059	1007	0.02808	2.632×10^{-5}	2.008×10^{-5}	1.896×10^{-5}	0.7202
70	1.028	1007	0.02881	2.780×10^{-5}	2.052×10^{-5}	1.995×10^{-5}	0.7177
80	0.9994	1008	0.02953	2.931×10^{-5}	2.096×10^{-5}	2.097×10^{-5}	0.7154
90	0.9718	1008	0.03024	3.086×10^{-5}	2.139×10^{-5}	2.201×10^{-5}	0.7132
100	0.9458	1009	0.03095	3.243×10^{-5}	2.181×10^{-5}	2.306×10^{-5}	0.7111
120	0.8977	1011	0.03235	3.565×10^{-5}	2.264×10^{-5}	2.522×10^{-5}	0.7073
140	0.8542	1013	0.03374	3.898×10^{-5}	2.345×10^{-5}	2.745×10^{-5}	0.7041
160	0.8148	1016	0.03511	4.241×10^{-5}	2.420×10^{-5}	2.975×10^{-5}	0.7014
180	0.7788	1019	0.03646	4.593×10^{-5}	2.504×10^{-5}	3.212×10^{-5}	0.6992
200	0.7459	1023	0.03779	4.954×10^{-5}	2.577×10^{-5}	3.455×10^{-5}	0.6974
250	0.6746	1033	0.04104	5.890×10^{-5}	2.760×10^{-5}	4.091×10^{-5}	0.6946
300	0.6158	1044	0.04418	6.871×10^{-5}	2.934×10^{-5}	4.765×10^{-5}	0.6935
350	0.5664	1056	0.04721	7.892×10^{-5}	3.101×10^{-5}	5.475×10^{-5}	0.6937
400	0.5243	1069	0.05015	8.951×10^{-5}	3.261×10^{-5}	6.219×10^{-5}	0.6948
450	0.4880	1081	0.05298	1.004×10^{-4}	3.415×10^{-5}	6.997×10^{-5}	0.6965
500	0.4565	1093	0.05572	1.117×10^{-4}	3.563×10^{-5}	7.806×10^{-5}	0.6986
600	0.4042	1115	0.06093	1.352×10^{-4}	3.846×10^{-5}	9.515×10^{-5}	0.7037
700	0.3627	1135	0.06581	1.598×10^{-4}	4.111×10^{-5}	1.133×10^{-4}	0.7092
800	0.3289	1153	0.07037	1.855×10^{-4}	4.362×10^{-5}	1.326×10^{-4}	0.7149
900	0.3008	1169	0.07465	2.122×10^{-4}	4.600×10^{-5}	1.529×10^{-4}	0.7206
1000	0.2772	1184	0.07868	2.398×10^{-4}	4.826×10^{-5}	1.741×10^{-4}	0.7260
1500	0.1990	1234	0.09599	3.908×10^{-4}	5.817×10^{-5}	2.922×10^{-4}	0.7478
2000	0.1553	1264	0.11113	5.664×10^{-4}	6.630×10^{-5}	4.270×10^{-4}	0.7539

Note: For ideal gases, the properties c_p, k, μ, and Pr are independent of pressure. The properties ρ, ν, and α at a pressure P (in atm) other than 1 atm are determined by multiplying the values of ρ at the given temperature by P and by dividing ν and α by P.

Source: Data generated from the EES software developed by S. A. Klein and F. L. Alvarado. Original sources: Keenan, Chao, Keyes, Gas Tables, Wiley, 1984; and Thermophysical Properties of Matter. Vol. 3: Thermal Conductivity, Y. S. Touloukian, P. E. Liley, S. C. Saxena, Vol. 11: Viscosity, Y. S. Touloukian, S. C. Saxena, and P. Hestermans, IFI/Plenun, NY, 1970, ISBN 0-306067020-8.

B

Calculations of convection coefficients

This appendix is added to give the details of the calculations of convection coefficients in each zone of the process as explained in Section 3.1.3. The scheme of the simulated zones is given in FigureB.1 and a summary of temperatures and web speeds simulated is given in Table B.1

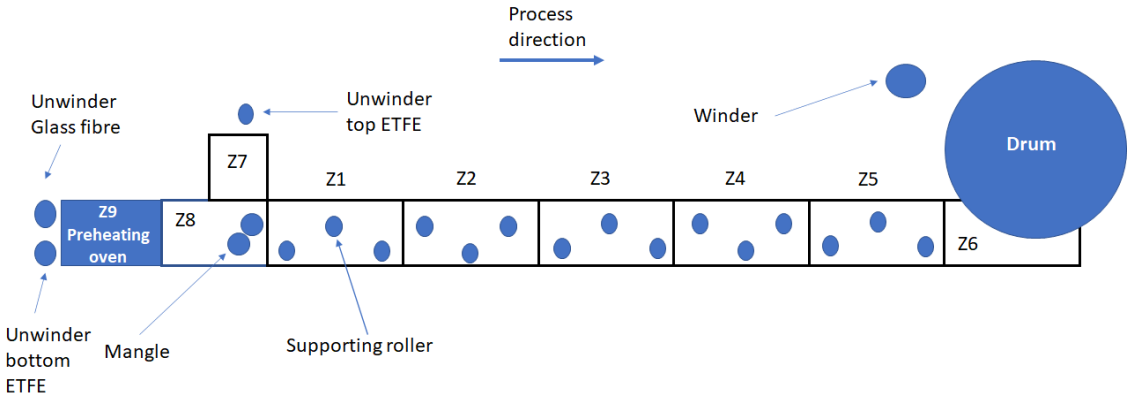

Figure B.1: Scheme of the machine used to produce the top encapsulation foil

Setting	Web Speed m/min	Z9 °C	Z8 °C	Z1 °C	Z2 °C	Z3 °C	Z4 °C	Z5 °C	Z6 °C
Baseline	Variable 0.64 - 3.00	48	75	100	120	120	128	135	145
Scenario 1	0.64	48	85	100	110	120	128	135	145
Scenario 2	0.64	48	85	100	120	130	140	150	150
Scenario 3	1.20	48	85	100	110	120	128	135	145
Scenario 4	1.20	48	100	110	120	130	140	150	160
Scenario 5	0.64	48	75	90	110	120	128	135	145

Table B.1: Summary of the parameters used in simulations

Convection coefficient calculations for web speed of 0.3 m/min and baseline zone temperatures

		Upper surface							
	Unit	**Z9**	**Z8**	**Z1**	**Z2**	**Z3**	**Z4**	**Z5**	**Z6**
h	**[W/m2.K]**	**1.09**	**1.41**	**1.25**	**1.24**	**0.88**	**1.18**	**1.20**	**0.97**
Nu	[-]	4.33E+01	3.91E+01	3.76E+01	3.50E+01	2.57E+01	3.22E+01	3.14E+01	3.31E+01
Nu_N	[-]	1.24E+01	1.13E+01	1.07E+01	9.47E+00	0.00E+00	7.30E+00	6.90E+00	7.90E+00
Nu_F	[-]	3.10E+01	2.79E+01	2.70E+01	2.56E+01	2.57E+01	2.49E+01	2.45E+01	2.52E+01
Ra	[-]	4.39E+06	3.04E+06	2.44E+06	1.51E+06	0.00E+00	5.34E+05	4.28E+05	7.32E+05
Gr	[-]	6.03E+06	4.21E+06	3.40E+06	2.12E+06	0.00E+00	7.51E+05	6.02E+05	1.03E+06
Pr	[-]	0.7282	0.7228	0.7177	0.7132	0.7132	0.7111	0.7102	0.7092
Re	[-]	2.69E+03	2.19E+03	2.06E+03	1.86E+03	1.87E+03	1.77E+03	1.71E+03	1.82E+03
T	[°C]	41.7	62.4	81.6	96.9	96.9	103.0	108.4	116.0
T_f	[C]	33.37355	52.08405	71.99225	89.2205	96.8775	99.9403	105.6831	112.1915
L	[m]	1.03	0.76	0.865	0.855	0.88	0.845	0.82	1.08
A_s	[m2]	0.412	0.304	0.346	0.342	0.352	0.338	0.328	0.432
p	[m]	2.86	2.32	2.53	2.51	2.56	2.49	2.44	2.96
L_c	[m]	0.144056	0.131034	0.136759	0.136255	0.1375	0.135743	0.134426	0.145946
ρ	[kg/m3]	1.164	1.092	1.028	0.9718	0.9718	0.9458	0.933775	0.92175
k	[W/m.K]	0.02588	0.02735	0.02881	0.03024	0.03024	0.03095	0.0313	0.03165
μ	[Pa.s]	1.87E-05	1.96E-05	2.05E-05	2.14E-05	2.14E-05	2.18E-05	2.2E-05	2.22E-05

Table B.2: Calculations for the convection coefficients of the upper surface of the produced foil for web speed of 0.3 m/min and baseline zone temperatures

		Lower surface							
	Unit	**Z9**	**Z8**	**Z1**	**Z2**	**Z3**	**Z4**	**Z5**	**Z6**
h	**[W/m2.K]**	**1.42**	**1.90**	**1.68**	**1.65**	**0.88**	**1.50**	**1.52**	**1.25**
Nu	[-]	5.64E+01	5.28E+01	5.06E+01	4.65E+01	2.57E+01	4.06E+01	3.98E+01	4.27E+01
NuN	[-]	2.54E+01	2.50E+01	2.36E+01	2.09E+01	0.00E+00	1.60E+01	1.53E+01	1.75E+01
NuF	[-]	3.10E+01	2.79E+01	2.70E+01	2.56E+01	2.57E+01	2.47E+01	2.45E+01	2.52E+01
Ra	[-]	3.45E+06	3.20E+06	2.56E+06	1.59E+06	0.00E+00	5.37E+05	4.49E+05	7.65E+05
Gr	[-]	4.74E+06	4.43E+06	3.57E+06	2.22E+06	0.00E+00	7.53E+05	6.30E+05	1.08E+06
Pr	[-]	0.7282	0.7228	0.7177	0.7154	0.7132	0.7132	0.713	0.7092
Re	[-]	2.69E+03	2.19E+03	2.06E+03	1.86E+03	1.87E+03	1.73E+03	1.71E+03	1.82E+03
T	[C]	38.0	59.6	79.6	95.6	95.6	102.0	107.6	115.6
Tf	[C]	31.5086	48.81315	69.60535	87.5986	95.5956	98.7944	104.7922	111.5896
L	[m]	1.03	0.76	0.865	0.855	0.88	0.845	0.82	1.08
As	[m2]	0.412	0.304	0.346	0.342	0.352	0.338	0.328	0.432
p	[m]	2.86	2.32	2.53	2.51	2.56	2.49	2.44	2.96
Lc	[m]	0.144056	0.131034	0.136759	0.136255	0.1375	0.135743	0.134426	0.145946
ρ	[kg/m3]	1.164	1.092	1.028	0.9718	0.9718	0.933775	0.933775	0.92175
k	[W/m.K]	0.02588	0.02735	0.02881	0.03024	0.03024	0.0313	0.0313	0.03165
μ	[Pa.s]	1.87E-05	1.96E-05	2.05E-05	2.14E-05	2.14E-05	2.2E-05	2.2E-05	2.22E-05

Table B.3: Calculations for the convection coefficients of the lower surface of the produced foil for web speed of 0.3 m/min and baseline zone temperatures

Convection coefficient calculations for web speed of 0.45 m/min and baseline zone temperatures

		Upper surface							
	Unit	**Z9**	**Z8**	**Z1**	**Z2**	**Z3**	**Z4**	**Z5**	**Z6**
h	**[W/m2.K]**	**1.26**	**1.63**	**1.45**	**1.44**	**1.08**	**1.38**	**1.41**	**1.14**
Nu	[-]	5.03E+01	4.54E+01	4.37E+01	4.08E+01	3.15E+01	3.78E+01	3.69E+01	3.88E+01
NuN	[-]	1.24E+01	1.13E+01	1.07E+01	9.47E+00	0.00E+00	7.30E+00	6.90E+00	7.90E+00
NuF	[-]	3.79E+01	3.41E+01	3.30E+01	3.13E+01	3.15E+01	3.05E+01	3.00E+01	3.09E+01
Ra	[-]	4.39E+06	3.04E+06	2.44E+06	1.51E+06	0.00E+00	5.34E+05	4.28E+05	7.32E+05
Gr	[-]	6.03E+06	4.21E+06	3.40E+06	2.12E+06	0.00E+00	7.51E+05	6.02E+05	1.03E+06
Pr	[-]	0.7282	0.7228	0.7177	0.7132	0.7132	0.7111	0.7102	0.7092
Re	[-]	4.03E+03	3.28E+03	3.08E+03	2.79E+03	2.81E+03	2.65E+03	2.57E+03	2.72E+03
T	[C]	41.7	62.4	81.6	96.9	96.9	103.0	108.4	116.0
Tf	[C]	33.37355	52.08405	71.99225	89.2205	96.8775	99.9403	105.6831	112.1915
L	[m]	1.03	0.76	0.865	0.855	0.88	0.845	0.82	1.08
As	[m2]	0.412	0.304	0.346	0.342	0.352	0.338	0.328	0.432
p	[m]	2.86	2.32	2.53	2.51	2.56	2.49	2.44	2.96
Lc	[m]	0.144056	0.131034	0.136759	0.136255	0.1375	0.135743	0.134426	0.145946
ρ	[kg/m3]	1.164	1.092	1.028	0.9718	0.9718	0.9458	0.933775	0.92175
k	[W/m.K]	0.02588	0.02735	0.02881	0.03024	0.03024	0.03095	0.0313	0.03165
μ	[Pa.s]	1.87E-05	1.96E-05	2.05E-05	2.14E-05	2.14E-05	2.18E-05	2.2E-05	2.22E-05

Table B.4: Calculations for the convection coefficients of the upper surface of the produced foil for web speed of 0.45 m/min and baseline zone temperatures

		Lower surface							
	Unit	**Z9**	**Z8**	**Z1**	**Z2**	**Z3**	**Z4**	**Z5**	**Z6**
h	**[W/m2.K]**	**1.59**	**2.13**	**1.89**	**1.85**	**1.08**	**1.71**	**1.73**	**1.42**
Nu	[-]	6.34E+01	5.91E+01	5.66E+01	5.23E+01	3.15E+01	4.62E+01	4.53E+01	4.84E+01
NuN	[-]	2.54E+01	2.50E+01	2.36E+01	2.09E+01	0.00E+00	1.60E+01	1.53E+01	1.75E+01
NuF	[-]	3.79E+01	3.41E+01	3.30E+01	3.13E+01	3.15E+01	3.02E+01	3.00E+01	3.09E+01
Ra	[-]	3.45E+06	3.20E+06	2.56E+06	1.59E+06	0.00E+00	5.37E+05	4.49E+05	7.65E+05
Gr	[-]	4.74E+06	4.43E+06	3.57E+06	2.22E+06	0.00E+00	7.53E+05	6.30E+05	1.08E+06
Pr	[-]	0.7282	0.7228	0.7177	0.7154	0.7132	0.7132	0.713	0.7092
Re	[-]	4.03E+03	3.28E+03	3.08E+03	2.79E+03	2.81E+03	2.59E+03	2.57E+03	2.72E+03
T	[C]	38.0	59.6	79.6	95.6	95.6	102.0	107.6	115.6
Tf	[C]	31.5086	48.81315	69.60535	87.5986	95.5956	98.7944	104.7922	111.5896
L	[m]	1.03	0.76	0.865	0.855	0.88	0.845	0.82	1.08
As	[m2]	0.412	0.304	0.346	0.342	0.352	0.338	0.328	0.432
p	[m]	2.86	2.32	2.53	2.51	2.56	2.49	2.44	2.96
Lc	[m]	0.144056	0.131034	0.136759	0.136255	0.1375	0.135743	0.134426	0.145946
ρ	[kg/m3]	1.164	1.092	1.028	0.9718	0.9718	0.933775	0.933775	0.92175
k	[W/m.K]	0.02588	0.02735	0.02881	0.03024	0.03024	0.0313	0.0313	0.03165
μ	[Pa.s]	1.87E-05	1.96E-05	2.05E-05	2.14E-05	2.14E-05	2.2E-05	2.2E-05	2.22E-05

Table B.5: Calculations for the convection coefficients of the lower surface of the produced foil for web speed of 0.45 m/min and baseline zone temperatures

Convection coefficient calculations for web speed of 0.64 m/min and baseline zone temperatures

		Upper surface							
	Unit	**Z9**	**Z8**	**Z1**	**Z2**	**Z3**	**Z4**	**Z5**	**Z6**
h	**[W/m2.K]**	**1.45**	**1.87**	**1.67**	**1.66**	**1.29**	**1.60**	**1.63**	**1.31**
Nu	[-]	5.76E+01	5.20E+01	5.00E+01	4.68E+01	3.75E+01	4.37E+01	4.27E+01	4.48E+01
NuN	[-]	1.24E+01	1.13E+01	1.07E+01	9.47E+00	0.00E+00	7.30E+00	6.90E+00	7.90E+00
NuF	[-]	4.52E+01	4.07E+01	3.94E+01	3.73E+01	3.75E+01	3.64E+01	3.58E+01	3.69E+01
Ra	[-]	4.39E+06	3.04E+06	2.44E+06	1.51E+06	0.00E+00	5.34E+05	4.28E+05	7.32E+05
Gr	[-]	6.03E+06	4.21E+06	3.40E+06	2.12E+06	0.00E+00	7.51E+05	6.02E+05	1.03E+06
Pr	[-]	0.7282	0.7228	0.7177	0.7132	0.7132	0.7111	0.7102	0.7092
Re	[-]	5.73E+03	4.67E+03	4.38E+03	3.96E+03	4.00E+03	3.77E+03	3.65E+03	3.87E+03
T	[C]	41.7	62.4	81.6	96.9	96.9	103.0	108.4	116.0
Tf	[C]	33.37355	52.08405	71.99225	89.2205	96.8775	99.9403	105.6831	112.1915
L	[m]	1.03	0.76	0.865	0.855	0.88	0.845	0.82	1.08
As	[m2]	0.412	0.304	0.346	0.342	0.352	0.338	0.328	0.432
p	[m]	2.86	2.32	2.53	2.51	2.56	2.49	2.44	2.96
Lc	[m]	0.144056	0.131034	0.136759	0.136255	0.1375	0.135743	0.134426	0.145946
ρ	[kg/m3]	1.164	1.092	1.028	0.9718	0.9718	0.9458	0.933775	0.92175
k	[W/m.K]	0.02588	0.02735	0.02881	0.03024	0.03024	0.03095	0.0313	0.03165
μ	[Pa.s]	1.87E-05	1.96E-05	2.05E-05	2.14E-05	2.14E-05	2.18E-05	2.2E-05	2.22E-05

Table B.6: Calculations for the convection coefficients of the upper surface of the produced foil for web speed of 0.64 m/min and baseline zone temperatures

		Lower surface							
	Unit	**Z9**	**Z8**	**Z1**	**Z2**	**Z3**	**Z4**	**Z5**	**Z6**
h		**1.78**	**2.36**	**2.10**	**2.06**	**1.29**	**1.93**	**1.95**	**1.59**
Nu	[-]	7.07E+01	6.57E+01	6.30E+01	5.83E+01	3.75E+01	5.20E+01	5.11E+01	5.43E+01
NuN	[-]	2.54E+01	2.50E+01	2.36E+01	2.09E+01	0.00E+00	1.60E+01	1.53E+01	1.75E+01
NuF	[-]	4.52E+01	4.07E+01	3.94E+01	3.74E+01	3.75E+01	3.60E+01	3.58E+01	3.69E+01
Ra	[-]	3.45E+06	3.20E+06	2.56E+06	1.59E+06	0.00E+00	5.37E+05	4.49E+05	7.65E+05
Gr	[-]	4.74E+06	4.43E+06	3.57E+06	2.22E+06	0.00E+00	7.53E+05	6.30E+05	1.08E+06
Pr	[-]	0.7282	0.7228	0.7177	0.7154	0.7132	0.7132	0.713	0.7092
Re	[-]	5.73E+03	4.67E+03	4.38E+03	3.96E+03	4.00E+03	3.68E+03	3.65E+03	3.87E+03
T	[C]	38.0	59.6	79.6	95.6	95.6	102.0	107.6	115.6
Tf	[C]	31.5086	48.81315	69.60535	87.5986	95.5956	98.7944	104.7922	111.5896
L	[m]	1.03	0.76	0.865	0.855	0.88	0.845	0.82	1.08
As	[m2]	0.412	0.304	0.346	0.342	0.352	0.338	0.328	0.432
p	[m]	2.86	2.32	2.53	2.51	2.56	2.49	2.44	2.96
Lc	[m]	0.144056	0.131034	0.136759	0.136255	0.1375	0.135743	0.134426	0.145946
ρ	[kg/m3]	1.164	1.092	1.028	0.9718	0.9718	0.933775	0.933775	0.92175
k	[W/m.K]	0.02588	0.02735	0.02881	0.03024	0.03024	0.0313	0.0313	0.03165
μ	[Pa.s]	1.87E-05	1.96E-05	2.05E-05	2.14E-05	2.14E-05	2.2E-05	2.2E-05	2.22E-05

Table B.7: Calculations for the convection coefficients of the upper surface of the produced foil for web speed of 0.64 m/min and baseline zone temperatures

Convection coefficient calculations for web speed of 1 m/min and baseline zone temperatures

		Upper surface							
	Unit	**Z9**	**Z8**	**Z1**	**Z2**	**Z3**	**Z4**	**Z5**	**Z6**
h	**[W/m2.K]**	**1.73**	**2.24**	**1.99**	**1.99**	**1.61**	**1.93**	**1.97**	**1.58**
Nu	[-]	6.89E+01	6.22E+01	5.99E+01	5.61E+01	4.69E+01	5.28E+01	5.16E+01	5.40E+01
NuN	[-]	1.24E+01	1.13E+01	1.07E+01	9.47E+00	0.00E+00	7.30E+00	6.90E+00	7.90E+00
NuF	[-]	5.65E+01	5.09E+01	4.92E+01	4.67E+01	4.69E+01	4.55E+01	4.47E+01	4.61E+01
Ra	[-]	4.39E+06	3.04E+06	2.44E+06	1.51E+06	0.00E+00	5.34E+05	4.28E+05	7.32E+05
Gr	[-]	6.03E+06	4.21E+06	3.40E+06	2.12E+06	0.00E+00	7.51E+05	6.02E+05	1.03E+06
Pr	[-]	0.7282	0.7228	0.7177	0.7132	0.7132	0.7111	0.7102	0.7092
Re	[-]	8.96E+03	7.29E+03	6.85E+03	6.19E+03	6.25E+03	5.89E+03	5.70E+03	6.05E+03
T	[C]	41.7	62.4	81.6	96.9	96.9	103.0	108.4	116.0
Tf	[C]	33.37355	52.08405	71.99225	89.2205	96.8775	99.9403	105.6831	112.1915
L	[m]	1.03	0.76	0.865	0.855	0.88	0.845	0.82	1.08
As	[m2]	0.412	0.304	0.346	0.342	0.352	0.338	0.328	0.432
p	[m]	2.86	2.32	2.53	2.51	2.56	2.49	2.44	2.96
Lc	[m]	0.144056	0.131034	0.136759	0.136255	0.1375	0.135743	0.134426	0.145946
ρ	[kg/m3]	1.164	1.092	1.028	0.9718	0.9718	0.9458	0.933775	0.92175
k	[W/m.K]	0.02588	0.02735	0.02881	0.03024	0.03024	0.03095	0.0313	0.03165
μ	[Pa.s]	1.87E-05	1.96E-05	2.05E-05	2.14E-05	2.14E-05	2.18E-05	2.2E-05	2.22E-05

Table B.8: Calculations for the convection coefficients of the upper surface of the produced foil for web speed of 1.00 m/min and baseline zone temperatures

		Lower surface							
	Unit	**Z9**	**Z8**	**Z1**	**Z2**	**Z3**	**Z4**	**Z5**	**Z6**
h	**[W/m2.K]**	**2.06**	**2.73**	**2.43**	**2.39**	**1.61**	**2.26**	**2.29**	**1.86**
Nu	[-]	8.20E+01	7.58E+01	7.28E+01	6.77E+01	4.69E+01	6.10E+01	6.01E+01	6.35E+01
NuN	[-]	2.54E+01	2.50E+01	2.36E+01	2.09E+01	0.00E+00	1.60E+01	1.53E+01	1.75E+01
NuF	[-]	5.65E+01	5.09E+01	4.92E+01	4.67E+01	4.69E+01	4.50E+01	4.48E+01	4.61E+01
Ra	[-]	3.45E+06	3.20E+06	2.56E+06	1.59E+06	0.00E+00	5.37E+05	4.49E+05	7.65E+05
Gr	[-]	4.74E+06	4.43E+06	3.57E+06	2.22E+06	0.00E+00	7.53E+05	6.30E+05	1.08E+06
Pr	[-]	0.7282	0.7228	0.7177	0.7154	0.7132	0.7132	0.713	0.7092
Re	[-]	8.96E+03	7.29E+03	6.85E+03	6.19E+03	6.25E+03	5.76E+03	5.70E+03	6.05E+03
T	[C]	38.0	59.6	79.6	95.6	95.6	102.0	107.6	115.6
Tf	[C]	31.5086	48.81315	69.60535	87.5986	95.5956	98.7944	104.7922	111.5896
L	[m]	1.03	0.76	0.865	0.855	0.88	0.845	0.82	1.08
As	[m2]	0.412	0.304	0.346	0.342	0.352	0.338	0.328	0.432
p	[m]	2.86	2.32	2.53	2.51	2.56	2.49	2.44	2.96
Lc	[m]	0.144056	0.131034	0.136759	0.136255	0.1375	0.135743	0.134426	0.145946
ρ	[kg/m3]	1.164	1.092	1.028	0.9718	0.9718	0.933775	0.933775	0.92175
k	[W/m.K]	0.02588	0.02735	0.02881	0.03024	0.03024	0.0313	0.0313	0.03165
μ	[Pa.s]	1.87E-05	1.96E-05	2.05E-05	2.14E-05	2.14E-05	2.2E-05	2.2E-05	2.22E-05

Table B.9: Calculations for the convection coefficients of the lower surface of the produced foil for web speed of 1.00 m/min and baseline zone temperatures

Convection coefficient calculations for web speed of 1.2 m/min and baseline zone temperatures

		Upper surface							
	Unit	**Z9**	**Z8**	**Z1**	**Z2**	**Z3**	**Z4**	**Z5**	**Z6**
h	**[W/m2.K]**	**1.87**	**2.41**	**2.15**	**2.14**	**1.77**	**2.09**	**2.13**	**1.71**
Nu	[-]	7.43E+01	6.70E+01	6.46E+01	6.06E+01	5.14E+01	5.71E+01	5.59E+01	5.84E+01
NuN	[-]	1.24E+01	1.13E+01	1.07E+01	9.47E+00	0.00E+00	7.30E+00	6.90E+00	7.90E+00
NuF	[-]	6.19E+01	5.57E+01	5.39E+01	5.11E+01	5.14E+01	4.98E+01	4.90E+01	5.05E+01
Ra	[-]	4.39E+06	3.04E+06	2.44E+06	1.51E+06	0.00E+00	5.34E+05	4.28E+05	7.32E+05
Gr	[-]	6.03E+06	4.21E+06	3.40E+06	2.12E+06	0.00E+00	7.51E+05	6.02E+05	1.03E+06
Pr	[-]	0.7282	0.7228	0.7177	0.7132	0.7132	0.7111	0.7102	0.7092
Re	[-]	1.07E+04	8.75E+03	8.22E+03	7.43E+03	7.50E+03	7.06E+03	6.84E+03	7.26E+03
T	[C]	41.7	62.4	81.6	96.9	96.9	103.0	108.4	116.0
Tf	[C]	33.37355	52.08405	71.99225	89.2205	96.8775	99.9403	105.6831	112.1915
L	[m]	1.03	0.76	0.865	0.855	0.88	0.845	0.82	1.08
As	[m2]	0.412	0.304	0.346	0.342	0.352	0.338	0.328	0.432
p	[m]	2.86	2.32	2.53	2.51	2.56	2.49	2.44	2.96
Lc	[m]	0.144056	0.131034	0.136759	0.136255	0.1375	0.135743	0.134426	0.145946
ρ	[kg/m3]	1.164	1.092	1.028	0.9718	0.9718	0.9458	0.933775	0.92175
k	[W/m.K]	0.02588	0.02735	0.02881	0.03024	0.03024	0.03095	0.0313	0.03165
μ	[Pa.s]	1.87E-05	1.96E-05	2.05E-05	2.14E-05	2.14E-05	2.18E-05	2.2E-05	2.22E-05

Table B.10: Calculations for the convection coefficients of the upper surface of the produced foil for web speed of 1.20 m/min and baseline zone temperatures

		Lower surface							
	Unit	**Z9**	**Z8**	**Z1**	**Z2**	**Z3**	**Z4**	**Z5**	**Z6**
h	**[W/m2.K]**	**2.20**	**2.90**	**2.58**	**2.55**	**1.77**	**2.42**	**2.46**	**1.99**
Nu	[-]	8.74E+01	8.07E+01	7.75E+01	7.21E+01	5.14E+01	6.53E+01	6.43E+01	6.79E+01
NuN	[-]	2.54E+01	2.50E+01	2.36E+01	2.09E+01	0.00E+00	1.60E+01	1.53E+01	1.75E+01
NuF	[-]	6.19E+01	5.57E+01	5.39E+01	5.12E+01	5.14E+01	4.93E+01	4.91E+01	5.05E+01
Ra	[-]	3.45E+06	3.20E+06	2.56E+06	1.59E+06	0.00E+00	5.37E+05	4.49E+05	7.65E+05
Gr	[-]	4.74E+06	4.43E+06	3.57E+06	2.22E+06	0.00E+00	7.53E+05	6.30E+05	1.08E+06
Pr	[-]	0.7282	0.7228	0.7177	0.7154	0.7132	0.7132	0.713	0.7092
Re	[-]	1.07E+04	8.75E+03	8.22E+03	7.43E+03	7.50E+03	6.91E+03	6.84E+03	7.26E+03
T	[C]	38.0	59.6	79.6	95.6	95.6	102.0	107.6	115.6
Tf	[C]	31.5086	48.81315	69.60535	87.5986	95.5956	98.7944	104.7922	111.5896
L	[m]	1.03	0.76	0.865	0.855	0.88	0.845	0.82	1.08
As	[m2]	0.412	0.304	0.346	0.342	0.352	0.338	0.328	0.432
p	[m]	2.86	2.32	2.53	2.51	2.56	2.49	2.44	2.96
Lc	[m]	0.144056	0.131034	0.136759	0.136255	0.1375	0.135743	0.134426	0.145946
ρ	[kg/m3]	1.164	1.092	1.028	0.9718	0.9718	0.933775	0.933775	0.92175
k	[W/m.K]	0.02588	0.02735	0.02881	0.03024	0.03024	0.0313	0.0313	0.03165
μ	[Pa.s]	1.87E-05	1.96E-05	2.05E-05	2.14E-05	2.14E-05	2.2E-05	2.2E-05	2.22E-05

Table B.11: Calculations for the convection coefficients of the lower surface of the produced foil for web speed of 1.20 m/min and baseline zone temperatures

Convection coefficient calculations for web speed of 2 m/min and baseline zone temperatures

		Upper surface							
	Unit	**Z9**	**Z8**	**Z1**	**Z2**	**Z3**	**Z4**	**Z5**	**Z6**
h	**[W/m2.K]**	**2.32**	**3.00**	**2.67**	**2.67**	**2.28**	**2.62**	**2.68**	**2.14**
Nu	[-]	9.23E+01	8.32E+01	8.03E+01	7.55E+01	6.63E+01	7.16E+01	7.02E+01	7.30E+01
NuN	[-]	1.24E+01	1.13E+01	1.07E+01	9.47E+00	0.00E+00	7.30E+00	6.90E+00	7.90E+00
NuF	[-]	8.00E+01	7.20E+01	6.96E+01	6.60E+01	6.63E+01	6.43E+01	6.33E+01	6.52E+01
Ra	[-]	4.39E+06	3.04E+06	2.44E+06	1.51E+06	0.00E+00	5.34E+05	4.28E+05	7.32E+05
Gr	[-]	6.03E+06	4.21E+06	3.40E+06	2.12E+06	0.00E+00	7.51E+05	6.02E+05	1.03E+06
Pr	[-]	0.7282	0.7228	0.7177	0.7132	0.7132	0.7111	0.7102	0.7092
Re	[-]	1.79E+04	1.46E+04	1.37E+04	1.24E+04	1.25E+04	1.18E+04	1.14E+04	1.21E+04
T	[C]	41.7	62.4	81.6	96.9	96.9	103.0	108.4	116.0
Tf	[C]	33.37355	52.08405	71.99225	89.2205	96.8775	99.9403	105.6831	112.1915
L	[m]	1.03	0.76	0.865	0.855	0.88	0.845	0.82	1.08
As	[m2]	0.412	0.304	0.346	0.342	0.352	0.338	0.328	0.432
p	[m]	2.86	2.32	2.53	2.51	2.56	2.49	2.44	2.96
Lc	[m]	0.144056	0.131034	0.136759	0.136255	0.1375	0.135743	0.134426	0.145946
ρ	[kg/m3]	1.164	1.092	1.028	0.9718	0.9718	0.9458	0.933775	0.92175
k	[W/m.K]	0.02588	0.02735	0.02881	0.03024	0.03024	0.03095	0.0313	0.03165
μ	[Pa.s]	1.87E-05	1.96E-05	2.05E-05	2.14E-05	2.14E-05	2.18E-05	2.2E-05	2.22E-05

Table B.12: Calculations for the convection coefficients of the upper surface of the produced foil for web speed of 2.00 m/min and baseline zone temperatures

		Lower surface							
	Unit	**Z9**	**Z8**	**Z1**	**Z2**	**Z3**	**Z4**	**Z5**	**Z6**
h	**[W/m2.K]**	**2.65**	**3.49**	**3.10**	**3.08**	**2.28**	**2.95**	**3.00**	**2.42**
Nu	[-]	1.05E+02	9.69E+01	9.32E+01	8.70E+01	6.63E+01	7.96E+01	7.86E+01	8.26E+01
NuN	[-]	2.54E+01	2.50E+01	2.36E+01	2.09E+01	0.00E+00	1.60E+01	1.53E+01	1.75E+01
NuF	[-]	8.00E+01	7.20E+01	6.96E+01	6.61E+01	6.63E+01	6.37E+01	6.33E+01	6.52E+01
Ra	[-]	3.45E+06	3.20E+06	2.56E+06	1.59E+06	0.00E+00	5.37E+05	4.49E+05	7.65E+05
Gr	[-]	4.74E+06	4.43E+06	3.57E+06	2.22E+06	0.00E+00	7.53E+05	6.30E+05	1.08E+06
Pr	[-]	0.7282	0.7228	0.7177	0.7154	0.7132	0.7132	0.713	0.7092
Re	[-]	1.79E+04	1.46E+04	1.37E+04	1.24E+04	1.25E+04	1.15E+04	1.14E+04	1.21E+04
T	[C]	38.0	59.6	79.6	95.6	95.6	102.0	107.6	115.6
Tf	[C]	31.5086	48.81315	69.60535	87.5986	95.5956	98.7944	104.7922	111.5896
L	[m]	1.03	0.76	0.865	0.855	0.88	0.845	0.82	1.08
As	[m2]	0.412	0.304	0.346	0.342	0.352	0.338	0.328	0.432
p	[m]	2.86	2.32	2.53	2.51	2.56	2.49	2.44	2.96
Lc	[m]	0.144056	0.131034	0.136759	0.136255	0.1375	0.135743	0.134426	0.145946
ρ	[kg/m3]	1.164	1.092	1.028	0.9718	0.9718	0.933775	0.933775	0.92175
k	[W/m.K]	0.02588	0.02735	0.02881	0.03024	0.03024	0.0313	0.0313	0.03165
μ	[Pa.s]	1.87E-05	1.96E-05	2.05E-05	2.14E-05	2.14E-05	2.2E-05	2.2E-05	2.22E-05

Table B.13: Calculations for the convection coefficients of the lower surface of the produced foil for web speed of 2.00 m/min and baseline zone temperatures

Convection coefficient calculations for web speed of 3 m/min and baseline zone temperatures

		Upper surface							
	Unit	**Z9**	**Z8**	**Z1**	**Z2**	**Z3**	**Z4**	**Z5**	**Z6**
h	**[W/m2.K]**	**2.77**	**3.58**	**3.19**	**3.19**	**2.79**	**3.15**	**3.22**	**2.57**
Nu	[-]	1.10E+02	9.94E+01	9.59E+01	9.03E+01	8.12E+01	8.61E+01	8.44E+01	8.77E+01
NuN	[-]	1.24E+01	1.13E+01	1.07E+01	9.47E+00	0.00E+00	7.30E+00	6.90E+00	7.90E+00
NuF	[-]	9.79E+01	8.81E+01	8.52E+01	8.08E+01	8.12E+01	7.88E+01	7.75E+01	7.98E+01
Ra	[-]	4.39E+06	3.04E+06	2.44E+06	1.51E+06	0.00E+00	5.34E+05	4.28E+05	7.32E+05
Gr	[-]	6.03E+06	4.21E+06	3.40E+06	2.12E+06	0.00E+00	7.51E+05	6.02E+05	1.03E+06
Pr	[-]	0.7282	0.7228	0.7177	0.7132	0.7132	0.7111	0.7102	0.7092
Re	[-]	2.69E+04	2.19E+04	2.06E+04	1.86E+04	1.87E+04	1.77E+04	1.71E+04	1.82E+04
T	[C]	41.7	62.4	81.6	96.9	96.9	103.0	108.4	116.0
Tf	[C]	33.37355	52.08405	71.99225	89.2205	96.8775	99.9403	105.6831	112.1915
L	[m]	1.03	0.76	0.865	0.855	0.88	0.845	0.82	1.08
As	[m2]	0.412	0.304	0.346	0.342	0.352	0.338	0.328	0.432
p	[m]	2.86	2.32	2.53	2.51	2.56	2.49	2.44	2.96
Lc	[m]	0.144056	0.131034	0.136759	0.136255	0.1375	0.135743	0.134426	0.145946
ρ	[kg/m3]	1.164	1.092	1.028	0.9718	0.9718	0.9458	0.933775	0.92175
k	[W/m.K]	0.02588	0.02735	0.02881	0.03024	0.03024	0.03095	0.0313	0.03165
μ	[Pa.s]	1.87E-05	1.96E-05	2.05E-05	2.14E-05	2.14E-05	2.18E-05	2.2E-05	2.22E-05

Table B.14: Calculations for the convection coefficients of the upper surface of the produced foil for web speed of 3.00 m/min and baseline zone temperatures

		Lower surface							
	Unit	**Z9**	**Z8**	**Z1**	**Z2**	**Z3**	**Z4**	**Z5**	**Z6**
h	**[W/m2.K]**	**3.10**	**4.07**	**3.62**	**3.60**	**2.79**	**3.48**	**3.54**	**2.85**
Nu	[-]	1.23E+02	1.13E+02	1.09E+02	1.02E+02	8.12E+01	9.39E+01	9.29E+01	9.72E+01
NuN	[-]	2.54E+01	2.50E+01	2.36E+01	2.09E+01	0.00E+00	1.60E+01	1.53E+01	1.75E+01
NuF	[-]	9.79E+01	8.81E+01	8.52E+01	8.09E+01	8.12E+01	7.80E+01	7.76E+01	7.98E+01
Ra	[-]	3.45E+06	3.20E+06	2.56E+06	1.59E+06	0.00E+00	5.37E+05	4.49E+05	7.65E+05
Gr	[-]	4.74E+06	4.43E+06	3.57E+06	2.22E+06	0.00E+00	7.53E+05	6.30E+05	1.08E+06
Pr	[-]	0.7282	0.7228	0.7177	0.7154	0.7132	0.7132	0.713	0.7092
Re	[-]	2.69E+04	2.19E+04	2.06E+04	1.86E+04	1.87E+04	1.73E+04	1.71E+04	1.82E+04
T	[C]	38.0	59.6	79.6	95.6	95.6	102.0	107.6	115.6
Tf	[C]	31.5086	48.81315	69.60535	87.5986	95.5956	98.7944	104.7922	111.5896
L	[m]	1.03	0.76	0.865	0.855	0.88	0.845	0.82	1.08
As	[m2]	0.412	0.304	0.346	0.342	0.352	0.338	0.328	0.432
p	[m]	2.86	2.32	2.53	2.51	2.56	2.49	2.44	2.96
Lc	[m]	0.144056	0.131034	0.136759	0.136255	0.1375	0.135743	0.134426	0.145946
ρ	[kg/m3]	1.164	1.092	1.028	0.9718	0.9718	0.933775	0.933775	0.92175
k	[W/m.K]	0.02588	0.02735	0.02881	0.03024	0.03024	0.0313	0.0313	0.03165
μ	[Pa.s]	1.87E-05	1.96E-05	2.05E-05	2.14E-05	2.14E-05	2.2E-05	2.2E-05	2.22E-05

Table B.15: Calculations for the convection coefficients of the lower surface of the produced foil for web speed of 3.00 m/min and baseline zone temperatures

Convection coefficient calculations for Scenario 1

		Upper surface							
	Unit	**Z9**	**Z8**	**Z1**	**Z2**	**Z3**	**Z4**	**Z5**	**Z6**
h	**[W/m2.K]**	**1.45**	**1.90**	**1.62**	**1.60**	**1.56**	**1.60**	**1.63**	**1.31**
Nu	[-]	5.76E+01	5.28E+01	4.88E+01	4.53E+01	4.55E+01	4.37E+01	4.27E+01	4.48E+01
NuN	[-]	1.24E+01	1.21E+01	9.39E+00	8.00E+00	8.02E+00	7.30E+00	6.90E+00	7.90E+00
NuF	[-]	4.52E+01	4.07E+01	3.94E+01	3.73E+01	3.75E+01	3.64E+01	3.58E+01	3.69E+01
Ra	[-]	4.39E+06	4.07E+06	1.46E+06	7.72E+05	7.77E+05	5.34E+05	4.28E+05	7.32E+05
Gr	[-]	6.03E+06	5.64E+06	2.04E+06	1.08E+06	1.09E+06	7.51E+05	6.02E+05	1.03E+06
Pr	[-]	0.7282	0.7228	0.7177	0.7132	0.7132	0.7111	0.7102	0.7092
Re	[-]	5.73E+03	4.67E+03	4.38E+03	3.96E+03	4.00E+03	3.77E+03	3.65E+03	3.87E+03
T	[C]	41.7	70.1	81.6	89.2	96.9	103.0	108.4	116.0
Tf	[C]	33.37355	55.91255	75.82075	85.392	93.049	99.9403	105.6831	112.1915
L	[m]	1.03	0.76	0.865	0.855	0.88	0.845	0.82	1.08
As	[m2]	0.412	0.304	0.346	0.342	0.352	0.338	0.328	0.432
p	[m]	2.86	2.32	2.53	2.51	2.56	2.49	2.44	2.96
Lc	[m]	0.144056	0.131034	0.136759	0.136255	0.1375	0.135743	0.134426	0.145946
ρ	[kg/m3]	1.164	1.092	1.028	0.9718	0.9718	0.9458	0.933775	0.92175
k	[W/m.K]	0.02588	0.02735	0.02881	0.03024	0.03024	0.03095	0.0313	0.03165
μ	[Pa.s]	1.87E-05	1.96E-05	2.05E-05	2.14E-05	2.14E-05	2.18E-05	2.2E-05	2.22E-05

Table B.16: Calculations for the convection coefficients of the upper surface of the produced foil for Scenario 1

		Lower surface							
	Unit	**Z9**	**Z8**	**Z1**	**Z2**	**Z3**	**Z4**	**Z5**	**Z6**
h	**[W/m2.K]**	**1.78**	**2.36**	**2.11**	**1.94**	**1.89**	**1.89**	**1.95**	**1.59**
Nu	[-]	7.07E+01	6.57E+01	6.35E+01	5.49E+01	5.50E+01	5.11E+01	5.11E+01	5.43E+01
NuN	[-]	2.54E+01	2.50E+01	2.41E+01	1.75E+01	1.75E+01	1.51E+01	1.53E+01	1.75E+01
NuF	[-]	4.52E+01	4.07E+01	3.94E+01	3.74E+01	3.75E+01	3.60E+01	3.58E+01	3.69E+01
Ra	[-]	3.45E+06	3.20E+06	2.80E+06	7.74E+05	7.77E+05	4.29E+05	4.49E+05	7.65E+05
Gr	[-]	4.74E+06	4.43E+06	3.90E+06	1.08E+06	1.09E+06	6.02E+05	6.30E+05	1.08E+06
Pr	[-]	0.7282	0.7228	0.7177	0.7154	0.7132	0.7132	0.713	0.7092
Re	[-]	5.73E+03	4.67E+03	4.38E+03	3.96E+03	4.00E+03	3.68E+03	3.65E+03	3.87E+03
T	[C]	38.0	59.6	81.6	89.2	96.9	102.0	107.6	115.6
Tf	[C]	31.5086	48.81315	70.5863	85.392	93.049	99.43535	104.7922	111.5896
L	[m]	1.03	0.76	0.865	0.855	0.88	0.845	0.82	1.08
As	[m2]	0.412	0.304	0.346	0.342	0.352	0.338	0.328	0.432
p	[m]	2.86	2.32	2.53	2.51	2.56	2.49	2.44	2.96
Lc	[m]	0.144056	0.131034	0.136759	0.136255	0.1375	0.135743	0.134426	0.145946
ρ	[kg/m3]	1.164	1.092	1.028	0.9718	0.9718	0.933775	0.933775	0.92175
k	[W/m.K]	0.02588	0.02735	0.02881	0.03024	0.03024	0.0313	0.0313	0.03165
μ	[Pa.s]	1.87E-05	1.96E-05	2.05E-05	2.14E-05	2.14E-05	2.2E-05	2.2E-05	2.22E-05

Table B.17: Calculations for the convection coefficients of the lower surface of the produced foil for Scenario 1

Convection coefficient calculations for Scenario 2

		Upper surface							
	Unit	**Z9**	**Z8**	**Z1**	**Z2**	**Z3**	**Z4**	**Z5**	**Z6**
h	**[W/m2.K]**	**1.45**	**1.90**	**1.62**	**1.60**	**1.56**	**1.60**	**1.63**	**1.31**
Nu	[-]	5.76E+01	5.28E+01	4.88E+01	4.53E+01	4.55E+01	4.37E+01	4.27E+01	4.48E+01
NuN	[-]	1.24E+01	1.21E+01	9.39E+00	8.00E+00	8.02E+00	7.30E+00	6.90E+00	7.90E+00
NuF	[-]	4.52E+01	4.07E+01	3.94E+01	3.73E+01	3.75E+01	3.64E+01	3.58E+01	3.69E+01
Ra	[-]	4.39E+06	4.07E+06	1.46E+06	7.72E+05	7.77E+05	5.34E+05	4.28E+05	7.32E+05
Gr	[-]	6.03E+06	5.64E+06	2.04E+06	1.08E+06	1.09E+06	7.51E+05	6.02E+05	1.03E+06
Pr	[-]	0.7282	0.7228	0.7177	0.7132	0.7132	0.7111	0.7102	0.7092
Re	[-]	5.73E+03	4.67E+03	4.38E+03	3.96E+03	4.00E+03	3.77E+03	3.65E+03	3.87E+03
T	[C]	41.7	70.1	81.6	89.2	96.9	103.0	108.4	116.0
Tf	[C]	33.37355	55.91255	75.82075	85.392	93.049	99.9403	105.6831	112.1915
L	[m]	1.03	0.76	0.865	0.855	0.88	0.845	0.82	1.08
As	[m2]	0.412	0.304	0.346	0.342	0.352	0.338	0.328	0.432
p	[m]	2.86	2.32	2.53	2.51	2.56	2.49	2.44	2.96
Lc	[m]	0.144056	0.131034	0.136759	0.136255	0.1375	0.135743	0.134426	0.145946
ρ	[kg/m3]	1.164	1.092	1.028	0.9718	0.9718	0.9458	0.933775	0.92175
k	[W/m.K]	0.02588	0.02735	0.02881	0.03024	0.03024	0.03095	0.0313	0.03165
μ	[Pa.s]	1.87E-05	1.96E-05	2.05E-05	2.14E-05	2.14E-05	2.18E-05	2.2E-05	2.22E-05

Table B.18: Calculations for the convection coefficients of the upper surface of the produced foil for Scenario 2

		Lower surface							
	Unit	**Z9**	**Z8**	**Z1**	**Z2**	**Z3**	**Z4**	**Z5**	**Z6**
h	**[W/m2.K]**	**1.78**	**2.36**	**2.11**	**1.94**	**1.89**	**1.89**	**1.95**	**1.59**
Nu	[-]	7.07E+01	6.57E+01	6.35E+01	5.49E+01	5.50E+01	5.11E+01	5.11E+01	5.43E+01
NuN	[-]	2.54E+01	2.50E+01	2.41E+01	1.75E+01	1.75E+01	1.51E+01	1.53E+01	1.75E+01
NuF	[-]	4.52E+01	4.07E+01	3.94E+01	3.74E+01	3.75E+01	3.60E+01	3.58E+01	3.69E+01
Ra	[-]	3.45E+06	3.20E+06	2.80E+06	7.74E+05	7.77E+05	4.29E+05	4.49E+05	7.65E+05
Gr	[-]	4.74E+06	4.43E+06	3.90E+06	1.08E+06	1.09E+06	6.02E+05	6.30E+05	1.08E+06
Pr	[-]	0.7282	0.7228	0.7177	0.7154	0.7132	0.7132	0.713	0.7092
Re	[-]	5.73E+03	4.67E+03	4.38E+03	3.96E+03	4.00E+03	3.68E+03	3.65E+03	3.87E+03
T	[C]	38.0	59.6	81.6	89.2	96.9	102.0	107.6	115.6
Tf	[C]	31.5086	48.81315	70.5863	85.392	93.049	99.43535	104.7922	111.5896
L	[m]	1.03	0.76	0.865	0.855	0.88	0.845	0.82	1.08
As	[m2]	0.412	0.304	0.346	0.342	0.352	0.338	0.328	0.432
p	[m]	2.86	2.32	2.53	2.51	2.56	2.49	2.44	2.96
Lc	[m]	0.144056	0.131034	0.136759	0.136255	0.1375	0.135743	0.134426	0.145946
ρ	[kg/m3]	1.164	1.092	1.028	0.9718	0.9718	0.933775	0.933775	0.92175
k	[W/m.K]	0.02588	0.02735	0.02881	0.03024	0.03024	0.0313	0.0313	0.03165
μ	[Pa.s]	1.87E-05	1.96E-05	2.05E-05	2.14E-05	2.14E-05	2.2E-05	2.2E-05	2.22E-05

Table B.19: Calculations for the convection coefficients of the lower surface of the produced foil for Scenario 2

Convection coefficient calculations for Scenario 3

	Upper surface							
	Unit	**Z9**	**Z8**	**Z1**	**Z2**	**Z3**	**Z4**	**Z5**	**Z6**
h	**[W/m2.K]**	**1.87**	**2.41**	**2.15**	**2.14**	**1.77**	**2.09**	**2.13**	**1.71**
Nu	[-]	7.43E+01	6.70E+01	6.46E+01	6.06E+01	5.14E+01	5.71E+01	5.59E+01	5.83E+01
NuN	[-]	1.24E+01	1.13E+01	1.07E+01	9.47E+00	0.00E+00	7.29E+00	6.92E+00	7.88E+00
NuF	[-]	6.19E+01	5.57E+01	5.39E+01	5.11E+01	5.14E+01	4.98E+01	4.90E+01	5.05E+01
Ra	[-]	4.39E+06	3.04E+06	2.45E+06	1.51E+06	0.00E+00	5.32E+05	4.31E+05	7.27E+05
Gr	[-]	6.03E+06	4.20E+06	3.41E+06	2.12E+06	0.00E+00	7.48E+05	6.07E+05	1.02E+06
Pr	[-]	0.7282	0.7228	0.7177	0.7132	0.7132	0.7111	0.7102	0.7092
Re	[-]	1.07E+04	8.75E+03	8.22E+03	7.43E+03	7.50E+03	7.06E+03	6.84E+03	7.26E+03
T	[C]	41.7	62.4	81.6	96.9	96.9	103.0	108.4	116.0
Tf	[C]	33.37355	52.07355	72	89.25	96.9	99.95	105.7	112.2
L	[m]	1.03	0.76	0.865	0.855	0.88	0.845	0.82	1.08
As	[m2]	0.412	0.304	0.346	0.342	0.352	0.338	0.328	0.432
p	[m]	2.86	2.32	2.53	2.51	2.56	2.49	2.44	2.96
Lc	[m]	0.144056	0.131034	0.136759	0.136255	0.1375	0.135743	0.134426	0.145946
ρ	[kg/m3]	1.164	1.092	1.028	0.9718	0.9718	0.9458	0.933775	0.92175
k	[W/m.K]	0.02588	0.02735	0.02881	0.03024	0.03024	0.03095	0.0313	0.03165
μ	[Pa.s]	1.87E-05	1.96E-05	2.05E-05	2.14E-05	2.14E-05	2.18E-05	2.2E-05	2.22E-05

Table B.20: Calculations for the convection coefficients of the upper surface of the produced foil for Scenario 3

	Lower surface							
	Unit	**Z9**	**Z8**	**Z1**	**Z2**	**Z3**	**Z4**	**Z5**	**Z6**
h	**[W/m2.K]**	**2.20**	**2.93**	**2.57**	**2.54**	**1.77**	**2.41**	**2.45**	**1.98**
Nu	[-]	8.74E+01	8.14E+01	7.72E+01	7.19E+01	5.14E+01	6.51E+01	6.42E+01	6.77E+01
NuN	[-]	2.54E+01	2.57E+01	2.33E+01	2.07E+01	0.00E+00	1.58E+01	1.51E+01	1.72E+01
NuF	[-]	6.19E+01	5.57E+01	5.39E+01	5.12E+01	5.14E+01	4.93E+01	4.91E+01	5.05E+01
Ra	[-]	3.45E+06	3.59E+06	2.45E+06	1.52E+06	0.00E+00	5.10E+05	4.33E+05	7.27E+05
Gr	[-]	4.74E+06	4.96E+06	3.41E+06	2.12E+06	0.00E+00	7.16E+05	6.07E+05	1.02E+06
Pr	[-]	0.7282	0.7228	0.7177	0.7154	0.7132	0.7132	0.713	0.7092
Re	[-]	1.07E+04	8.75E+03	8.22E+03	7.43E+03	7.50E+03	6.91E+03	6.84E+03	7.26E+03
T	[C]	38.0	62.4	81.6	96.9	96.9	103.0	108.4	116.0
Tf	[C]	31.5086	50.2086	72	89.25	96.9	99.95	105.7	112.2
L	[m]	1.03	0.76	0.865	0.855	0.88	0.845	0.82	1.08
As	[m2]	0.412	0.304	0.346	0.342	0.352	0.338	0.328	0.432
p	[m]	2.86	2.32	2.53	2.51	2.56	2.49	2.44	2.96
Lc	[m]	0.144056	0.131034	0.136759	0.136255	0.1375	0.135743	0.134426	0.145946
ρ	[kg/m3]	1.164	1.092	1.028	0.9718	0.9718	0.933775	0.933775	0.92175
k	[W/m.K]	0.02588	0.02735	0.02881	0.03024	0.03024	0.0313	0.0313	0.03165
μ	[Pa.s]	1.87E-05	1.96E-05	2.05E-05	2.14E-05	2.14E-05	2.2E-05	2.2E-05	2.22E-05

Table B.21: Calculations for the convection coefficients of the lower surface of the produced foil for Scenario 3

Convection coefficient calculations for Scenario 4

	Upper surface							
	Unit	**Z9**	**Z8**	**Z1**	**Z2**	**Z3**	**Z4**	**Z5**	**Z6**
h	**[W/m2.K]**	**1.87**	**2.48**	**2.08**	**2.09**	**2.04**	**2.11**	**2.16**	**1.71**
Nu	[-]	7.43E+01	6.88E+01	6.23E+01	5.91E+01	5.93E+01	5.75E+01	5.65E+01	5.83E+01
NuN	[-]	1.24E+01	1.31E+01	8.44E+00	7.96E+00	7.97E+00	7.67E+00	7.49E+00	7.84E+00
NuF	[-]	6.19E+01	5.57E+01	5.39E+01	5.11E+01	5.14E+01	4.98E+01	4.90E+01	5.05E+01
Ra	[-]	4.39E+06	5.54E+06	9.55E+05	7.56E+05	7.61E+05	6.52E+05	5.93E+05	7.11E+05
Gr	[-]	6.03E+06	7.67E+06	1.33E+06	1.06E+06	1.07E+06	9.17E+05	8.35E+05	1.00E+06
Pr	[-]	0.7282	0.7228	0.7177	0.7132	0.7132	0.7111	0.7102	0.7092
Re	[-]	1.07E+04	8.75E+03	8.22E+03	7.43E+03	7.50E+03	7.06E+03	6.84E+03	7.26E+03
T	[C]	41.7	81.6	89.2	96.9	104.5	112.2	119.8	127.5
Tf	[C]	33.37355	61.6553	85.392	93.049	100.706	108.363	116.02	123.677
L	[m]	1.03	0.76	0.865	0.855	0.88	0.845	0.82	1.08
As	[m2]	0.412	0.304	0.346	0.342	0.352	0.338	0.328	0.432
p	[m]	2.86	2.32	2.53	2.51	2.56	2.49	2.44	2.96
Lc	[m]	0.144056	0.131034	0.136759	0.136255	0.1375	0.135743	0.134426	0.145946
ρ	[kg/m3]	1.164	1.092	1.028	0.9718	0.9718	0.9458	0.933775	0.92175
k	[W/m.K]	0.02588	0.02735	0.02881	0.03024	0.03024	0.03095	0.0313	0.03165
μ	[Pa.s]	1.87E-05	1.96E-05	2.05E-05	2.14E-05	2.14E-05	2.18E-05	2.2E-05	2.22E-05

Table B.22: Calculations for the convection coefficients of the upper surface of the produced foil for Scenario 4

	Lower surface							
	Unit	**Z9**	**Z8**	**Z1**	**Z2**	**Z3**	**Z4**	**Z5**	**Z6**
h	**[W/m2.K]**	**2.20**	**3.06**	**2.41**	**2.43**	**2.36**	**2.44**	**2.50**	**1.98**
Nu	[-]	8.74E+01	8.50E+01	7.23E+01	6.86E+01	6.88E+01	6.59E+01	6.55E+01	6.76E+01
NuN	[-]	2.54E+01	2.93E+01	1.84E+01	1.74E+01	1.74E+01	1.66E+01	1.64E+01	1.71E+01
NuF	[-]	6.19E+01	5.57E+01	5.39E+01	5.12E+01	5.14E+01	4.93E+01	4.91E+01	5.05E+01
Ra	[-]	3.45E+06	6.06E+06	9.55E+05	7.58E+05	7.61E+05	6.25E+05	5.95E+05	7.11E+05
Gr	[-]	4.74E+06	8.39E+06	1.33E+06	1.06E+06	1.07E+06	8.77E+05	8.35E+05	1.00E+06
Pr	[-]	0.7282	0.7228	0.7177	0.7154	0.7132	0.7132	0.713	0.7092
Re	[-]	1.07E+04	8.75E+03	8.22E+03	7.43E+03	7.50E+03	6.91E+03	6.84E+03	7.26E+03
T	[C]	38.0	81.6	89.2	96.9	104.5	112.2	119.8	127.5
Tf	[C]	31.5086	59.79035	85.392	93.049	100.706	108.363	116.02	123.677
L	[m]	1.03	0.76	0.865	0.855	0.88	0.845	0.82	1.08
As	[m2]	0.412	0.304	0.346	0.342	0.352	0.338	0.328	0.432
p	[m]	2.86	2.32	2.53	2.51	2.56	2.49	2.44	2.96
Lc	[m]	0.144056	0.131034	0.136759	0.136255	0.1375	0.135743	0.134426	0.145946
ρ	[kg/m3]	1.164	1.092	1.028	0.9718	0.9718	0.933775	0.933775	0.92175
k	[W/m.K]	0.02588	0.02735	0.02881	0.03024	0.03024	0.0313	0.0313	0.03165
μ	[Pa.s]	1.87E-05	1.96E-05	2.05E-05	2.14E-05	2.14E-05	2.2E-05	2.2E-05	2.22E-05

Table B.23: Calculations for the convection coefficients of the lower surface of the produced foil for Scenario 4

Convection coefficient calculations for Scenario 5

		Upper surface							
	Unit	**Z9**	**Z8**	**Z1**	**Z2**	**Z3**	**Z4**	**Z5**	**Z6**
h	**[W/m2.K]**	**1.45**	**1.87**	**1.63**	**1.66**	**1.29**	**1.66**	**1.63**	**1.31**
Nu	[-]	5.76E+01	5.20E+01	4.88E+01	4.69E+01	3.75E+01	4.53E+01	4.27E+01	4.48E+01
NuN	[-]	1.24E+01	1.13E+01	9.44E+00	9.52E+00	0.00E+00	8.94E+00	6.90E+00	7.90E+00
NuF	[-]	4.52E+01	4.07E+01	3.94E+01	3.73E+01	3.75E+01	3.64E+01	3.58E+01	3.69E+01
Ra	[-]	4.39E+06	3.04E+06	1.50E+06	1.54E+06	0.00E+00	1.20E+06	4.28E+05	7.32E+05
Gr	[-]	6.03E+06	4.21E+06	2.08E+06	2.16E+06	0.00E+00	1.69E+06	6.02E+05	1.03E+06
Pr	[-]	0.7282	0.7228	0.7177	0.7132	0.7132	0.7111	0.7102	0.7092
Re	[-]	5.73E+03	4.67E+03	4.38E+03	3.96E+03	4.00E+03	3.77E+03	3.65E+03	3.87E+03
T	[C]	41.7	62.4	73.9	89.2	89.2	103.0	108.4	116.0
Tf	[C]	33.37355	52.08405	68.16375	81.5635	89.2205	96.1118	105.6831	112.1915
L	[m]	1.03	0.76	0.865	0.855	0.88	0.845	0.82	1.08
As	[m2]	0.412	0.304	0.346	0.342	0.352	0.338	0.328	0.432
p	[m]	2.86	2.32	2.53	2.51	2.56	2.49	2.44	2.96
Lc	[m]	0.144056	0.131034	0.136759	0.136255	0.1375	0.135743	0.134426	0.145946
ρ	[kg/m3]	1.164	1.092	1.028	0.9718	0.9718	0.9458	0.933775	0.92175
k	[W/m.K]	0.02588	0.02735	0.02881	0.03024	0.03024	0.03095	0.0313	0.03165
μ	[Pa.s]	1.87E-05	1.96E-05	2.05E-05	2.14E-05	2.14E-05	2.18E-05	2.2E-05	2.22E-05

Table B.24: Calculations for the convection coefficients of the upper surface of the produced foil for Scenario 5

		Lower surface							
	Unit	**Z9**	**Z8**	**Z1**	**Z2**	**Z3**	**Z4**	**Z5**	**Z6**
h	**[W/m2.K]**	**1.78**	**2.36**	**2.04**	**2.06**	**1.29**	**2.04**	**1.95**	**1.59**
Nu	[-]	7.07E+01	6.57E+01	6.12E+01	5.82E+01	3.75E+01	5.50E+01	5.11E+01	5.43E+01
NuN	[-]	2.54E+01	2.50E+01	2.18E+01	2.08E+01	0.00E+00	1.90E+01	1.53E+01	1.75E+01
NuF	[-]	4.52E+01	4.07E+01	3.94E+01	3.74E+01	3.75E+01	3.60E+01	3.58E+01	3.69E+01
Ra	[-]	3.45E+06	3.20E+06	1.86E+06	1.55E+06	0.00E+00	1.07E+06	4.49E+05	7.65E+05
Gr	[-]	4.74E+06	4.43E+06	2.59E+06	2.16E+06	0.00E+00	1.50E+06	6.30E+05	1.08E+06
Pr	[-]	0.7282	0.7228	0.7177	0.7154	0.7132	0.7132	0.713	0.7092
Re	[-]	5.73E+03	4.67E+03	4.38E+03	3.96E+03	4.00E+03	3.68E+03	3.65E+03	3.87E+03
T	[C]	38.0	59.6	73.9	89.2	89.2	102.0	107.6	115.6
Tf	[C]	31.5086	48.81315	66.7578	81.5635	89.2205	95.60685	104.7922	111.5896
L	[m]	1.03	0.76	0.865	0.855	0.88	0.845	0.82	1.08
As	[m2]	0.412	0.304	0.346	0.342	0.352	0.338	0.328	0.432
p	[m]	2.86	2.32	2.53	2.51	2.56	2.49	2.44	2.96
Lc	[m]	0.144056	0.131034	0.136759	0.136255	0.1375	0.135743	0.134426	0.145946
ρ	[kg/m3]	1.164	1.092	1.028	0.9718	0.9718	0.933775	0.933775	0.92175
k	[W/m.K]	0.02588	0.02735	0.02881	0.03024	0.03024	0.0313	0.0313	0.03165
μ	[Pa.s]	1.87E-05	1.96E-05	2.05E-05	2.14E-05	2.14E-05	2.2E-05	2.2E-05	2.22E-05

Table B.25: Calculations for the convection coefficients of the lower surface of the produced foil for Scenario 5

C

Inputs and outputs of the thermal model

The thermal model takes the ambient temperature and convection coefficients as inputs and calculates the temperature profile as an output. The model takes inputs and gives outputs as a function of time, however, it is very easy to translate time to distance if we know the web speed using C.1. a table converting each zone length into time spent in that zone in seconds is given below.

$$x = v \times t \tag{C.1}$$

Where,
x: the distance covered in a certain time.
v: web speed.
t: time spent during the process.

Zone number	Length (m)	Web speed (m/min)						
		0.3	**0.45**	**0.64**	**1**	**1.2**	**2**	**3**
Z1	**0.865**	173	115.3333	81.09375	51.9	43.25	25.95	17.3
Z2	**0.855**	171	114	80.15625	51.3	42.75	25.65	17.1
Z3	**0.88**	176	117.3333	82.5	52.8	44	26.4	17.6
Z4	**0.845**	169	112.6667	79.21875	50.7	42.25	25.35	16.9
Z5	**0.82**	164	109.3333	76.875	49.2	41	24.6	16.4
Z6	**1.08**	216	144	101.25	64.8	54	32.4	21.6
Total	**5.345**	1069	712.6667	501.0938	320.7	267.25	160.35	106.9

Table C.1: Amount of time the foil spends in each zone under different web speeds

In addition, a scheme of the machine is given in the figure below with a table quantifying the lengths and temperatures in each zone.

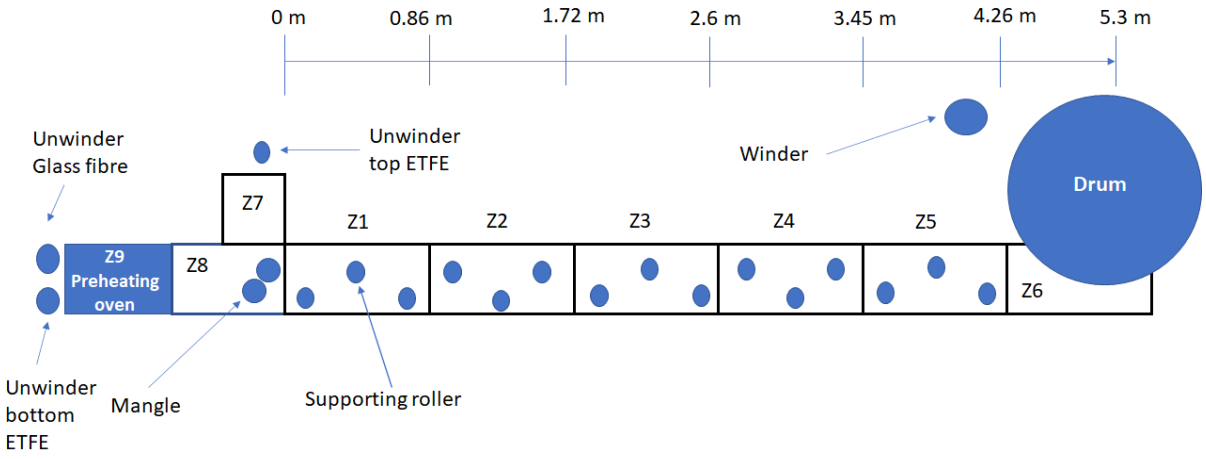

Figure C.1: The scheme of the machine where the process of laminating the top encapsulation foil takes place with the positions used in the model explained

Zone number	**Z9**	**Z8**	**Z1**	**Z2**	**Z3**	**Z4**	**Z5**	**Z6**	**Drum**
Set temperature (°C)	48	75	100	120	120	128	135	145	135
Length (cm)	103	76	86.5	85,5	88	84.5	82	108	N/A

Table C.2: Temperatures and lengths of each zone in the machine

Input and output parameters for web speed of 0.3 m/min

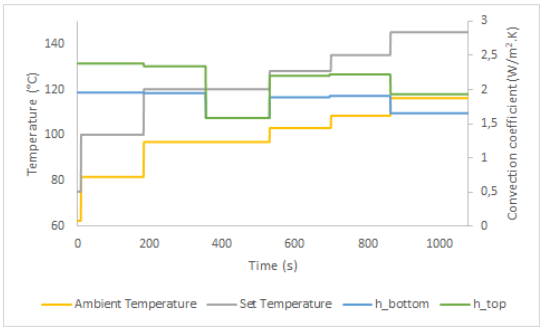

(a) Thermal model input parameters (h is the convection coefficient).

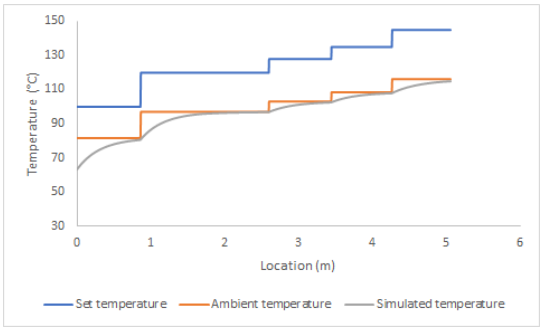

(b) Output of the thermal model compared to set and ambient temperatures

Figure C.2: Inputs and outputs of the thermal model for web speed of 0.3 m/min

Input and output parameters for web speed of 0.45 m/min

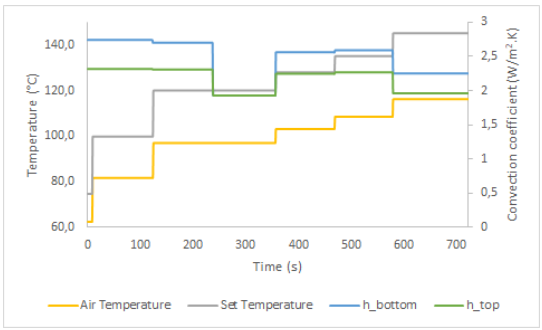

(a) Thermal model input parameters (h is the convection coefficient).

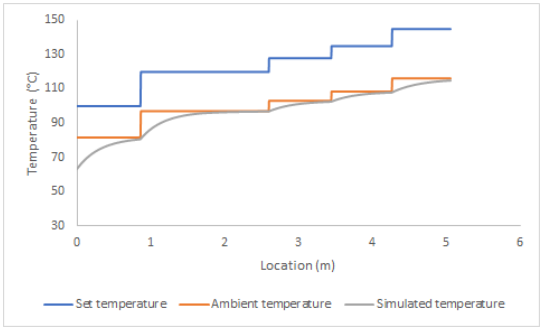

(b) Output of the thermal model compared to set and ambient temperatures

Figure C.3: Inputs and outputs of the thermal model for web speed of 0.45 m/min

Input and output parameters for web speed of 0.64 m/min

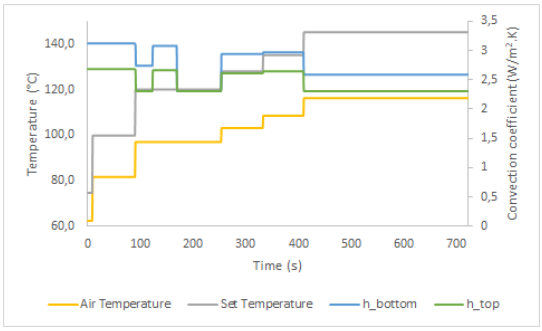

(a) Thermal model input parameters (h is the convection coefficient).

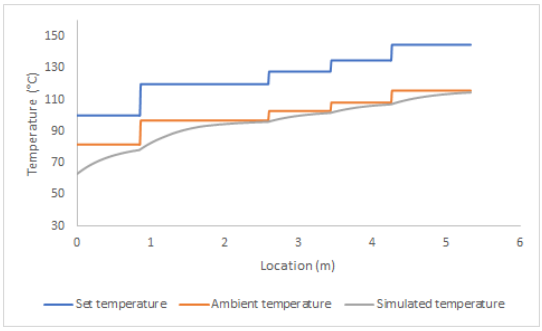

(b) Output of the thermal model compared to set and ambient temperatures

Figure C.4: Inputs and outputs of the thermal model for web speed of 0.64 m/min

Input and output parameters for web speed of 1.00 m/min

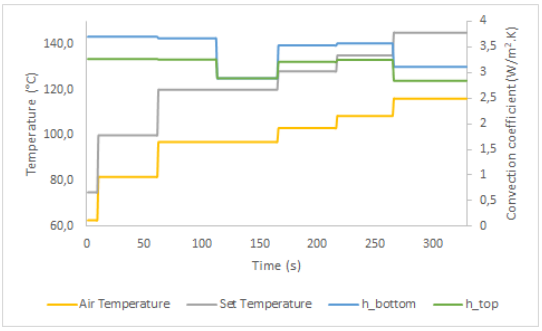

(a) Thermal model input parameters (h is the convection coefficient).

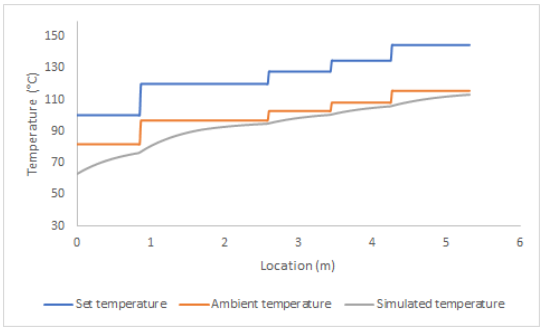

(b) Output of the thermal model compared to set and ambient temperatures

Figure C.5: Inputs and outputs of the thermal model for web speed of 1.00 m/min

Input and output parameters for web speed of 1.20 m/min

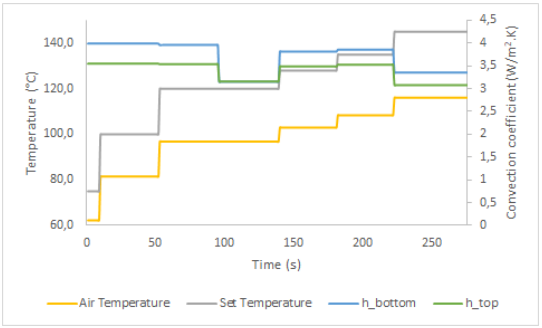

(a) Thermal model input parameters (h is the convection coefficient).

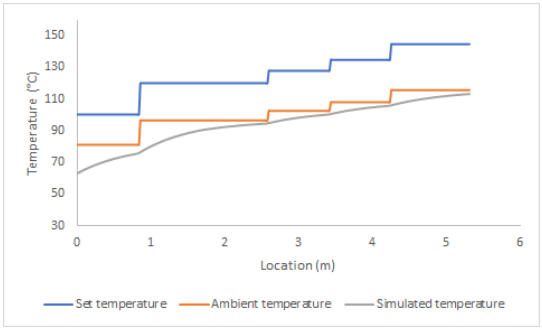

(b) Output of the thermal model compared to set and ambient temperatures

Figure C.6: Inputs and outputs of the thermal model for web speed of 1.20 m/min

Input and output parameters for web speed of 2.00 m/min

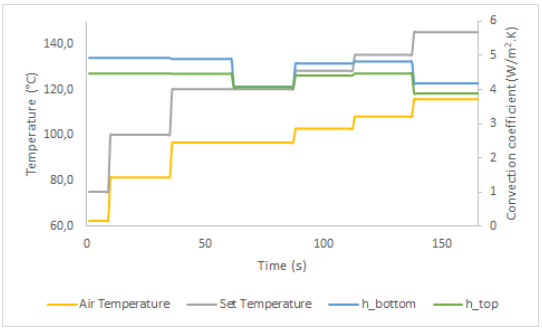

(a) Thermal model input parameters (h is the convection coefficient).

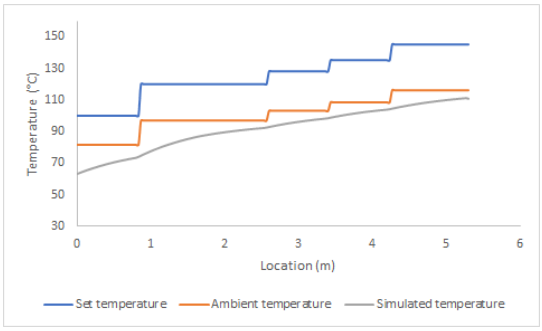

(b) Output of the thermal model compared to set and ambient temperatures

Figure C.7: Inputs and outputs of the thermal model for web speed of 2.00 m/min

Input and output parameters for web speed of 3.00 m/min

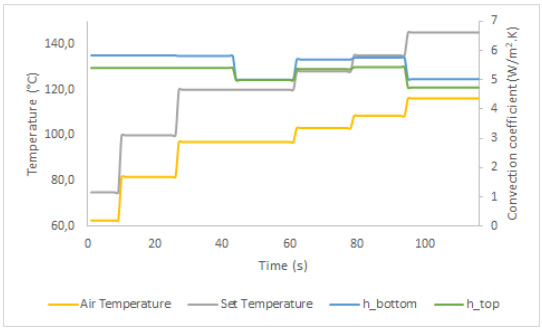

(a) Thermal model input parameters (h is the convection coefficient).

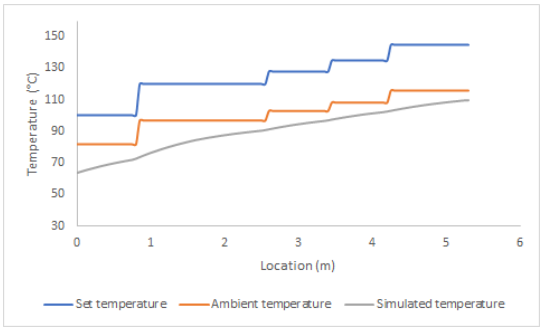

(b) Output of the thermal model compared to set and ambient temperatures

Figure C.8: Inputs and outputs of the thermal model for web speed of 3.00 m/min

Input and output parameters for web speed of Scenario 1

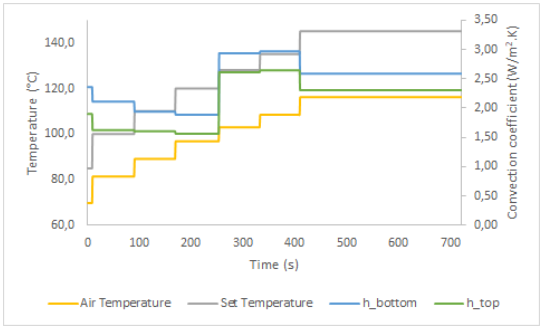

(a) Thermal model input parameters (h is the convection coefficient).

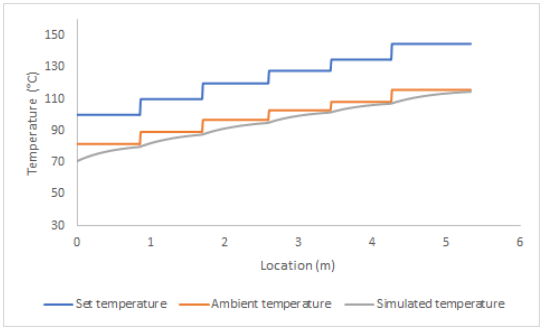

(b) Output of the thermal model compared to set and ambient temperatures

Figure C.9: Inputs and outputs of the thermal model for web speed of Scenario 1

Input and output parameters for web speed of Scenario 2

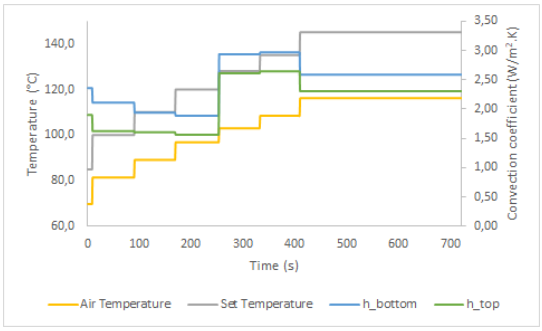

(a) Thermal model input parameters (h is the convection coefficient).

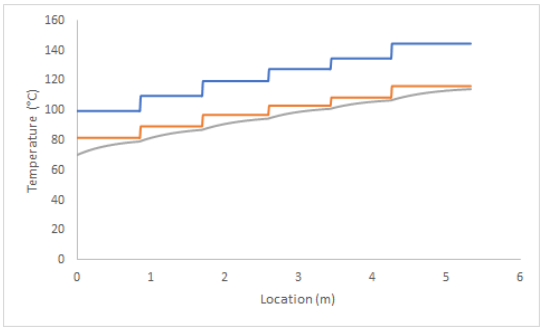

(b) Output of the thermal model compared to set and ambient temperatures

Figure C.10: Inputs and outputs of the thermal model for web speed of Scenario 2

Input and output parameters for web speed of Scenario 3

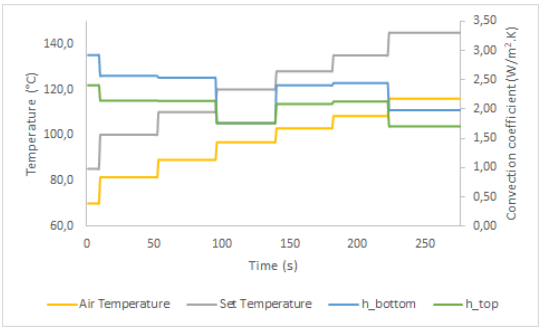

(a) Thermal model input parameters (h is the convection coefficient).

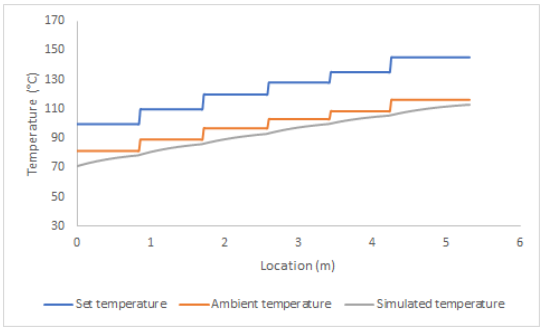

(b) Output of the thermal model compared to set and ambient temperatures

Figure C.11: Inputs and outputs of the thermal model for web speed of Scenario 3

Input and output parameters for web speed of Scenario 4

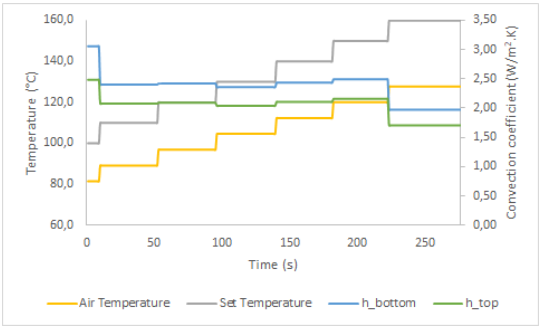

(a) Thermal model input parameters (h is the convection coefficient).

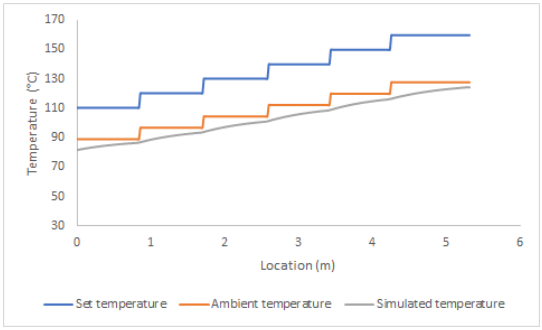

(b) Output of the thermal model compared to set and ambient temperatures

Figure C.12: Inputs and outputs of the thermal model for web speed of Scenario 4

Input and output parameters for web speed of Scenario 5

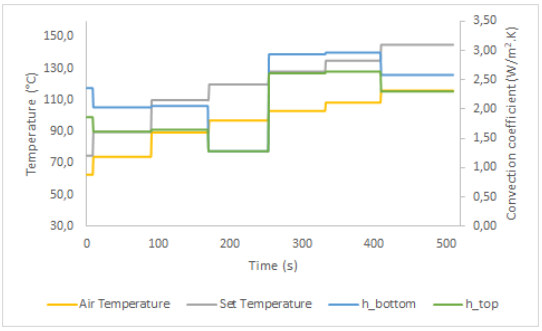

(a) Thermal model input parameters (h is the convection coefficient).

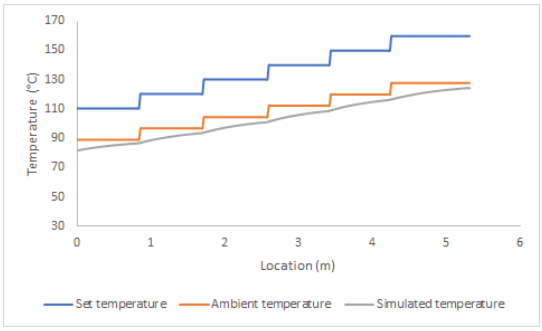

(b) Output of the thermal model compared to set and ambient temperatures

Figure C.13: Inputs and outputs of the thermal model for web speed of Scenario 5

D

Inputs and outputs of the mechanical model

In this appendix, the results obtained using the mechanical model are presented. The calculations of the stresses in the foil was explained in Section 3.2. The criteria for the critical stress has been explained in Section 2.4.3. A scheme of the machine with corresponding positions is given below with a table quantifying the lengths and temperatures of each zone.

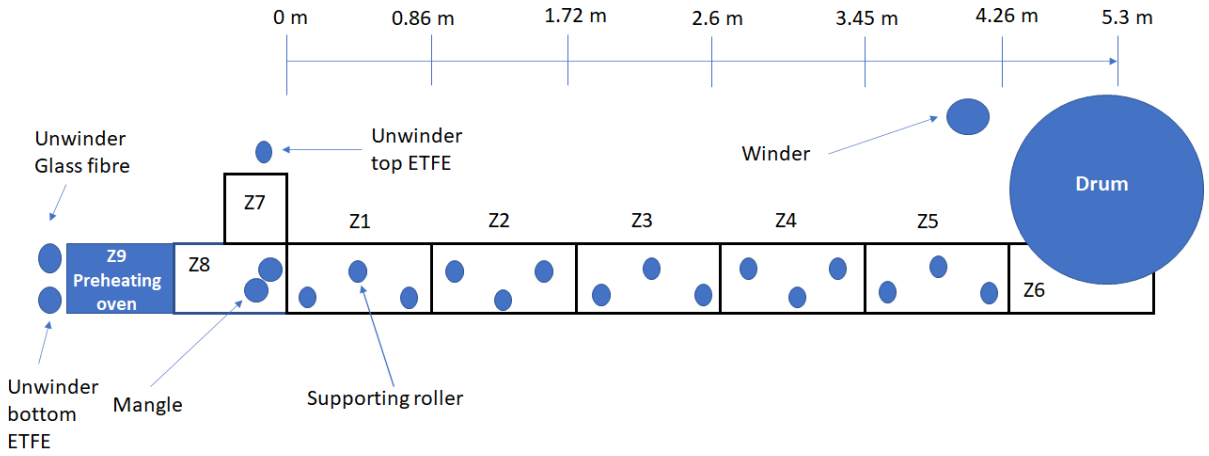

Figure D.1: The scheme of the machine where the process of laminating the top encapsulation foil takes place with the positions used in the model explained

Zone number	**Z9**	**Z8**	**Z1**	**Z2**	**Z3**	**Z4**	**Z5**	**Z6**	**Drum**
Set temperature (°C)	48	75	100	120	120	128	135	145	135
Length (cm)	103	76	86.5	85.5	88	84.5	82	108	N/A

Table D.1: Temperatures and lengths of each zone in the machine

Results for foil thickness of 25 μ m and width of 0.4 m under different web speeds:

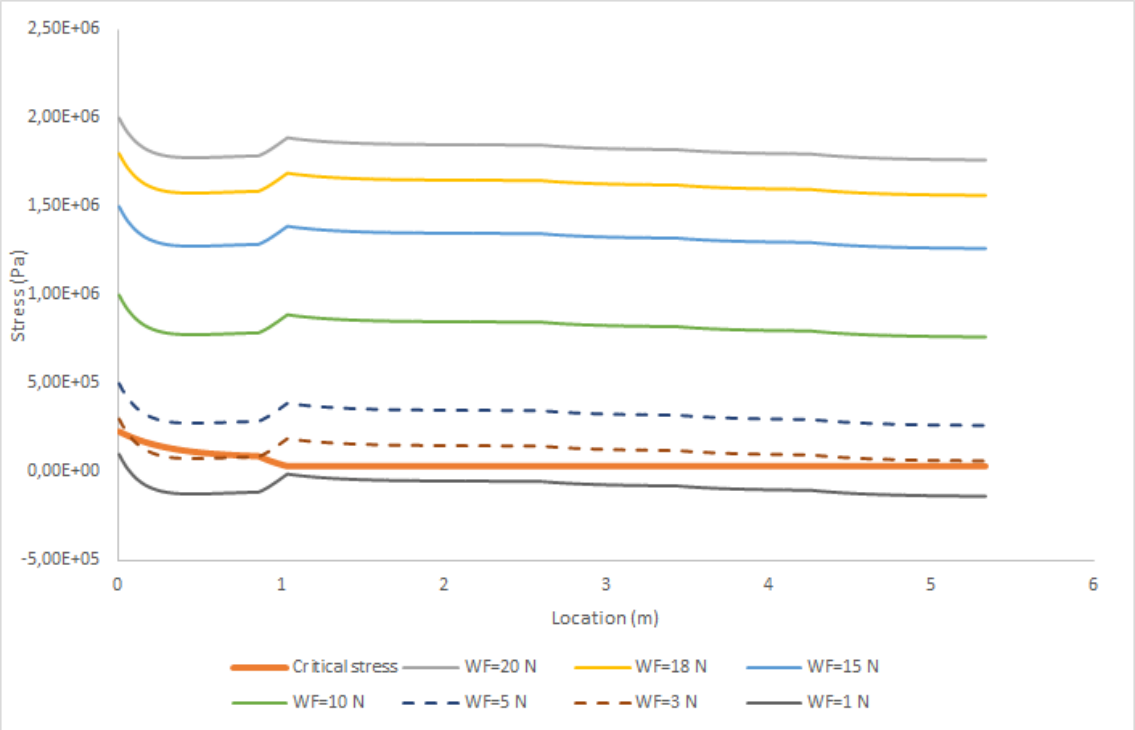

Figure D.2: The stress caused by different web forces in a 25 μm foil compared to the critical stress under web speed of 0.3 m/min

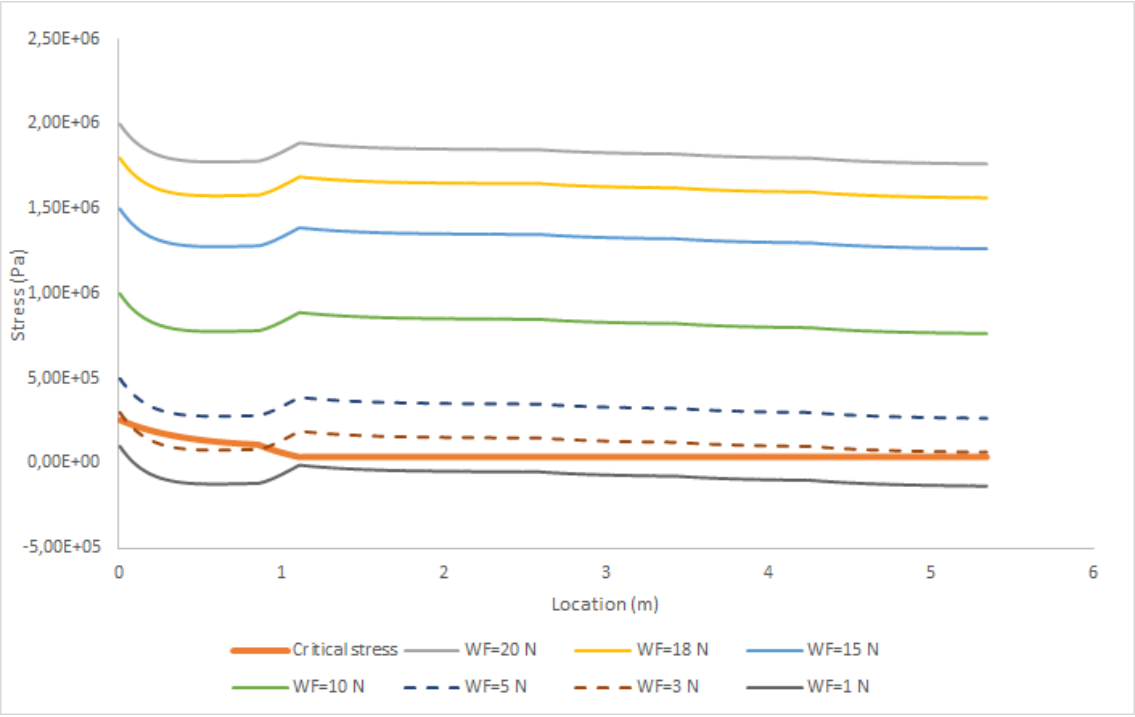

Figure D.3: The stress caused by different web forces in a 25 μm foil compared to the critical stress under web speed of 0.45 m/min

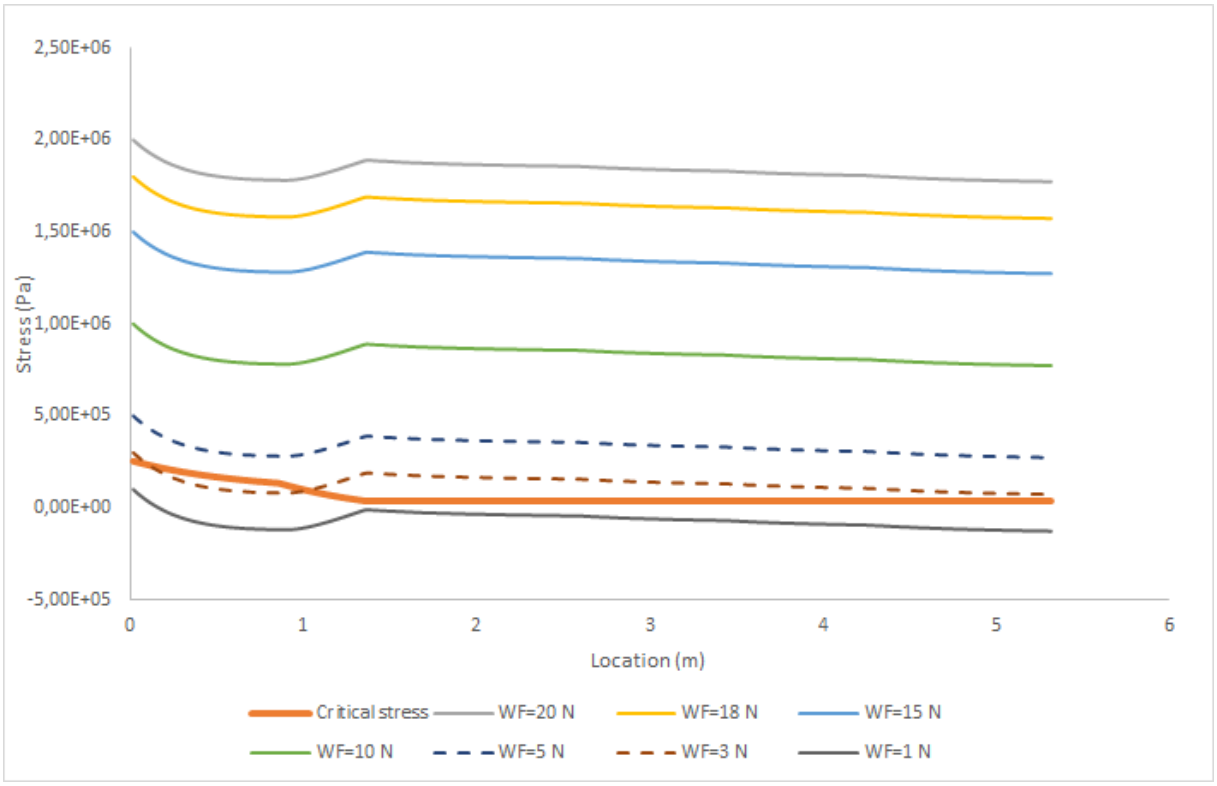

Figure D.4: The stress caused by different web forces in a 25 μm foil compared to the critical stress under web speed of 0.64 m/min

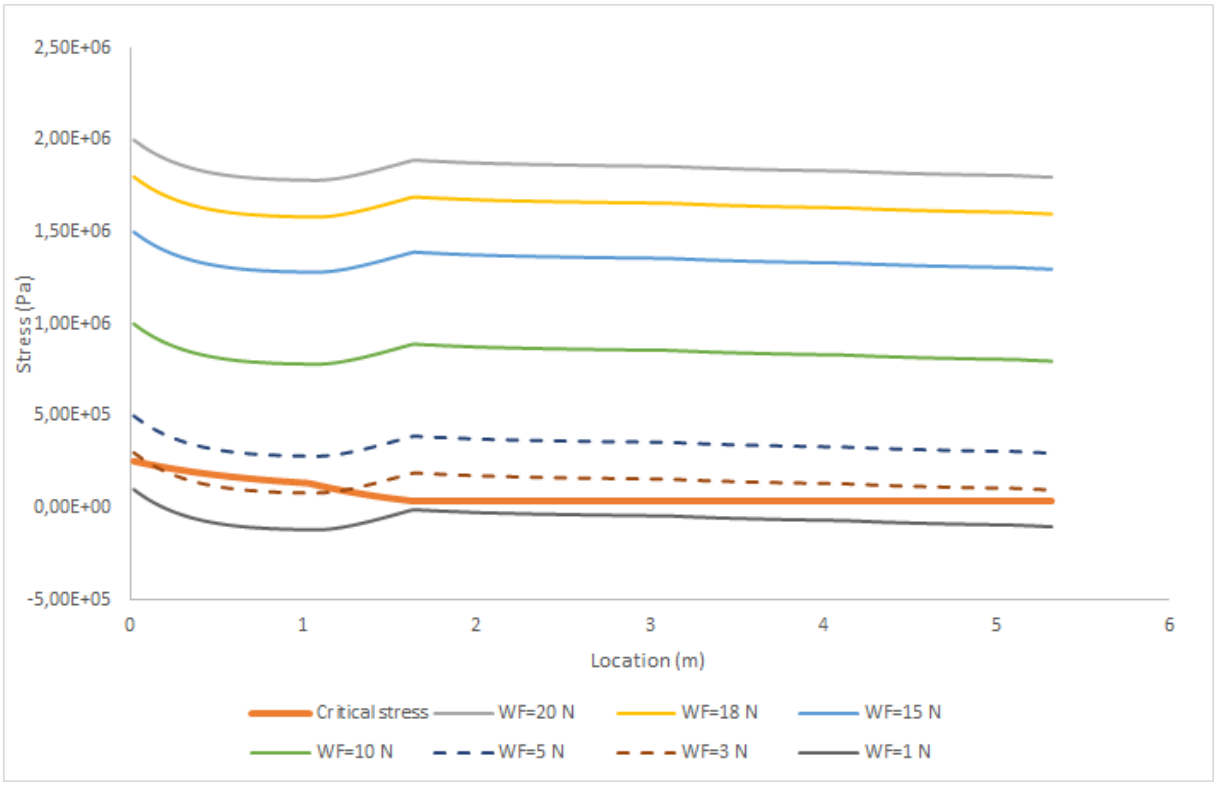

Figure D.5: The stress caused by different web forces in a 25 μm foil compared to the critical stress under web speed of 1 m/min

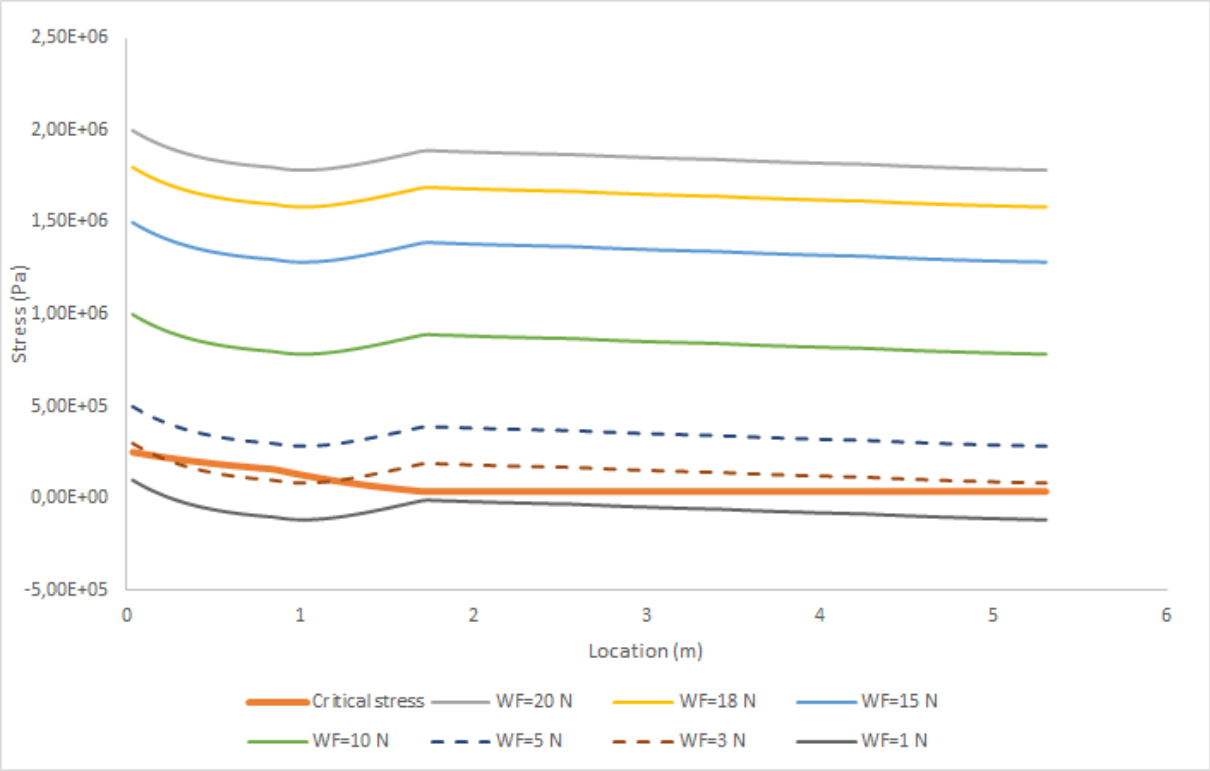

Figure D.6: The stress caused by different web forces in a 25 μm foil compared to the critical stress under web speed of 1.2 m/min

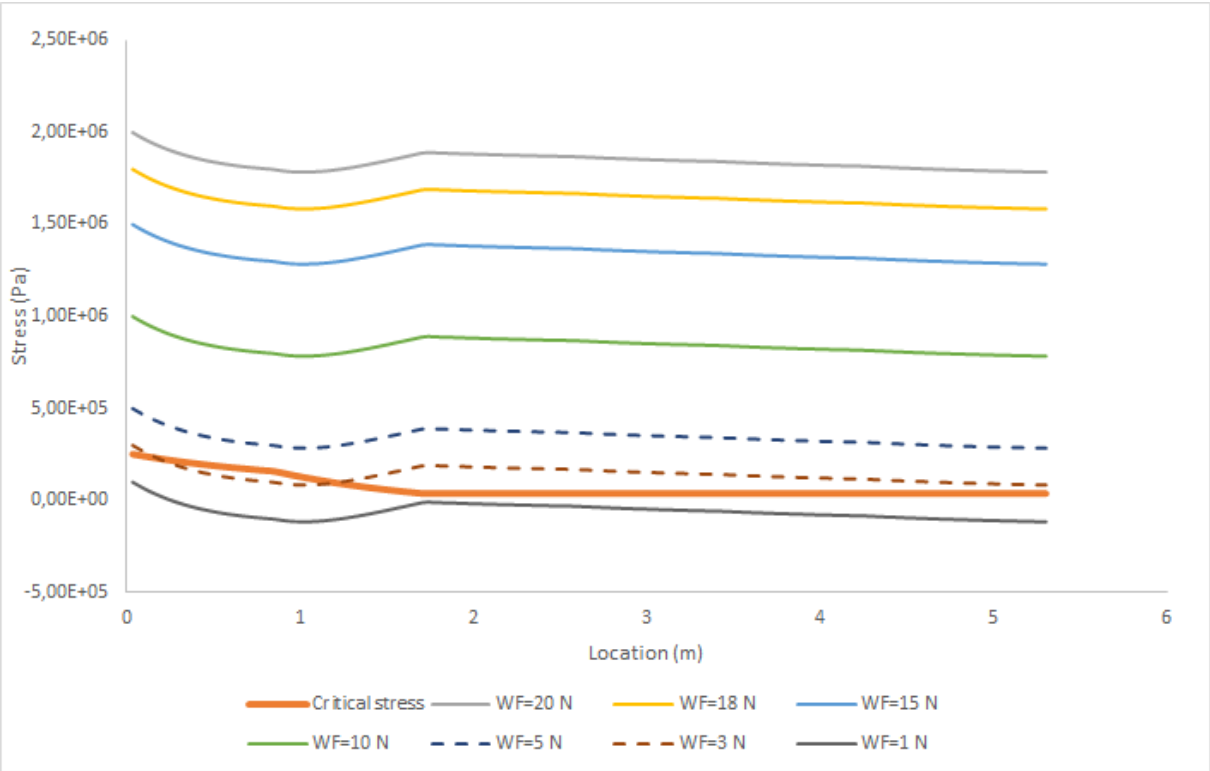

Figure D.7: The stress caused by different web forces in a 25 μm foil compared to the critical stress under web speed of 2 m/min

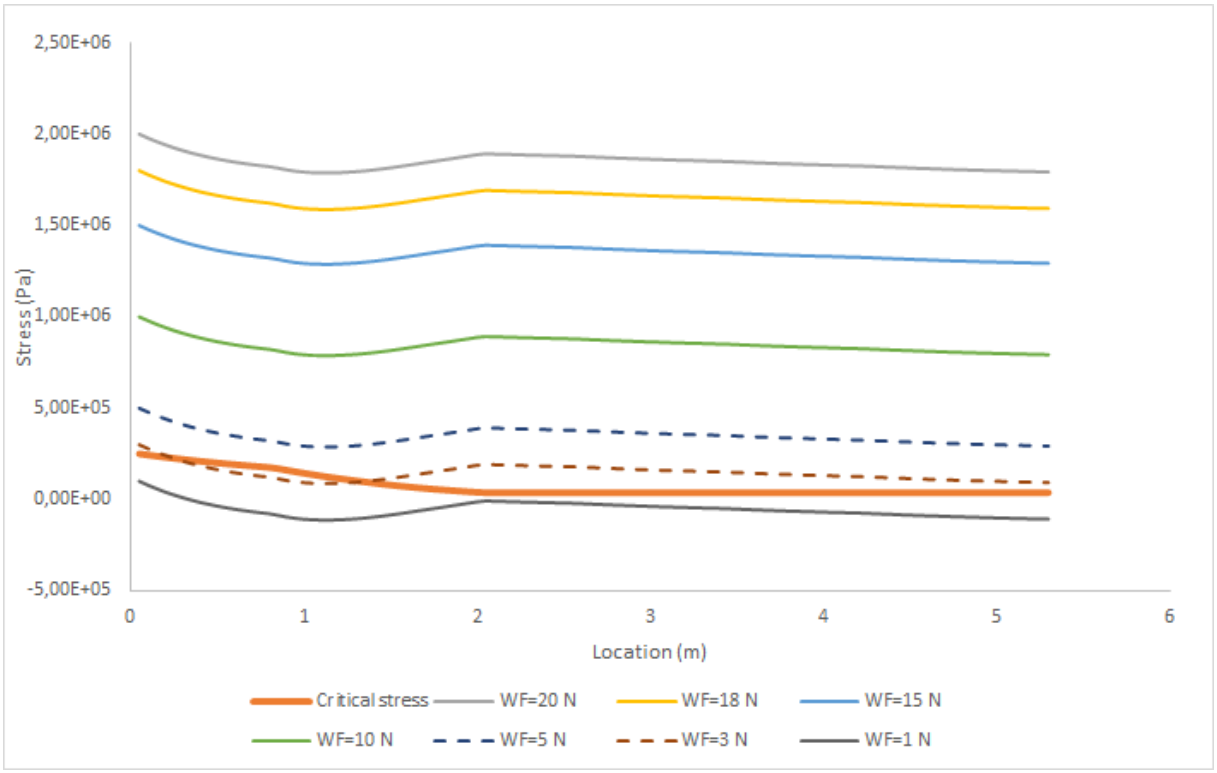

Figure D.8: The stress caused by different web forces in a 25 μm foil compared to the critical stress under web speed of 3 m/min

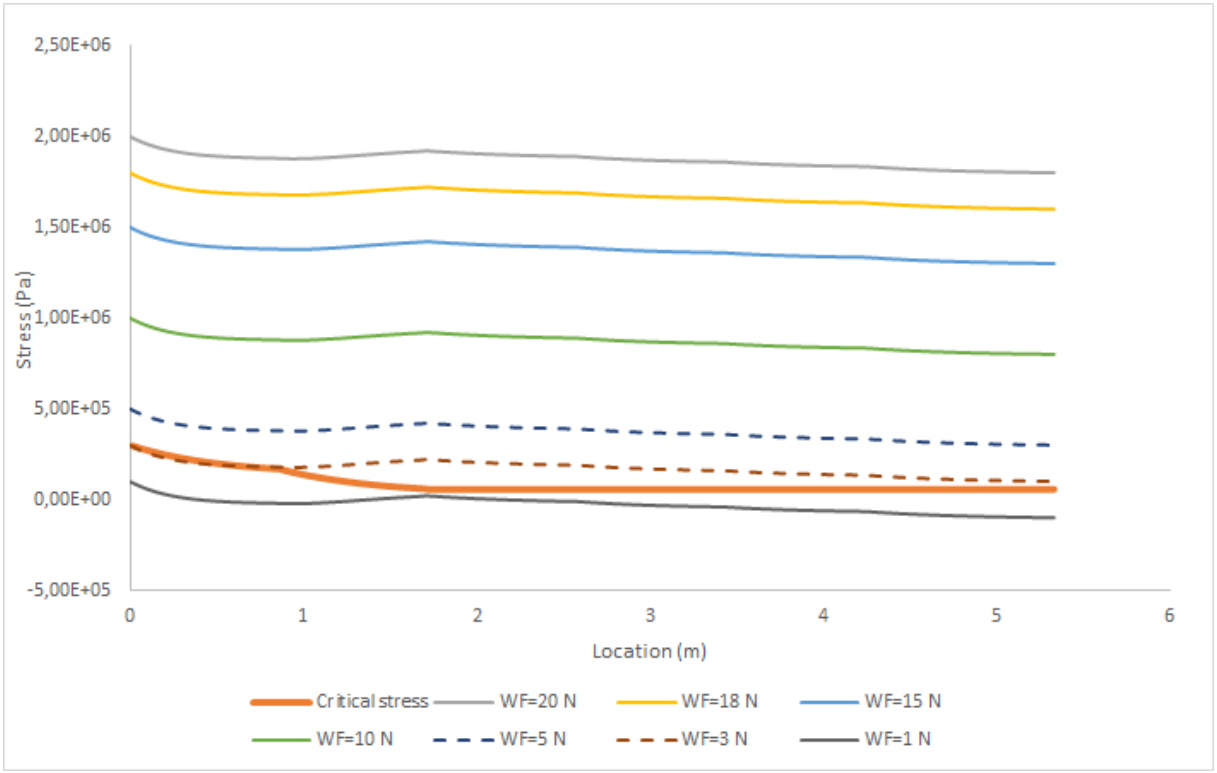

Figure D.9: The stress caused by different web forces in a 25 μm foil compared to the critical stress for Scenario 1

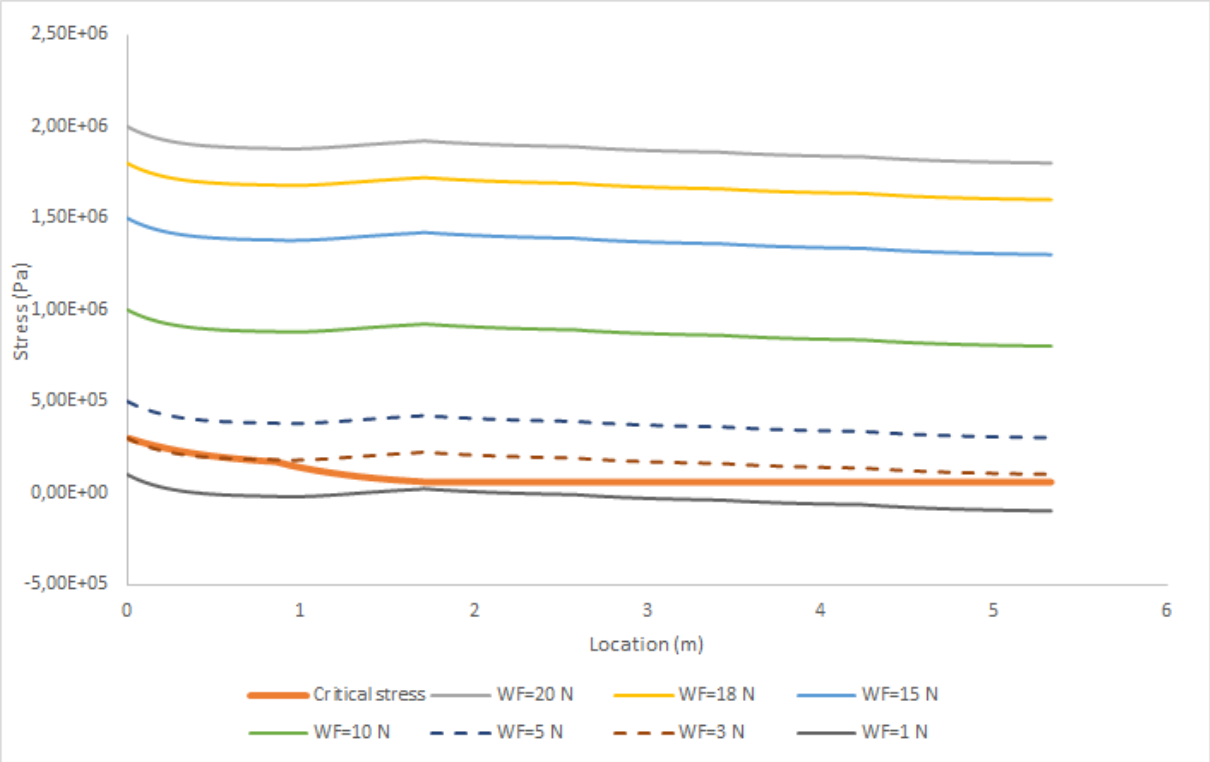

Figure D.10: The stress caused by different web forces in a 25 μm foil compared to the critical stress for Scenario 2

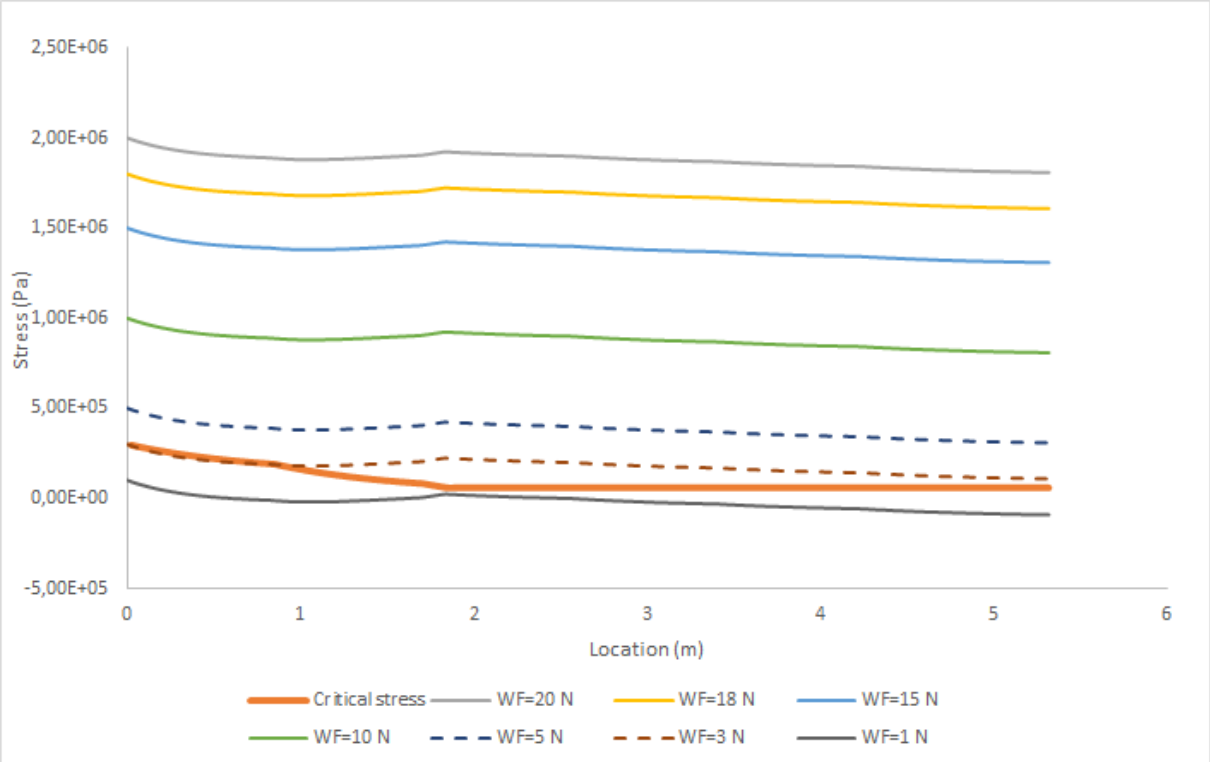

Figure D.11: The stress caused by different web forces in a 25 μm foil compared to the critical stress for Scenario 3

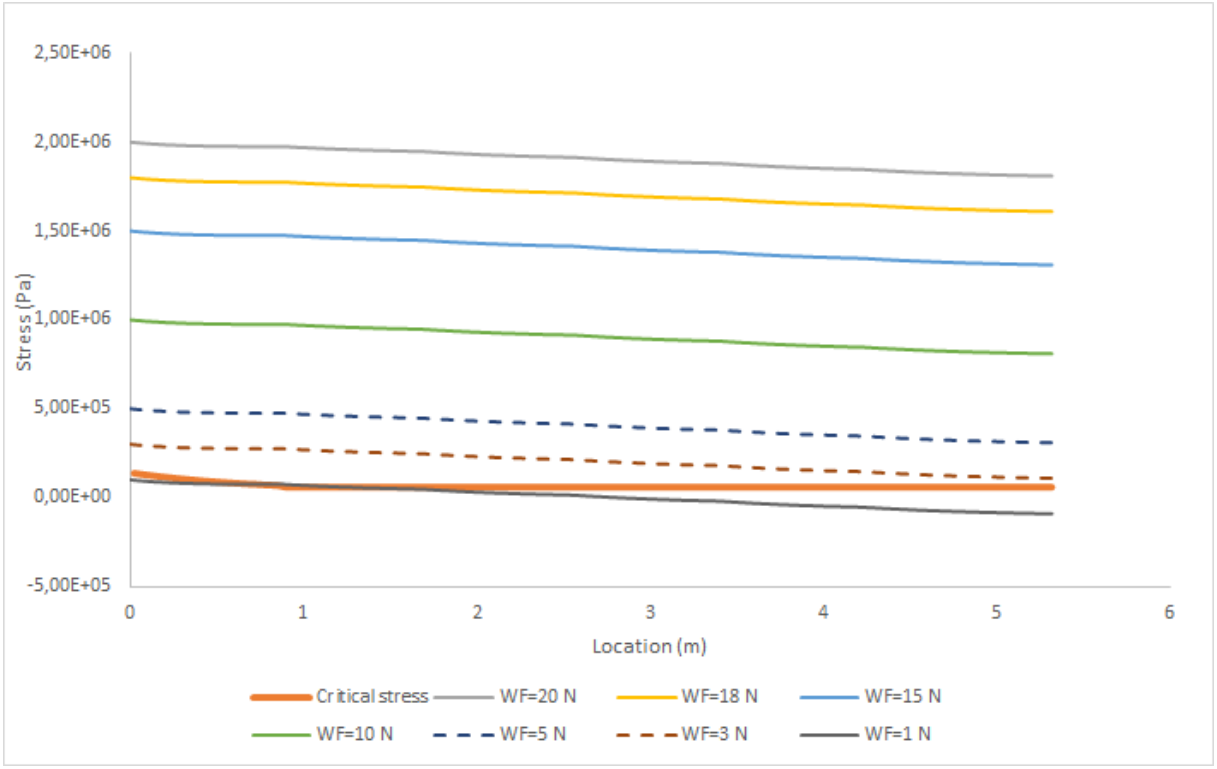

Figure D.12: The stress caused by different web forces in a 25 μm foil compared to the critical stress for Scenario 4

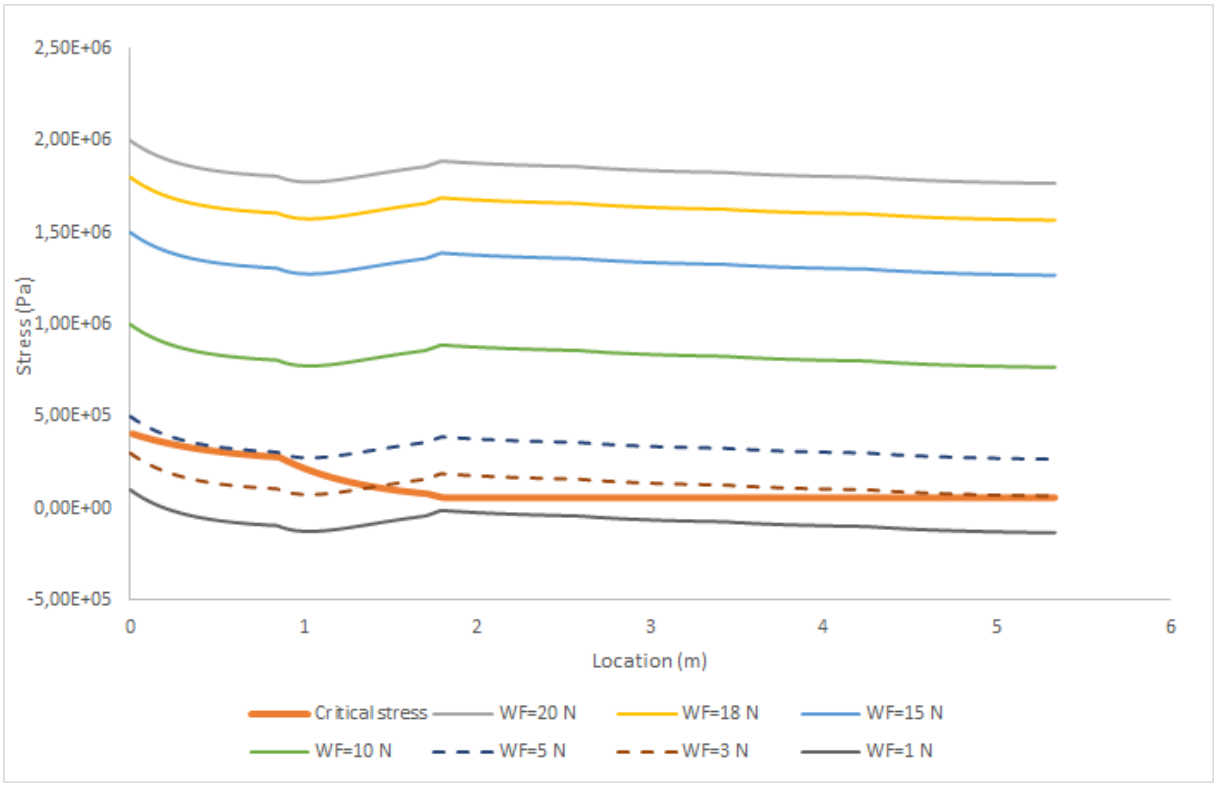

Figure D.13: The stress caused by different web forces in a 25 μm foil compared to the critical stress for Scenario 5

Results for foil thickness of 50 μ m and width of 0.4 m under different web speeds:

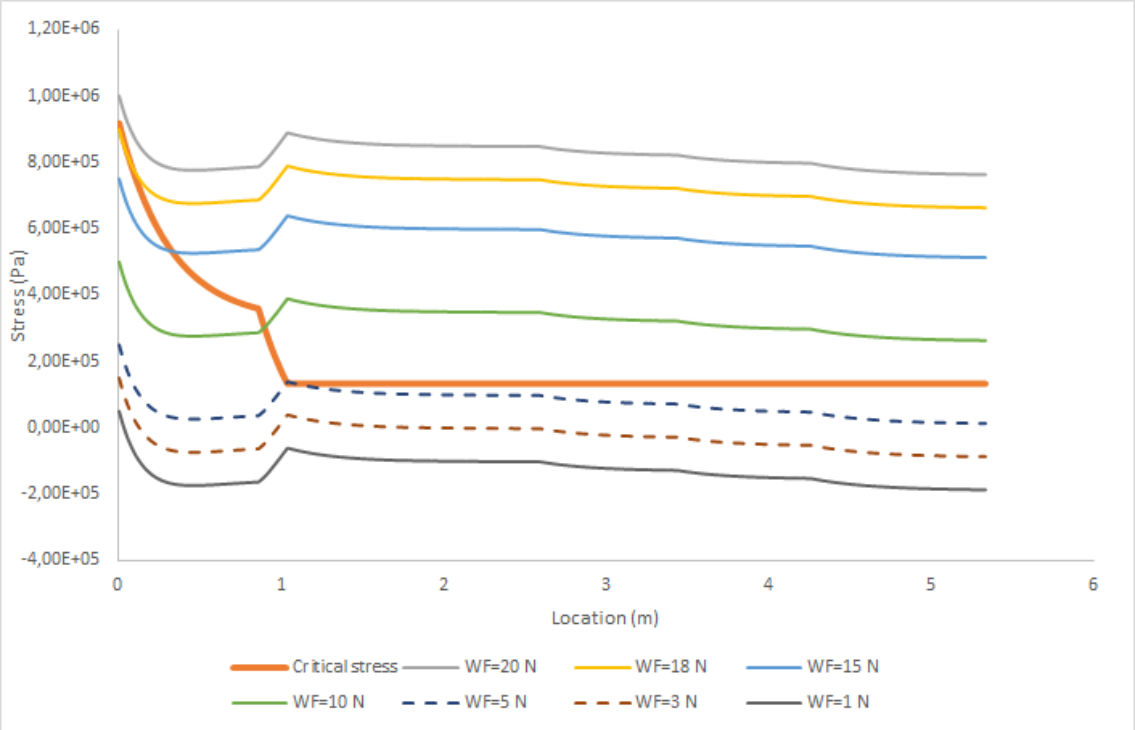

Figure D.14: The stress caused by different web forces in a 50 μm thick foil compared to the critical stress under web speed of 0.3 m/min

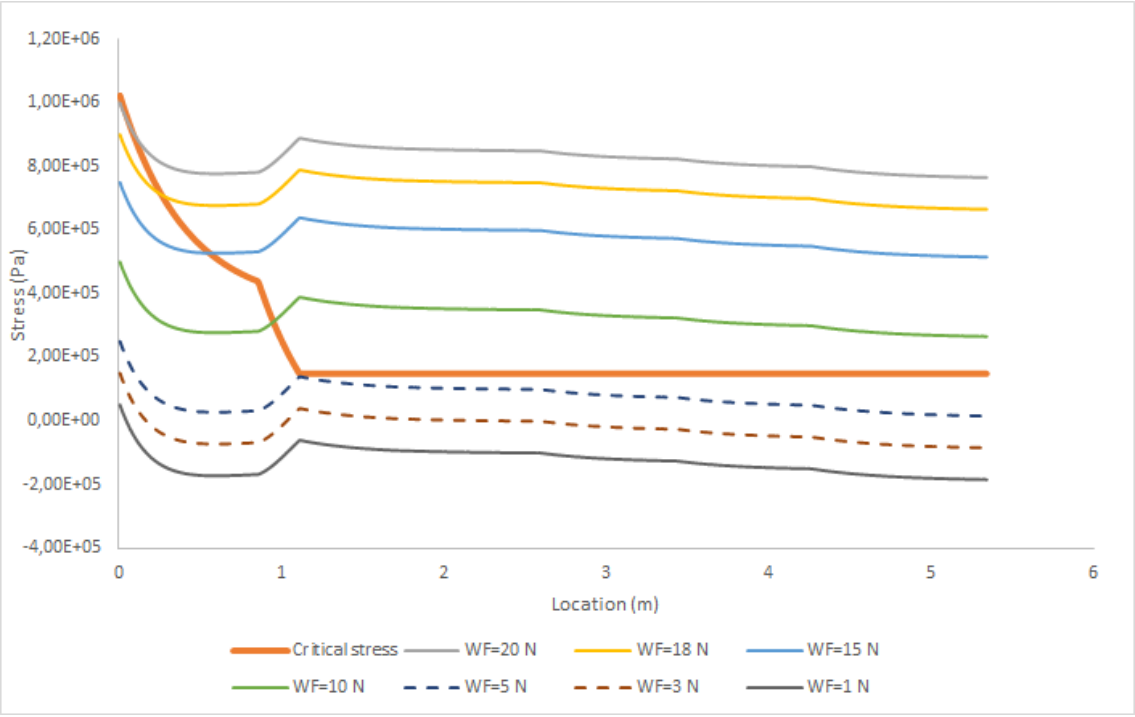

Figure D.15: The stress caused by different web forces in a 50 μm thick foil compared to the critical stress under web speed of 0.45 m/min

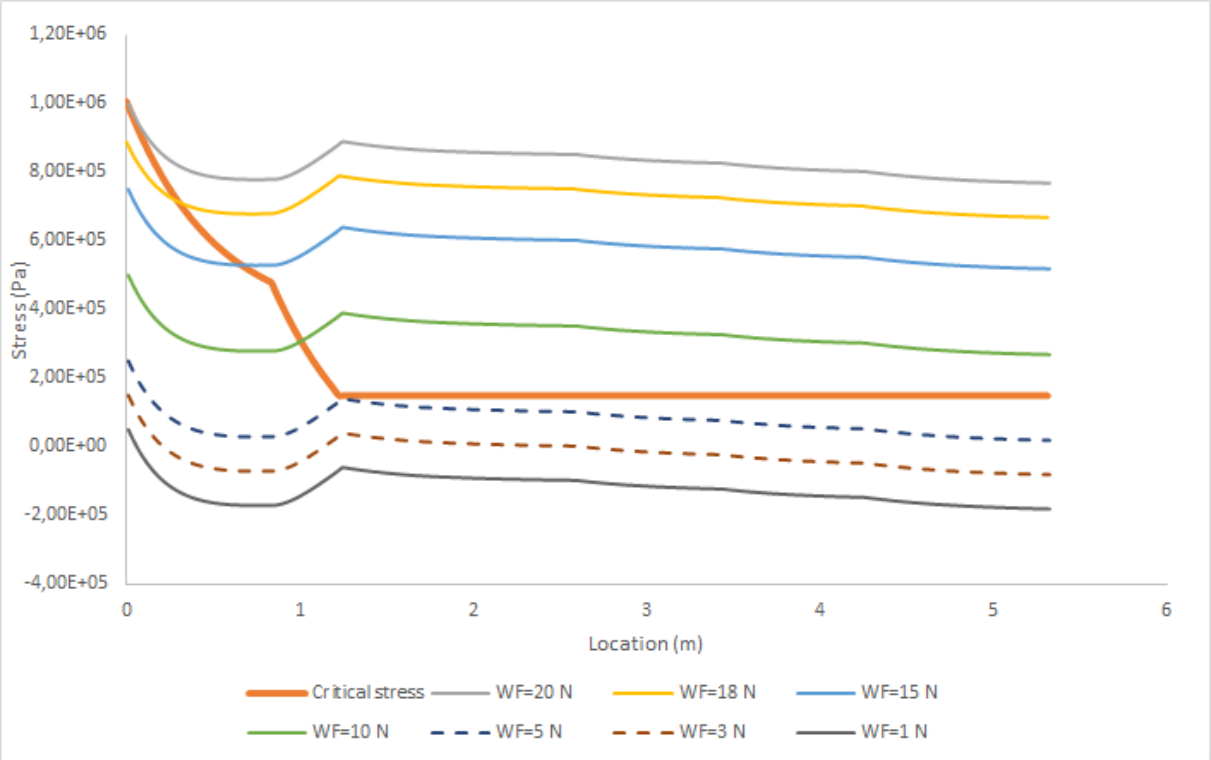

Figure D.16: The stress caused by different web forces in a 50 μm thick foil compared to the critical stress under web speed of 0.64 m/min

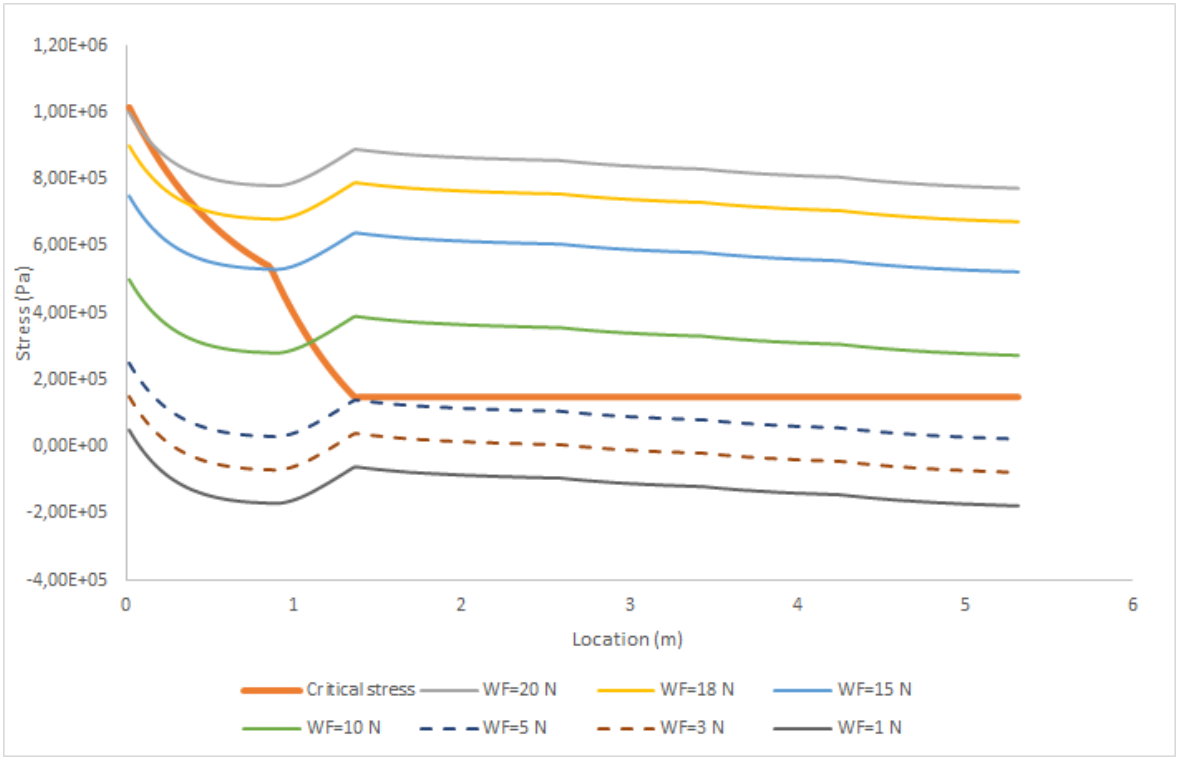

Figure D.17: The stress caused by different web forces in a 50 μm thick foil compared to the critical stress under web speed of 1.00 m/min

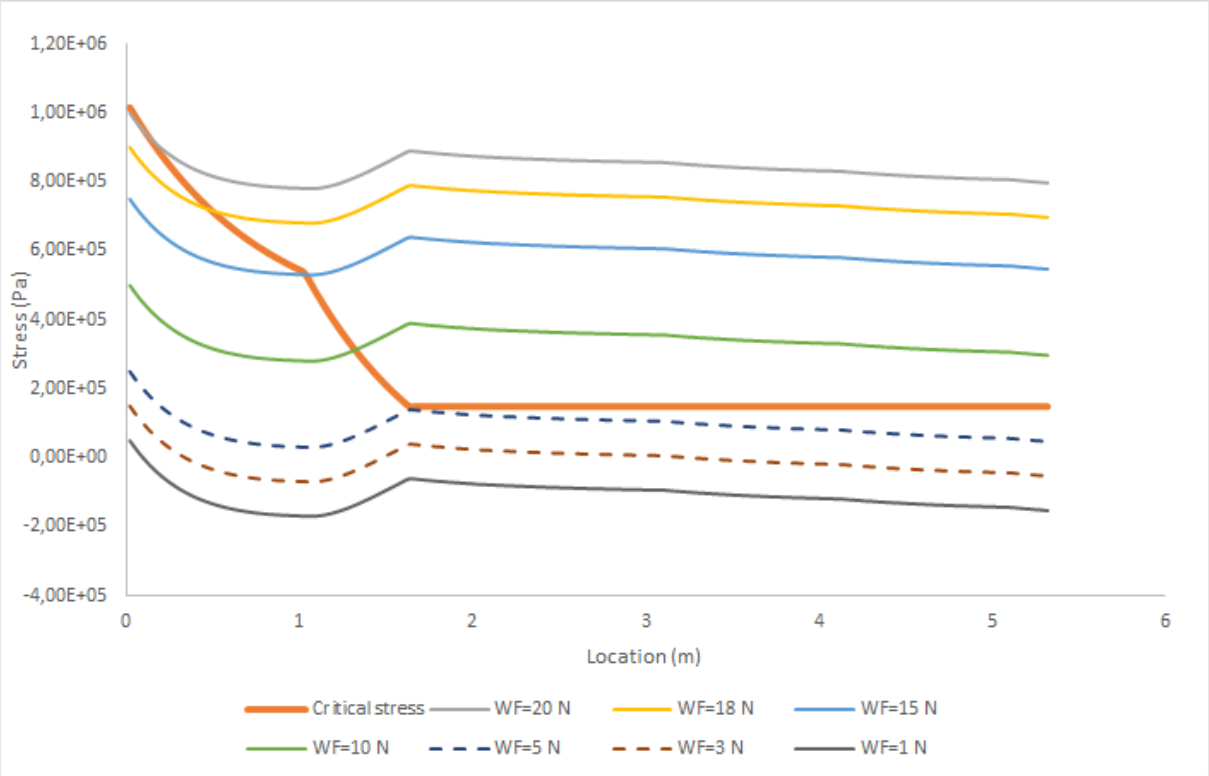

Figure D.18: The stress caused by different web forces in a 50 μm thick foil compared to the critical stress under web speed of 1.20 m/min

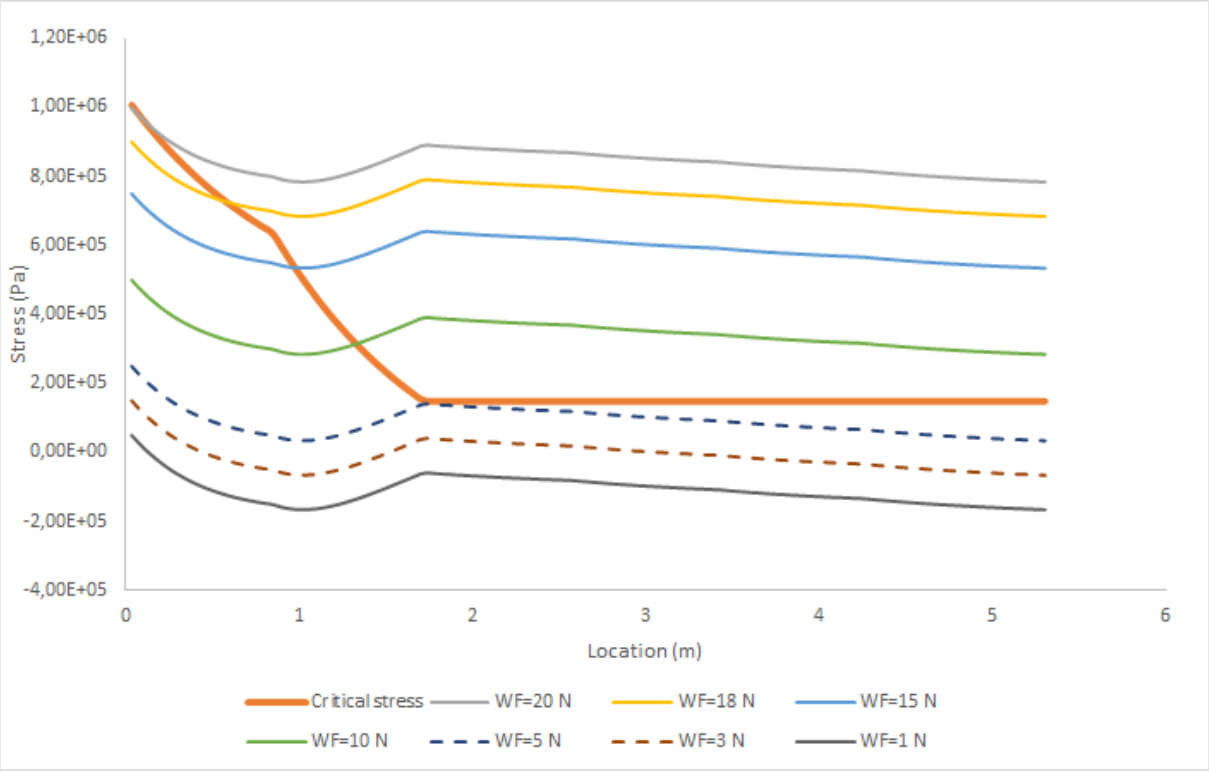

Figure D.19: The stress caused by different web forces in a 50 μm thick foil compared to the critical stress under web speed of 2.00 m/min

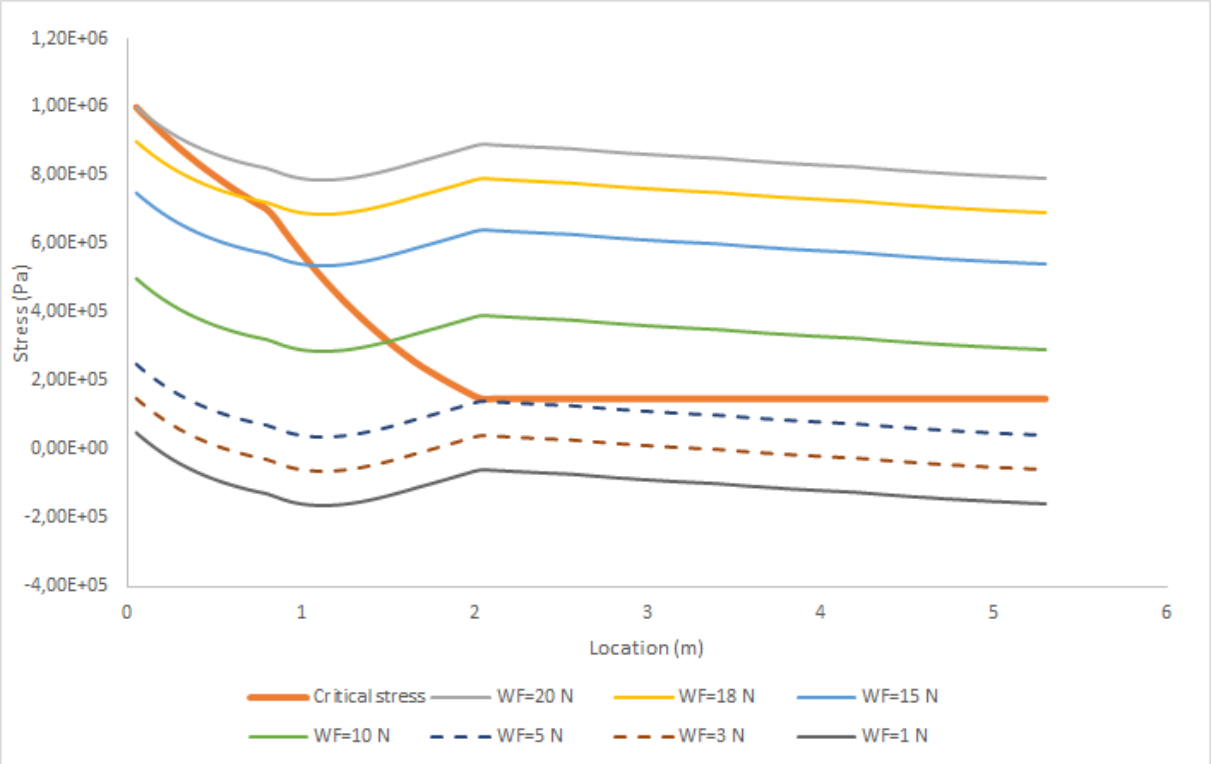

Figure D.20: The stress caused by different web forces in a 50 μm thick foil compared to the critical stress under web speed of 3.00 m/min

Bibliography

[1] What web tension should i run at on a roll to roll solution? URL https://www.kymc.com/msg/msg87.html.

[2] Etfe properties - fluorotherm™, Feb 2017. URL https://www.fluorotherm.com/technical-information/materials-overview/etfe-properties/.

[3] Cengel Yunus A. and Afshin J. Ghajar. *Heat and mass transfer: fundamentals applications*. McGraw-Hill Education, 2015.

[4] Wenjun Chen, Xuchun Gui, Leilei Yang, Hai Zhu, and Zikang Tang. Wrinkling of two-dimensional materials: methods, properties and applications. *Nanoscale Horiz*, 4:291–320, 2019. doi: 10.1039/C8NH00112J. URL http://dx.doi.org/10.1039/C8NH00112J.

[5] Cerda E. and Mahadevan L. Geometry and physics of wrinkling. *Physical review letters*, 90: 074302, 03 2003. doi: 10.1103/PhysRevLett.90.074302.

[6] Cerda E., K. Ravi-Chandar, and Mahadevan L. Wrinkling of an elastic sheet under tension. *Nature*, 419(6907):579–580, 2002. doi: 10.1038/419579b.

[7] Hamers E. Taak842- te, on air entrainment. Company internal report, 2017.

[8] Koenders E. Curing behaviour of the adhesives. Master's thesis, Hogeschool Utrecht, 2020.

[9] Rammerstorfer F.G. Friedl N. and Fischer F.d. Buckling of stretched strips. *Computers Structures*, 78(1-3):185–190, 2000. doi: 10.1016/s0045-7949(00)00072-9.

[10] Aditya Gotimukul. Prediction of amplitude and wavelength of troughs on polyethylene webs. Master's thesis, 2010.

[11] Pearson Glen Cakmak Miko Greener, Jehuda. 5.1 web handling, 2018. URL https://app.knovel.com/hotlink/khtml/id:kt011N7BGF/roll-roll-manufacturing/web-handling.

[12] Garcia J.P. van der Meulen G. Horstink J. Hamers E., Khadikova E. Strategy te1 trials (taak 1168). Company internal report, 2019.

[13] Honghao Hou, Yanchang Gan, Xuesong Jiang, and Jie Yin. Facile and robust strategy to antireflective photo-curing coating through self-wrinkling. *Chinese Chemical Letters*, 28(11):2147 – 2150, 2017. ISSN 1001-8417. doi: https://doi.org/10.1016/j.cclet.2017.08.027. URL http://www.sciencedirect.com/science/article/pii/S100184171730311X. SI: Young Scientists in Material Chemistry.

[14] Iea. Is exponential growth of solar pv the obvious conclusion? – analysis. URL https://www.iea.org/commentaries/is-exponential-growth-of-solar-pv-the-obvious-conclusion.

[15] Giese M. J. Corneal wrinkling in a hydrogel contact lens wearer with marfan syndrome. *Journal of the American Optometric Association*, 68:50–54, 1997.

[16] J.A. Beisel J.K. Good and H. Yurtcu. Instability of webs: the prediction of troughs and wrinkles. *In Advances in Pulp and Paper Research, Oxford 2009, Trans. of the XIVth Fund. Res. Symp.*, page 517–556, 2009. doi: 10.15376/frc.2009.1.517.

[17] Garcia J.P. Aging of te1 and modules with sand wrinkles and battleships (taak 977). Company internal report, 2019.

[18] Alkanbar T. Kadikova K. Te production - wrinkles formation -ansys heat model (taak1270). Company internal report, 2020.

[19] Dahl-Young Khang, Hanqing Jiang, Young Huang, and John A. Rogers. A stretchable form of single-crystal silicon for high-performance electronics on rubber substrates. *Science*, 311(5758): 208–212, 2006. ISSN 0036-8075. doi: 10.1126/science.1121401. URL https://science.sciencemag.org/content/311/5758/208.

[20] F. Kreith, Mark S. Bohn, and Raj M. Manglik. *Principles of heat transfer*. CL Engineering, 2010.

[21] T. D. Lee and A. U. Ebong. A review of thin film solar cell technologies and challenges. *Elsevier*, 322:1286–1297, 2017. doi: https://doi-org.tudelft.idm.oclc.org/10.1016/j.rser.2016.12.028.

[22] F. G. Rammerstorfer. Buckling of elastic structures under tensile loads. *Acta Mechanica*, 229(2): 881–900, 2017. doi: 10.1007/s00707-017-2006-1.

[23] D. Shaw and Y.H. Huang. Buckling behavior of a central cracked thin plate under tension. *Engineering Fracture Mechanics*, 35(6):1019 – 1027, 1990. ISSN 0013-7944. doi: https://doi.org/10.1016/0013-7944(90)90129-5. URL http://www.sciencedirect.com/science/article/pii/0013794490901295.

[24] Shigeru Shimizu, Shunya Yoshida, and Noriyasu Enomoto. Buckling of plates with a hole under tension. *Thin-Walled Structures*, 12(1):35 – 49, 1991. ISSN 0263-8231. doi: https://doi.org/10.1016/0263-8231(91)90025-E. URL http://www.sciencedirect.com/science/article/pii/026382319190025E.

[25] Isabella O. van Swaaaj R. Smets A., Jäger K. and Zeman M. *Solar energy: the physics and engineering of photovoltaic conversion, technologies and systems*. 01 2016.

[26] HyET Solar. Lcoe hyet solar: Hyet solar. URL https://www.hyetsolar.com/cost-effective/.

[27] Stephen P Timoshenko and James M Gere. *Theory of elastic stability*. Courier Corporation, 2009.

[28] Shiren Wang and Jingjing Qiu. Enhancing thermal conductivity of glass fiber/polymer composites through carbon nanotubes incorporation. *Composites Part B: Engineering*, 41(7):533–536, 2010. ISSN 1359-8368. doi: https://doi.org/10.1016/j.compositesb.2010.07.002. URL https://www.sciencedirect.com/science/article/pii/S1359836810001071.

[29] Tomasz Wierzbicki. 2.080j structural mechanics. *Massachusetts Institute of Technology: MIT OpenCourseWare*, Fall 2013. URL https://ocw.mit.edu. "License: Creative Commons BY-NC-SA".

[30] Wpengine. Fiberglass fabrics composites, Jun 2020. URL https://jpscm.com/resources/why-fiberglass/#:~:text=Thefiberglassyarnsusedin,cm/cm/°C.

[31] Mahmoud Zendehdel, Narges Yaghoobi Nia, and Mohammadreza Yaghoubinia. *Emerging Thin Film Solar Panels*. 01 2020. ISBN 978-1-78984-823-6. doi: 10.5772/intechopen.88733.

[32] Bing Zhao, Wujun Chen, Jianhui Hu, Jianwen Chen, Zhenyu Qiu, Jinyu Zhou, and Chengjun Gao. Mechanical properties of etfe foils in form-developing of inflated cushion through flat-patterning. *Construction and Building Materials*, 111:580 – 589, 2016. ISSN 0950-0618. doi: https://doi.org/10.1016/j.conbuildmat.2016.01.050. URL http://www.sciencedirect.com/science/article/pii/S0950061816300502.